Comparative histology of human skin.

COMPARATIVE HISTOLOGY OF HUMAN SKIN

KAMIL ASAAD

MPhil

UNIVERSITY OF BRADFORD

2010

Abstract

There are 5 distinct aspects to this study. (i) Two histological stains for collagen were compared against each other for the first time, namely Herovici's technique and picrosirius-polarization. (ii) Skin samples from embalmed cadaveric tissue from human cadavers were compared against samples taken from surgical patients. (iii) Skin samples were studied from different regions of the body to assess if dermal structure correlates with scarring potential. (iv) Skin samples were sectioned in a plane parallel to the epidermis to gain further insight into dermal structure. (v) A novel basement membrane stain was produced.

Type I and type III collagen are important structural constituents of dermis and play a crucial role in wound healing. Only two traditional histological methods are thought to differentiate between them, so avoiding the need for antibodies. These methods are picrosirius-polarization and Herovici's technique. These were compared against each other for the first time in order to establish differences in image quality and discrimination between Type I and type III collagen. Neither technique requires antibodies, however picrosirius requires polarisation microscopy. Herovici's technique was found to result in a clearer, consistently reproducible collagen staining pattern than the picrosirius method and more importantly did not require elaborate apparatus to analyze. Additionally other cellular elements were visible.

Skin samples for research are often obtained from surgical excision. This clearly limits which tissues are available for comparative study to those areas

operated on. Studying samples from embalmed medical school cadavers has the great advantage of studying areas of the body not routinely available from common surgical procedures. It was therefore desirable to assess whether embalmed cadaveric tissues exhibited different properties by virtue of their age and the embalming process compared to fresh surgical specimens, in order to give confidence that studies utilising the former would be equally valid. To test this, 58 skin samples from embalmed medical school cadavers were compared to skin samples from 38 fresh operative specimens. The levels of tissue preservation and processing artefacts were similar in both groups. Embalmed medical school cadavers clearly offer an opportunity to study tissue areas not routinely available during surgery. This is the first time such a comparison has been made.

Many things will affect the final appearance of the scar, but the single most important determinant is the body region affected. The most common areas for unfavourable scarring, specifically keloid or hypertrophic scarring have been shown to be the ear, deltoid and sternal areas. To test the hypothesis that there is no difference in histological structure of skin that correlates to body region, comparative histology was undertaken exploring the regional variations of skin characteristics in 58 cadaveric samples. Closely comparable samples were taken from the deltoid (9), abdomen (13), sternum (10), post-auricular (5), earlobe (12) and eyelid (9). Epidermal thickness, epidermal appendage density and collagen fibre orientation were examined and qualitative structural differences were assessed for each region

Skin samples were then grouped by both topographical location of the body and scarring potential. Skin samples exhibited qualitative and quantifiable regional variations in the characteristics studied. Epidermal thickness and appendage counts did not correlate with scarring potential. Both however were statistically significantly higher in skin sampled from the head compared to the trunk. Bundles of collagen fibres in the reticular dermis were grouped according to their orientation in relation to the coronal plane; either parallel, oblique or perpendicular. The ratio of oblique to parallel fibres was statistically significantly higher in body areas with poorer scarring prognosis. This corresponds to a more disorganised arrangement of collagen fibres in these areas.

Further qualitative understanding of dermal collagen fibres came from sectioning tissues in a plane parallel to the skin's surface. This is perpendicular to conventional histological samples. Further visualisation and clarification of the 'basket-weave' arrangement of fibres at different levels of the dermis was observed and greatly aided by the clarity of Herovici's stain.

In the process of optimising Herovici's stain, a novel histological stain for basement membranes was produced. This new method stained basement membranes purple, cytoplasm was stained greenish-brown and nuclei dark brown. Collagen fibres were either thin and blue or thick and green. This method was compared to PAS staining and although required more preparative steps allows greater identification of other cellular structures.

Keywords

Herovici's; Picrosirious-Polarisation; Cadaver; Keloid; Type I Collagen; Type III Collagen; Basement membrane; PAS staining; Histology.

Acknowledgements

To Dr Ian Naylor for his guidance and support throughout my research and thesis.

To Professor David Sharpe for giving me the opportunity to undertake this research at Bradford.

I would like to thank my parents for their continued love and support throughout my life.

To my brother Nabil for proofreading the discussion and explaining chemical structures.

To my sister Maha for always making me laugh. Never lose your sense of fun.

To Lucy for the conversations about histology, skin cancer and for being a true friend.

To Dr Pat McConnell at the University of Leeds for allowing me access to the dissection rooms and laboratories and cadaveric material, without which this would have been a very different project.

To Tim Lee at the University of Leeds for his help in processing the cadaveric tissue.

To my colleagues Shahid, Susan, and Shola. I shall miss the camaraderie of our office on H floor. Good luck in your respective careers. I know we haven't seen the last of each other.

To Emily, I will try to remember how you lived.

This thesis is dedicated to

the memory of

the 56 who died and the 270 injured

on May 11th 1985

at the Bradford City Football Stadium fire

disaster

Papers Derived from this Thesis

Published Abstracts

A Novel Picropolychrome Technique for the Selective Staining of Basement Membranes

Asaad K, DT Sharpe, Huq S, Stevenson S, Adekunle A, Naylor IL

J Path 2006 210(S1) 61A

Herovici's Stain Vs Picrosirius Polarization In Cutaneous Histology

Asaad K, Adekunle A, Huq S, Stevenson S, Naylor IL, Sharpe DT

J Path 2006 208(S1) 24A

Oral Presentations

Can dermal collagen structure predict scarring outcome?

Asaad K, Adekunle A, Huq S, Stevenson S, Naylor IL, Sharpe DT

BAPRAS, London Dec 2006

Can detailed knowledge of skin structure improve cosmetic outcome in skin grafts?

Asaad K, Adekunle A, Huq S, Stevenson S, Naylor IL, Sharpe DT

ISBI Fortaleza, Brazil September 2006

A Novel Picropolychrome Technique for the Selective Staining of Basement Membranes

Asaad K, DT Sharpe, Huq S, Stevenson S, Adekunle A, Naylor IL

The Pathological Society of Great Britain, Manchester Jul 2006

Histological Analysis of Skin from Embalmed Cadavers-a Possible Route for Studying the Complexities of Skin

Asaad K, McConnell P, Naylor IL, Sharpe DT

The Anatomical Society of Great Britain and Ireland, Cambridge Jan 2006

Poster Presentations

Herovici's Staining of the Papillary-Reticular Dermal Interface:

Does This Facilitate Clark's Staging of Melanoma?

Asaad K, Adekunle A, Huq S, Stevenson S, Naylor IL, Sharpe DT

BAPRAS, Sheffield Jul 2006

Herovici's Stain Vs Picrosirius Polarization In Cutaneous Histology

Asaad K, Adekunle A, Huq S, Stevenson S, Naylor IL, Sharpe DT

The Pathological Society of Great Britain, Oxford Jan 2006

Table of Contents

List of Figures

List of Tables

List of Graphs

Chapter 1 Introduction

1.1 Skin Anatomy

The skin is the largest organ in the body, forming 8% of the total body mass. It is continuous with the mucous membranes lining the body's orifices. Its functions are extremely diverse acting as a mechanical barrier and sense organ. It plays an important role in thermoregulation, immunity and UV protection as well as a cosmetic and social role. It is divided into three layers from superficial to deep: the epidermis, dermis and subcutaneous tissue. (Elder *et al* 2004, McKee *et al* 1996) It has two embryological origins; the epidermis is from the surface ectoderm and the dermis from the underlying mesenchyme (Sadler 1990). It is appropriate to first of all consider the epidermis.

1.1.1 The Epidermis

The epidermis is a keratinising stratified squamous epithelium. It contains two main cell populations, keratinocytes and dendritic cells. The dendritic or clear cell population include melanocytes and Langerhans cells. These are randomly arranged and provide protection in terms of melanin and the immune system. The keratinocytes are arranged into four layers or strata; these are:

The basal cell layer (stratum basale)

The prickle cell layer (stratum spinosum)

The granular cell layer (stratum granulosum)

The horny layer (stratum corneum)

Each layer will be considered in turn.

The basal cells form a single layer of columnar cells attached to the basement membrane zone by hemidesmosomes and connected to adjacent cells by desmosomes. They often contain melanin transferred from adjacent melanocytes. Most mitotic activity in normal human epidermis occurs in this layer

The prickle cell layer contains several layers of more mature polygonal keratinocytes that tend to become more flattened as they reach the surface. They have an eosinophillic cytoplasm and are attached via desmosomes.

The granular layer comprises cells that contain keratohyalin granules. The nuclei become pycnotic and begin to disintegrate. Membranous organelles degenerate and keratin filament bundles become more compact

The horny layer is the final product of epidermal differentiation or keratinisation. It contains closely packed layers of flattened corneocytes or squames. This ranges in thickness from a few cells to 50 cells deep depending on location within the body. The corneocytes are devoid of a nucleus and membranous organelles, consisting of a dense array of keratin filaments.

The epidermal cells rely on a supportive structure on which to exist and this will now be considered.

1.1.2 The Basement Membrane Zone

This separates the basal layer of the epidermis from the dermis. Using a suitable light microscopy stain it appears homogeneous. When the PAS reaction procedure is used, a positive region 0.5-1 μm in thickness is seen. A similar zone is seen around cutaneous appendages. In contrast to light microscopy, electron microscopy reveals that the basal lamina has 4 zones; these are:

The plasma membrane of basal cells containing hemidesmosomes and anchoring filaments. The lamina lucida, an electron lucid area 35nm wide composed of laminin. The lamina densa, an electron dense area 30-50nm wide composed of type IV collagen. The sub-basal lamina fibrous zone (sublamina densa, pars fibroreticularis) contains extensions of lamina densa and banded anchoring fibrils attaching the basal lamina to dermal connective tissue. The anchoring fibrils contain type VII collagen and elastic fibres.

The next structural layer to consider is the dermis.

1.1.3 The Dermis

Perhaps it is appropriate to begin with a quotation from a recent text that nicely summarizes our present concepts regarding the dermis. One can read…

"Not long ago, the dermis was considered to be a leathery cutaneous layer primarily responsible for housing and protection of vessels that served to nourish the keratinizing epidermis. Today we realize that the dermis is a dynamic microenvironment containing a repertoire of cells and matrix molecules arguably more complex and sophisticated than the epidermis and its appendages." (Elder *et al* 2004)

In the most basic structural terms the dermis is subdivided into a superficial papillary layer and a deeper reticular layer. The dermis comprises a fibrous connective tissue component, ground substance, epidermal appendages, blood vessels and nerves. In addition there is a cellular component distributed throughout the dermis, comprising mast cells, fibroblasts, myofibroblasts and macrophages. Collagen gives the dermis tensile strength, while elastin, which is distributed throughout helps to provide elastic recoil after stimulation.

The papillary dermis includes the subepidermal papillae located between the rete ridges, and extends to the superficial vascular plexus. In additional the thin meshwork of collagen fibres forming sheaths around the epidermal appendages, called the periadnexal dermis can be regarded a functional unit with the papillary dermis known as the adventitial dermis.

The remainder of the dermis, constituting a much larger portion, usually stated to be approximately 90% of the total, comprises thick bundles of collagen fibres and is called the reticular dermis.

Between all the filaments of both the papillary and reticular dermis is what is termed the ground substance. This extremely complex mixture consists mainly of fibronectin and glycosaminoglycans linked to form macromolecules. This extremely complex mixture of macromolecules serves as an embedding medium for cellular and fibrous components of the dermis and has a role in the transport of water, nutrients and electrolytes. Its ability to effectively connect all elements in the dermis is basic to dermal integrity.

Finally in the dermis are a group of less studied elements which are usually grouped together as elastic fibres. These have formed into a well developed network in the dermis by 32 weeks. They constitute 2-4% of the dermis (Uitto *et al* 1983). In the papillary dermis thin fibres run upwards perpendicular to the to the dermal-epidermal junction and terminate at the basement membrane zone. In the lower portions of the dermis the fibres are thicker and run parallel to the skin's surface. Their exact role is still the subject of speculation (Elder *et al* 2004, Gray *et al* 1995, McKee *et al* 1996).

A subject of less speculation is the essential role of blood vessels in the skin. This will be considered next.

1.1.4 Blood Supply

The dermal microvasculature is divided into two strata. The superficial vascular plexus occurs in the boundary between the papillary and reticular dermis and envelops adnexal structures. This plexus forms a layer of anastomosing arterioles and venules. Small capillary loops arise from this plexus extending into each dermal papilla.

The deep vascular plexus connects to the superficial plexus via vertical vessels in the reticular dermis and separates the reticular dermis from the underlying subcutaneous fat (Gray *et al* 1995).

1.1.5 Regional Variations

After a concise summary of the what elements are present in the skin it is perhaps appropriate to mention that although many people consider skin as a uniform structure this is far from true.

"There is considerable regional variation in structure, making a knowledge of the normal anatomy of skin at its varying sites essential for the accurate diagnosis of skin biopsies." (McKee *et al* 1996).

Whilst it is true that most texts draw an important distinction between thin, hairy skin that covers most of the body and the thick, hairless, glabrous skin covering the palms and soles there are also other areas of specialized skin at mucocutaneous junctions such as the lips and outer rim of the anal canal which do not fit in with this classification system. (Gray *et al* 1995). More generalised considerations are lacking. One illustration of this variability is shown by relaxed skin tension lines. These are determined by pinching the skin to determine the direction in which skin can be moved with least resistance. They vary considerably with the body region and it should be said that there is still some disagreement over their exact arrangement (Borges 1984). Another example of the variability in skin behaviour is its potential to scar differently at different locations. We shall now consider this in more detail.

1.2 Scar Prognosis

Scarring is the end product of a healed wound (Ferguson *et al* 1996). It is thought to be an evolutionary optimization for speed of healing under dirty conditions. This end product can be thought of as a continuum ranging from scarless healing to a fine line scar, a stretched, contracted or raised scar to a hypertrophic or keloid scar (Bayat *et al* 2003). Whilst some of these terms are self-explanatory, confusion exists when classifying scars as hypertrophic or keloid. Some authors have suggested the classification on the grounds of clinical behaviour (Brody 1990) or histological and biochemical differences (Rockwell *et al* 1988). Others have suggested the existence of an intermediate group of scars whose behaviour falls in between the two (Muir 1990).

Many different factors will influence the final appearance of scar. These include direction in relation to lines of skin tension; wound shape; surgical technique; wound tension; infection; nature of injury; and individual, racial or genetic factors. However the most important determinant in an individual is the region of the body that has been injured (Borges 1960) We can consider keloids to illustrate this point.

Several studies have looked at the relative incidence of keloids at different body regions. In 1947 Jacobsson reported on the treatment of 625 keloids. Of these 563 cases were localized to one region of the body. 121 were in the sternal region, 118 were on the shoulder and 97 on the neck.

13 years later, Cosman *et al* (1961) studied the treatment and behaviour of 340 lesions described clinically and/or pathologically as keloids excised from 247 patients. 35% of these lesions were from the ear, 20% from the face, and 16% from the neck. Whilst this appears to contradict other studies about the incidence of keloid formation it should be remembered that these are more cosmetically sensitive areas and the patients underwent surgery, thus introducing a strong element of bias into the analysis of incidence here.

In the same decade as the last study, Crockett (1964) examined 46 Sudanese patients with 250 keloid scars, of which 80 were severe (defined as greater than 1 inch of extension from the original scar in width or depth). 24 patients had keloids present in more than one body region. The body was divided into twelve regions for this study and the incidence of keloid, severe keloid and non-keloid scars was examined. It was found that the incidence of keloid scars in susceptible areas was inversely proportional to the incidence of non-keloid scars. Those areas with greatest tendency to form keloids were the midline front of chest, upper back, beard area, ear and pre-axial upper limb (includes deltoid region). The central face was the least likely area to form keloids. The beard area included pre-auricular skin, lower cheek and chin, and the front and sides of the neck above the level of the cricoid cartilage. It is of interest to note that males did not form keloids in this region after the development of facial hair.

Further studies followed, in India 1000 patients with keloids (Ramakrishnan *et al* 1974) showed that the greatest incidence of keloids was in the pre-sternal region, in 336 cases, followed by the deltoid region with 170 cases.

More recently a study of 211 cases of keloid scarring from the West Indies (Bayat *et al* 2005) showed 122 cases with keloids at a single site and 89 cases with a total of 369 keloids at multiple sites. Here it was found that the ear was the commonest site, followed by the chest and then trunk. Bayat *et al* (2004) also studied the morphology of these scars and found that this could vary greatly both within and between regions.

One study of the behaviour of keloids and regional susceptibility (Calnan *et al* 1967) excised a keloid from 10 patients (4 pre-sternal, 2 deltoid, 1 earlobe, 1 elbow, 1 buttock and 1 breast) and formed these into a 2.5cm circular graft 2-3mm thick and grafted this onto a similar sized defect created in the anterior abdominal wall. 9 of the keloids recurred at the site of original excision. In the grafted areas 1 graft did not take and a keloid formed at this site. In all other cases the grafts took and the keloids have regressed, becoming softer, paler and flatter within 3 years.

Whilst there are many other factors that may contribute to the formation of keloids including age, family history and race. These studies show that the skin has different scarring potential at different locations even in the same individual. When a keloid is transplanted it loses its ability to exert its keloidal nature. This may suggest local factors have a role in the behaviour of such cells.

After a broad perspective of the dermis, what of its constituent fibres, namely collagen?

1.3 Collagen

1.3.1 Collagen Biochemistry

Collagen is a family of basic glycoproteins containing high proportions of glycine and proline (Kiernan 1990). The basic molecule of collagen is the monomer tropocollagen composed of 3 α-chains with a total molecular weight of 300,000 A. Each α-chain is a left-handed helix with three residues per turn. The three chains are then interwoven around a central axis to form a right-handed superhelical molecule. Each α-chain is arranged in peptide units of three, with the amino acid glycine occupying every third position, allowing this tightly wound configuration. The two other sites of the alpha chain, conventionally denoted X and Y may be occupied by any number of amino acids, however the X position is frequently occupied by proline and the Y position by hydroxyproline, which is thought to contribute to the stability of the helix. (Prockop *et al* 1995, Murray *et al* 2003, Junqueira *et al* 2002)

Collagen is formed from the cleavage of precursors. Preprocollagen is synthesized on membrane bound ribosomes and contains a leader sequence that directs the peptide into the rough endoplasmic reticulum. This leader sequence is then cleaved to form procollagen, which still contains additional polypeptide residues at the amino and carboxyl terminals. This confers solubility to the molecule and prevents intra-cellular polymerization in the endoplasmic reticulum hydroxylation of the proline and lysine residues and glycosylation of hydroxylysine also occurs. Procollagen thus consists of three pro- α chains that develop the triple helix configuration. Next it is secreted into the intercellular fluid where it is cleaved to form collagen. Collagen molecules are rod shaped, measure 1.5 by 300nm and contain 1000 amino acids per chain. The diameter of composite fibres ranges from 2-15 μm. They are strengthened by covalent cross linkages, which may be side to side, end to end and overlapping. Collagen molecules intertwine to form microfibrils and then fibrils. Interweaving of fibrils results in the mature collagen fibre. Using electron microscopy longitudinal sections of collagen show cross striations with a periodicity of 64nm. These are seen because of the longitudinal overlap of individual molecules (Prockop *et al* 1995, Murray *et al* 2003, Junqueira *et al* 2002).

The position is made more complex as there is not just one type of collagen. 19 subtypes of collagen have been described, depending on morphology, amino acid composition, and physical properties (Prockop *et al* 1995). Reticulin fibres are a type of thin type III collagen fibres. They demonstrate argyrophillia and PAS positivity, due to their high sugar content (Glegg *et al* 1953), containing 6-12% hexoses compared to 1% in other collagen types. They are the first formed fibres in embryonic life and various conditions characterized by increased fibroblast activity (Junqueira *et al* 2002).

Table 1.1 Distribution of collagen subtypes within different tissues Adapted from Prockop *et al* 1995

Collagen Type	Tissue
I	Most connective tissues
II	Cartilage, vitreous humour
III	Extensible connective tissue
IV	Basement membranes
V	Tissues containing type I collagen
VI	Most connective tissues
VII	Anchoring fibrils
VIII	Endothelium
IX	Tissues containing type II collagen
X	Hypertrophic cartilage
XI	Tissues containing type II collagen
XII	Tissues containing type I collagen
XIII	Many tissues
XIV	Tissues containing type I collagen
XV	Many tissues
XVI	Many tissues
XVII	Skin hemidesmosomes
XVIII	Many tissues
XIX	Rhabdomyosarcoma cells

1.3.2 Dermal Collagen

Collagen is the most abundant constituent of dermal connective tissue. Fibres are present as a finely woven network or thick bundles. The majority (85-90%) of dermal collagen is type I. To the naked eye, type I fibres are colourless, but when they are present in great numbers they appear white. Their orientation imparts a good degree of natural birefringence on polarizing microscopy (see figure 3.3). The fibres orientated parallel to each other can form thick bundles especially in the reticular dermis. Type III collagen accounts for 8-11% of dermal collagen, though it forms a higher percentage in foetal skin. Type IV is present within the lamina densa of the basement membrane. Type V is present throughout the dermis and in the lamina lucida. Type VI surrounds dermal nerves and vessels. Type VII is present in anchoring fibrils (Prockop *et al* 1995)

Dermal collagen distribution has been a topic of debate. Immunological studies suggested that type III collagen was the main collagen in the papillary dermis and periadnexal dermis, while type I collagen was located on the thick bundles of the reticular dermis (Meigal *et al* 1977). However in 1978 Epstein *et al* used a biochemical assay for type I and III collagen in human dermis cut at different depths and showed that the ratio of the two collagens was the same at all levels even discounting epidermal appendages. This finding was later contradicted by a biochemical study of calf skin (Tajima *et al* 1980) when it was shown that the amount of type III collagen in the dermis decreased with increased dermal depth. In 1983

Junqueira *et al* used silver staining, picrosirius polarization and electron microscopy and found that the thin finely woven fibres of the papillary dermis were easily distinguished from the thick collagen fibres in the reticular dermis. Studying serial sections showed the fibres in the papillary dermis were arygophyllic and demonstrated a weak green birefringence contrasting with the thick red strongly birefringent fibres of the reticular dermis. Levame and Mayer (1987) compared immunohistochemistry of types I and III collagen with Herovici's stain and found that the areas of type III collagen were mainly in the superficial dermis and adnexal structures with type I fibres in the deeper dermis.

1.4 Collagen Staining

There are many different histological techniques for staining collagen however most are variants of two methods. The first group is typified by van Gieson's method and consists of a mixture of two anionic dyes; one imparts colour to collagen and the other to cytoplasm. The second group are trichrome methods, which use two or more anionic dyes in conjunction with phosphotungstic or phosphomolybdic acid. Collagen, cytoplasm and erythrocytes are coloured differently (Gabe 1976, Kiernan1990).

1.4.1 Competition between two dyestuffs

When a section is treated with two acidic dyestuffs with sufficiently different diffusion coefficients, the more diffusible fixes into the denser structures and the less diffusible one is restricted to the looser structures. One of these is always picric acid, the other can be acid fuschin, methyl blue, indigocarmine, ponceau, thiazine red or aniline blue. (Gabe 1976, Kiernan1990)

1.4.2 Stains involving phosphotungstic or phosphomolybdic acid

These are a group of stains derived from Mallory's method that uses phosphomolybdic acid to confine stains like aniline blue, methyl blue or light green to collagen fibres only. Phosphotungstic or phosphomolybdic acids are heterpolyacids that are freely soluble in water to give strong acid solutions. They bind to tissues in aqueous or alcoholic solutions and have been referred to as colourless ionic dyes. These acids compete with acidic dyes for collagen binding in loose structures which permit their diffusion and high molecular weight particles. With these methods cartilage and some mucous secretions may stain the same colour as collagen, though the intensity of staining is reported to be less (Gabe 1976, Kiernan1990).

Table 1.2 Staining patterns seen with different connective tissue stains adapted from Gabe (1976) and Carleton (1980)

Method	**Collagen**	**Nuclei**	**Cytoplasm**
Van Gieson's	Deep red	Black	Yellow
Nuclear fast-red picro-indigocarmine	Blue	Red	Pink, grey, yellow
Mallory's	Blue	Red	Red
Masson's	Green	Black	Red
Casson's	Blue	Black	Red
Gabe's	Bluish-green	Black, red	Pink, red, greyish purple

It is interesting to note that if one reads several different accounts of these stains different authors will ascribe different colours to the various components apparently stained by the same method. None of these stains are able to discriminate between different subtypes of collagen. Few histological methods are thought to be able to differentiate between types I and III collagen, picrosirius polarization is by far the most commonly used (see 1.4.4). Herovici's stain is much less popular (see 1.4.5). Two other methods are Lillie's (Lillie *et al* 1979) that has been claimed to stain loose and dense fibres collagen fibres green and blue respectively. Shoobridge's stain (Shoobridge 1983) was a complex method that was claimed to stain reticulin fibres blue, collagen fibres deep blue and basement membranes intense deep blue. These last two methods have seldom been used since and are only mentioned for completeness.

1.4.3 Reticulin staining

Reticulin can be stained due to its carbohydrate content and should be considered with other collagen stains. It may be stained by the periodic acid-Schiff procedure (PAS). However a more distinct staining relies on the deposition of metallic silver on the fibres. Hydroxyl groups on hexose sugars are oxidised to aldehydes by potassium permanganate or periodic acid. The aldehydes then reduce the silver diamine ion to the metal. Silver diamine is formed from addition of ammonium hydroxide to silver nitrate. At this stage there is not enough silver allow adequate visibility. However more silver can be precipitated by transferring solutions to an aqueous formaldehyde solution in a process similar to photographic development (Kiernan1990). There are several variations on this method (Carleton 1980). It has also been used with Sirius red to show differential staining with type I collagen and reticulin fibres (Montes *et al* 1980). It can be stated with confidence however that this type of staining is far more technically difficult than conventional H&E or triple staining. Consequently the literature on its use as a selective reticulin stain is extremely limited.

After an appraisal of the literature it is fair to say that, at present there is still no consensus on how best to stain collagen histologically. One technique that has been used by several workers is known as picrosirius-polarization. It is appropriate to consider it in some detail since it will be used in this study.

1.4.4 Picrosirius Polarization

Sirius red was originally developed as a textile dye in the 1920s. It is an elongated molecule containing 6 sulphonic acid groups. It is 46 A long. Picric acid was a silk dye in the eighteenth century.

In 1964 Sweat *et al* demonstrated that a 0.1% solution of Sirius red in saturated aqueous picric acid selectively stained connective tissue fibres, except elastic membranes, deep red. It was found to be superior to the earlier Van Gieson's picrofuschin stain, as the colours did not fade with time. It was also noted that Sirius red stained equally well with tissues fixed in a number of different solutions.

Four years later, Constantine and Mowry (1968) found that Sirius red greatly enhanced collagen's natural birefringence when combined with polarization microscopy. They reported a bright yellow colour that allowed small fibres to be clearly visualized.

Ten years later, in 1978 Junqueira *et al* demonstrated that the combination of Sirius red staining and polarization microscopy could differentiate between collagen types I, II and III. Samples from humans and other vertebrate species were collected and fixed in Bouin's solution. They were stained for 30 minutes in a 0.1% solution of Sirius red in saturated aqueous picric acid. Type I collagen was said to display a brilliant orange, yellow or red colour when viewed under crossed polarising filters. Type II collagen showed either a blue or light yellow colour depending on the orientation of the fibres. Type III collagen was seen as thin green fibres besides regions of thick bright yellow fibres, supporting the idea of type III collagen being mixed with type I collagen. The green colour was much less intense than the yellow and only observed when "very intense illumination" was used. Consequently these investigations in 1978 established that this combination of Sirius red, picric acid and polarisation microscopy could be used, but practical difficulties were still present as it was not clear how the method actually worked.

To try and explain the mechanism of action of Sirius red a number of experiments were carried out (Junqueira *et al* 1979). It was thought that as collagen is a basic protein the sulphonic groups of the dye might interact at low pH with the amino groups of lysine and hydroxylysine and the guanidine groups of arginine. These groups were blocked in specimens either by deamination with nitrous acid, which reduced the uptake of Sirius red to 43%. Chlorination with sodium hypochlorite reduced dye uptake to 15%. Acetylation with pyridine-acetic anhydride reduced the staining to 17%. This suggests that the reaction between Sirius red and collagen is between the sulphonic groups of the dye and the basic groups of the protein. When picric acid was omitted from the staining solution all tissue components stained red. It is thought that picric acid blocks the staining of non-collagenous structures by Sirius red. In addition to the uptake of the dye it was considered how the dye increased birefringence. It is thought that the elongated dye molecules attach to collagen in such a way that their long axes are parallel. The increased birefringence of collagen was quantified as greater than 700% when light intensities of slides stained with Sirius red or picric acid only were compared.

The conditions for optimal staining were determined in a series of experiments varying different parameters. This results with a concentration of Sirius red of 0.1%. The concentration of picric acid was found not to be critical. Staining saturation was reached at 1 hour. Greatest staining intensity was reached at pH 2.

Using solutions of known concentrations of pure collagen types I, II and III spread and dried onto glass slides and stained with Sirius red it was found that 126 molecules of Sirius red bind with each collagen molecule (Junqueira *et al* 1979).

Montes *et al* (1980) compared picrosirius-polarization with electron microscopy and silver impregnation methods to examine reticular fibres in several different organs in different mammals. He found that as the different fibres were localized in the tissue sections it was possible to differentiate between thin, pale, green, weakly birefringent reticular fibres and the thick, red, strongly birefringent collagen fibres. The distribution of the reticular fibres corresponded with fibres that stained positively with silver impregnation techniques on serial sections. This was further confirmed with electron microscopic studies. It is however important to note that this study did not include skin.

`One important finding of these experiments was that it was shown that increasing thickness of tissue sections resulted in a gradual shift in colour from greenish in thinner sections to yellow and red as tissue thickness increased. The degree of birefringence also increases with tissue section thickness. This is most noticeable where there are folds in the section. The optimal tissue section thickness has been shown to be 5-7μm. (Junqueira *et al* 1982)

It has never been claimed that a specific interaction occurs between picrosirius and different collagen types. The differences in colour and intensity of birefringence shown by collagen types I, II and III were initially thought to be due to fibre thickness. Experiments showed that decreasing fibre size resulted in a reduced intensity of birefringence and a colour shift from red to yellow to green. (Perez-Tamayo *et al* 1980) This idea has also been suggested when comparing the colour of native fibrillar collagen with formalin fixed tissue stained with Sirius Red (Lopez-De Leon *et al* 1985). Dayan *et al* (1989) strengthened this idea showing that the different colours are not solely dependant on fibre diameter, but also due to the different patterns of their physical aggregation. In this study 12 different types of thin (8 μm or less) and 12 thick (1.6-2.4 μm) pure collagen I, II, and III fibres were subjected to routine histological processing and stained with the picrosirius polarization method. It was shown that the colours of all fibres displayed great variability, on a scale ranging from green to yellow and orange to red.

It is fair to say that the picrosirius polarization method has undoubtedly greatly aided our understanding of collagen biology. There are currently over 100 citations on PubMed or Medline involving its use. It has been used to study the arrangement of different collagen subtypes in different tissues as outlined earlier. Its scope of application in the study of healthy tissue includes medial collagen organization in human arteries (Canham *et al* 1991). Age related changes of the human heart (Gazoti-Debessa *et al* 2001) distribution of collagen in the human vocal fold (Madruga de Melo *et al* 2003). It has been used to study disease processes including capsular invasion of follicular thyroid neoplasms (Koren *et al* 2001) connective tissue nevi collagens (Trau *et al* 1991). It has also been used to provide histological information on various experimental models including collagen alignment in undermined and non-undermined skin stretched with a skin stretching device {Melis *et al* 2002} scar maturation in intralesional cryotherapy for hypertrophic scars and keloids (Har-Shai *et al* 2003). Aging of wound healing in an experimental model of mice (Hiss 1988). These are a few examples that illustrate the scope of a histological stain that can differentiate between different collagen subtypes, albeit with the complexities of having to use polarization microscopy to “see” the staining patterns.

There is an alternative to picrosirius-polarization and this is known as Herovici’s stain. For the reader who has not come across it before, a few words are appropriate.

1.4.5 Herovici’s Stain

Herovici developed a stain in 1961 with separate components to stain nuclei, cytoplasm and collagen fibres. This technique revealed a differential staining pattern of collagen fibres, with smaller finer fibres staining blue and thicker fibres staining red (Herovici 1961). This technique was modified two years later to enhance nuclear and cytoplasmic staining however the collagen staining remained the same (Herovici 1963).

Levame and Mayer (1987) showed that the blue staining fibres corresponded to type III collagen and the red fibres to type I collagen. Use of Herovici’s stain in both experimental medical sciences and for routine pathological analysis has been relatively limited compared with other connective tissue stains, including picrosirius polarization.

Fitzgerald *et al* (1996) studied normal skin sections with Herovici's and found a distinctive, reproducible staining pattern. The papillary dermis demonstrated thin blue fibres in the subepidermal region with an absence of red staining fibres. As dermal depth increased so did the amount of red staining fibres. Some blue fibres coexisted with the red fibres in the reticular dermis.

Herovici's stain has been used to study different aspects of wound healing, either on its own or as an adjunct to other research techniques. Mackay *et al* (1972) studied the histology of reconstruction of rabbit fallopian tube and different time intervals, demonstrating the replacement of muscle by fibrous tissue. Griffioen *et al* (1987) studied repair of different types of surgically created cleft palates in rabbits. Lamme *et al* (1998) examined dermal substitute degradation of an artificial dermal substitute seeded with fibroblasts in experimental porcine full thickness wounds. Ranne *et al* (2000) studied dermal healing inn denervated rat groin flap wounds. More recently Rawlins *et al* (2006**)** have assessed the ratio of type I and III collagen in scar tissue from surgical wounds, keloids and burns scars using Herovici's stain and image analysis software.

Other conditions studied include Dupuytrens disease (Fitzgerald *et al* 1995) and synovial tissue in rheumatoid arthritis (Furuzawa-Carballeda *et al* 2002).

As with picrosirius-polarization we can see the diverse potential of a histological stain that differentiates between collagen subtypes, although less popular it is curious that the two staining methods have not been compared. One of the objectives of this thesis will be to undertake such a comparison.

Chapter 2 Materials and Methods

2.1 Basic Procedures and Tissue Processing

2.1.1 Poly-L-lysine Coated Slides

Slides (Menzel-Glaser, Braunschweig, Germany) cleaned in Pyroneg in distilled water 5 minutes

Rinse several times in distilled water until stops bubbling

100% alcohol 5 minutes

Drying cabinet 5-10 minutes

0.01% solution poly-L-lysine (Sigma-Aldrich, St Louis, USA) in distilled water 5 minutes

Drying cabinet 2 hours at 60C

2.1.2 Phosphate Buffered Saline (PBS) Solution

1000ml Distilled water

8g NaCl

0.2g KCl

1.44g Na_2HPO_4

0.24g KH_2PO_4

NaOH titrated to pH 7.4

2.1.3 Tissue Fixation

Cadaveric tissues samples are orientated, pulled out length and attached to thick card with dressmaker pins and placed in 10% solution of formaldehyde in PBS (formaldehyde 38%, VWR, Poole, UK) for 1 week. During wax embedding a marker stitch was used to facilitate tissue orientation.

Operative tissue samples were placed directly in 10% solution of formaldehyde in PBS (formaldehyde 38%, VWR, Poole, UK) for minimum 48 hours

2.1.4 Cadaveric Embalming

Embalming fluid (Leeds Formulation, Vickers Laboratories, Pudsey, UK)

1 litre contains

Industrial Methylated Spirits 99% 756ml

Phenol 80% 125ml

Formaldehyde 40% 40ml

Glycerol 22ml

Water 57ml

Approximately 50 litres are introduced via a cannula in the carotid artery over 2-3 days.

2.1.5 Wax Embedding

Automated Programme

70% Alcohol 3 hours

80% Alcohol 3 hours

90% Alcohol 3 hours

100% Alcohol 1 hour

100% Alcohol 2 hours

100% Alcohol 2 hours

Histoclear 1 hour

Histoclear 2 hours

Histoclear 2 hours

Wax (paraplast) 2 hours

Wax (paraplast) 2 hours

Total time 23 hours

2.1.6 Tissue sectioning

Tissues were carefully embedded in wax and cut into sections 5 μm thick in a plane perpendicular to the epidermal surface. In addition a number of tissues were orientated to allow sectioning at a plane parallel to the epidermal surface. Sections were placed onto poly-L-lysine coated slides in a water bath allowed to dry overnight at room temperature.

2.2 Staining Protocols

2.2.1 Picrosirius-Polarization

Dewaxing:

Histoclear 5 minutes

Histoclear 5 minutes

100% Ethanol 5 minutes

100% Ethanol 5 minutes

50% Ethanol 5 minutes

Distilled water 5 minutes

Sirius red F3B (RA Lamb, Eastbourne, UK) in saturated aqueous picric acid solution at 0.1% (w/v) concentration

1 hour

Wash tap water

Dehydration:

Distilled water 5 minutes

70% Ethanol 5 minutes

100% Ethanol 5 minutes

100% Ethanol 5 minutes

Histoclear 5 minutes

Histoclear 5 minutes

Mount slides with histomount (Agar Scientific, Stanstead, UK) and coverslips (Menzel-Glaser, Braunschweig, Germany)

2.3 Variations of the picrosirius polarization method

A number of variations of the picrosirius polarization method were tried. These were:

2.3.1 Picrosirius Polarization with Haematoxylin Counterstain

Dewaxing as in 2.2.1

Sirius red F3B (RA Lamb, Eastbourne, UK) in saturated aqueous picric acid solution at 0.1% (w/v) concentration

1 hour

Wash tap water

Harris' Haematoxylin 5 minutes

Wash tap water

Dehydrate and mount slides as in 2.2.1.

2.3.2 Picrosirius Polarization with Acetic Acid

Dewaxing as in 2.2.1

Sirius red F3B (RA Lamb, Eastbourne, UK) in saturated aqueous picric acid solution at 0.1% (w/v) concentration 1 hour

Wash tap water

0.1% Acetic acid 30 mins

Wash distilled water

Dehydrate and mount slides as in 2.2.1.

2.4 Herovici's Staining

2.4.1 Herovici's Solutions

Make up the following solutions {Herovici 1963}

A:Celestine blue 1.25g

Iron Alum 15g

Distilled water 300ml

Heat and boil for 3 minutes

When cool add 60ml glycerol

B:5% aqueous solution aluminium sulphate

Heat and add 100ml 1% alcoholic haematoxylin

Boil 3 minutes

When cool add 200ml distilled water

20ml 4% aqueous $FeCl_3$

2ml concentrated HCl

C:Metanil Yellow 1.25g

Distilled water 300ml

Acetic acid 25 drops

D:Distilled water 300ml

Acetic acid 25 drops

E:Distilled water 300ml

10 drops saturated aqueous Li_2CO_3

F:

Solution 1.

Methyl blue 0.15g

Distilled water 150ml

Solution 2.

Acid fuschin 0.2g

Saturated aqueous picric acid 150ml

Mix solutions 1 and 2, add 30ml glycerol and 0.15ml saturated aqueous Li_2CO_3

2.4.2 Herovici's Staining Method

Dewaxing as 2.2.1

Solution A 5 minutes

Wash tap water 2 minutes

Solution B 5 minutes

Wash tap water 2 minutes

Solution C 2 minutes

Solution D 2 minutes

Wash tap water 2 minutes

Solution E 2 minutes

Solution F 2 minutes

1% Acetic acid 2 minutes

Dehydration:

100% Ethanol 1 minute

100% Ethanol 1 minute

Histoclear 2 minutes

Histoclear 2 minutes

Mount slides as in 2.2.1

2.5 Variations of Herovici's Method

A number of variations of Herovici's method were tried.

These were:

2.5.1 Methyl Blue in Distilled Water

Make up solutions A to E as in 2.4.1

Dewaxing as in 2.2.1

Solution A 5 minutes

Wash tap water 2 minutes

Solution B 5 minutes

Wash tap water 2 minutes

Solution C 2 minutes

Solution D 2 minutes

Wash tap water 2 minutes

Solution E 2 minutes

Methyl blue 0.3g in 300ml distilled water

2 minutes

1% Acetic acid 2 minutes

Dehydration as in 2.4.2

Mount slides as in 2.2.1

2.5.2 Methyl Blue in Picric acid

Dewaxing as in 2.2.1

Solution A 5 minutes

Wash tap water 2 minutes

Solution B 5 minutes

Wash tap water 2 minutes

Solution C 2 minutes

Solution D 2 minutes

Wash tap water 2 minutes

Solution E 2 minutes

Methyl blue 0.3g in 300ml picric acid

2 minutes

1% Acetic acid 2 minutes

Dehydration as in 2.4.2

Mount slides as in 2.2.1

2.5.3 Sirius Red in Place of Acid Fuschin

Dewaxing as in 2.2.1

Solution A 5 minutes

Wash tap water 2 minutes

Solution B 5 minutes

Wash tap water 2 minutes

Solution C 2 minutes

Solution D 2 minutes

Wash tap water 2 minutes

Solution E 2 minutes

Methyl blue 0.15g in 150ml distilled water

Sirius red 0.15g in 150ml picric acid

Mix together and add 30ml glycerol and 0.15ml saturated aqueous Li_2O_3 2 minutes

1% Acetic acid 2 minutes

Dehydration as in 2.4.2

Mount slides as in 2.2.1

2.6 PAS staining

Dewaxing as in 2.2.1

Wash tap water 5 mins

1% periodic acid 10 mins

Wash distilled water 5 mins

Schiff’s reagent 10 mins

Wash tap water 5 mins

Dehydration:

Distilled water 2 mins

70% Ethanol 2 minutes

100% Ethanol 2 minutes

100% Ethanol 2 minutes

Histoclear 2 minutes

Histoclear 2 minutes

Mount slides as in 2.2.1

2.7 Tissue Samples

2.7.1 Rat Wounds

Sections of full thickness rat wounds (n=4) were obtained from archived specimens. The tissues were from full thickness dorsal skin wounds (original size 15 X 15mm) 14 days after infliction. The specimens were in the middle of the wound in a transverse direction.

2.7.2 Rat Kidneys

Normal rat kidneys (n=4) were obtained from 1 day old rats.

2.7.3 Operative Samples

Samples of normal skin (n=38) were obtained from surgical procedures including abdominoplasty, reduction mammoplasty, otoplasty and blepharoplasty procedures. In addition archived samples of mature scar tissue (n=6) from a variety of causes were also studied. Tissue fixation was as described in section 2.1.3.

2.7.4 Cadaveric Samples

Skin samples taken from embalmed cadavers (n=58) for anatomical study by medical students were studied. Samples were carefully orientated as described in section 2.1.3 to facilitate accurate comparisons as described in sections 2.7 – 2.10. Tissue fixation was as described in section 2.1.3.

Different regions of the body were studied, namely deltoid (n=9), abdomen (n=13), pre-sternal area (n=10), post-auricular (n=5), earlobe (n=12) and upper eyelid (n=9).

2.8 Microscopy and Photography

Slides were examined using a Nikon Eclipse 80i microscope and camera. Photographs were taken on a PC using ACT-2U image capture software. For polarizing microscopy polaroid filters crossed perpendicular to each other were used.

2.9 Epidermal Appendage Counts

For the cadaveric skin only, 5 random fields were examined on each slide at X20 magnification. Counts were made of hair follicles, sebaceous glands and sweat glands in each field. The total numbers and mean of each were determined for different body regions.

2.10 Epidermal thickness

Photographs of all skin samples at X20 magnification, with a scale bar, were taken and printed onto A4 paper. 5 vertical measurements of the epidermis were taken at points that excluded epidermal appendages, but were otherwise randomly selected. Using the scale bar the actual epidermal thickness was calculated and the mean was determined.

2.11 Collagen fibre orientation

Photographs of all cadaveric skin samples were taken at X20 magnification. Squares measuring 15mm were printed onto acetate. 5 areas of deep dermis that excluded epidermal appendages were otherwise randomly selected. Collagen fibres were traced onto the acetate using different colours for fibres parallel, perpendicular or oblique to the plane of the section. Two counts were made for each sample and the mean determined.

Chapter 3 - Results

3.1 Picrosirius Polarization

3.1.1 Picrosirius-Polarization without Counterstain

Rat wounds

These sampled the full thickness dorsal skin through the entire width of the wound including edges of normal skin. 4 samples were studied. Within these tissues there were distinct areas of normal dermis and areas of granulation tissue. In addition numerous epidermal appendages particularly hair follicles and sebaceous glands were seen.

Under crossed polarized filters granulation tissue was visible as thin weakly birefringent fibres that varied in colour from green and yellow to orange and red (Fig 3.1). Some of this colour variability was seen on the same fibres. Normal dermis consisted of a very thin superficial region beneath the epidermis and surrounding epidermal appendages that was of a very similar appearance to granulation tissue with fibres orientated parallel to the epidermis. The deeper dermis mainly comprised thick red strongly birefringent fibres organized into a basket weave pattern. Some thin green and yellow weakly birefringent fibres were seen to coexist in the deeper dermis. Some weak birefringence was seen in areas of the stratum corneum.

When viewed under normal light microscopy granulation tissue appeared as thin pale red and pink fibres (Fig 3.2). Normal dermis appeared as thick red fibres indistinguishable from any thin fibres that may be present.
Cytoplasmic staining in the epidermis and all other structures was pale pink. Nuclei appeared pink.

Fig 3.1 Rat wound stained with picrosirius solution and viewed under crossed polarized filters at X20 magnification. Thick, red and yellow strongly birefringent fibres of normal reticular dermis are visible on the right of the picture. Contrast this with the thin red, green and yellow weakly birefringent fibres of the granulation tissue on the left.

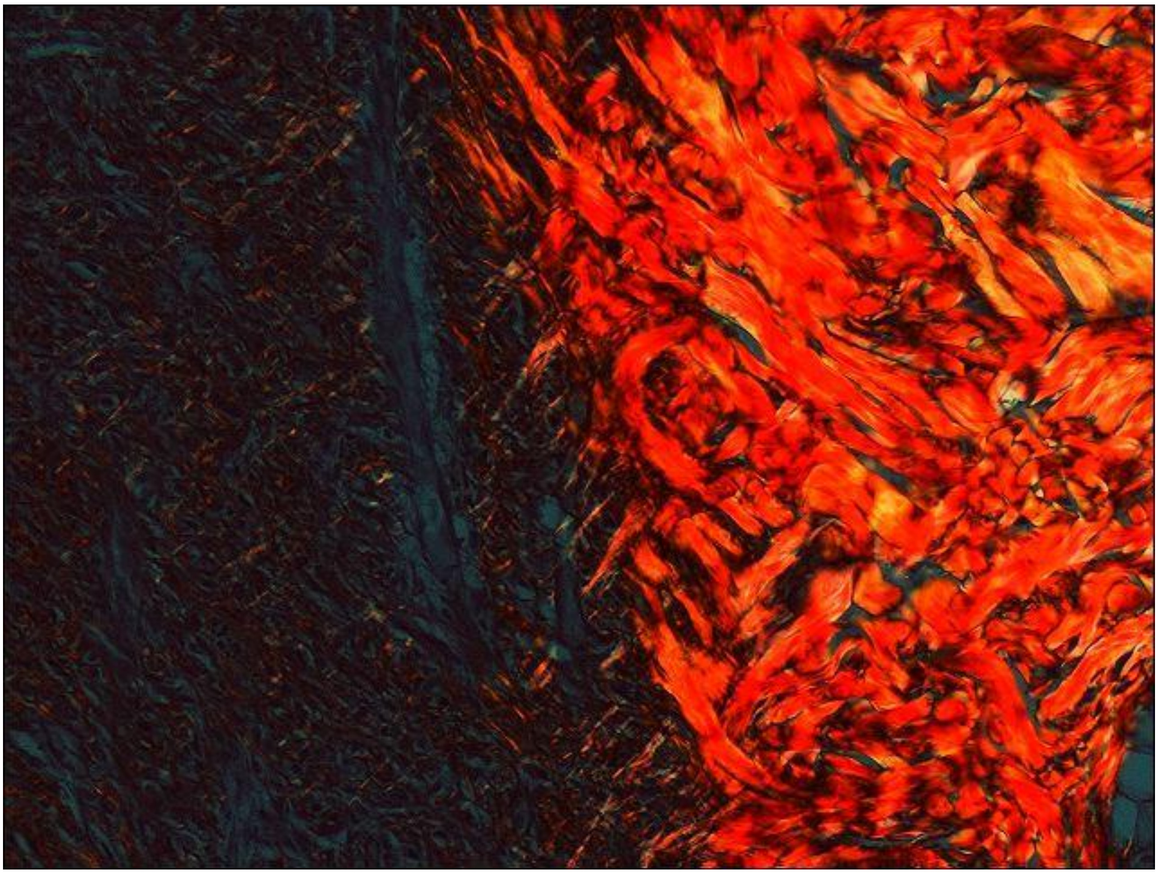

Fig 3.2 A section from the same tissue block of rat wound stained with picrosirius solution viewed under normal microscopy. Note the pale pink staining of the granulation tissue on the left. Compare this to the intense red staining of normal dermal collagen on the right. Also note the dark red staining of the superficial epidermis.

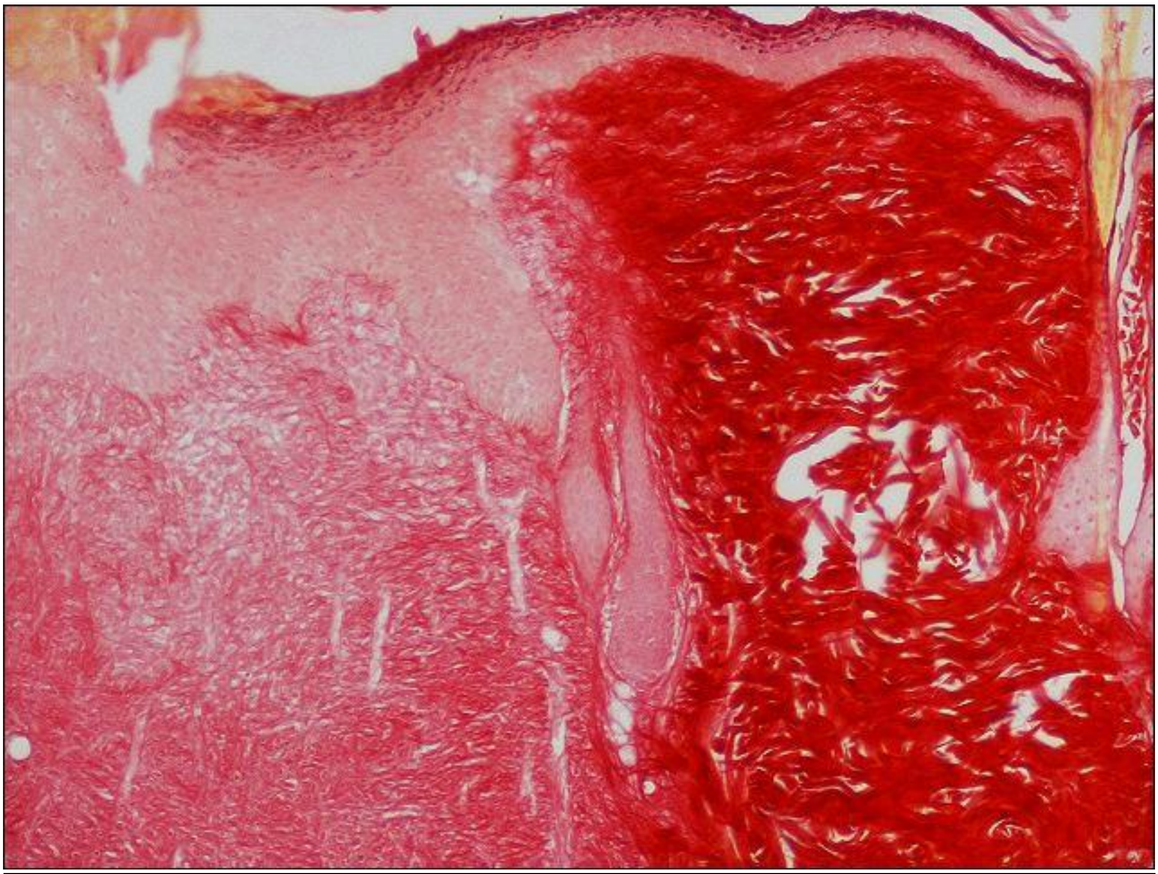

Normal human skin

Under polarizing filters

Most areas of skin studied followed the same general staining pattern (Figs 3.3, 3.4). The exception is skin from upper and lower eyelids and this will be discussed separately.

Superficial dermis

Thin green yellow and red weakly birefringent fibres were present in a random arrangement and were most concentrated in the subepidermal and superficial papillary dermis.

Deep dermis

Thick red strongly birefringent fibres were present in a basket weave arrangement. A large proportion of fibres displayed variability of colour, being red in the centre but yellow on the periphery. Some thin red and green weakly birefringent fibres coexisted with thicker fibres.

Adnexal dermis

Thin red orange yellow and green fibres surrounded epidermal appendages and blood vessels in a concentric pattern (Fig 3.5).

Fig 3.3 Human abdominal skin stained with picrosirius solution and viewed under crossed polarized filters at X20 magnification. Observe the thin yellow, red, green and orange fibres in the superficial dermis (S). Contrast this with the thick red fibres of the deeper dermis (D). Also note the birefringence of the Epidermis (E).

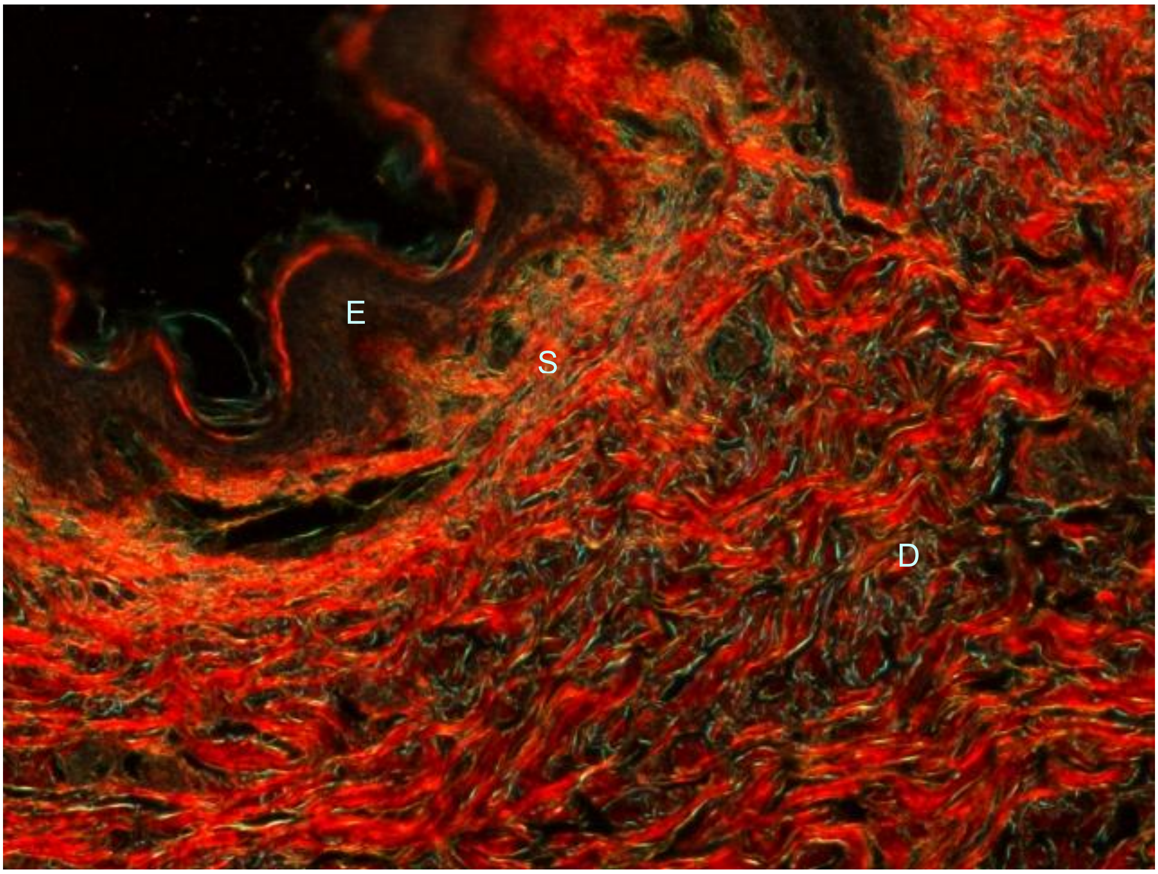

Fig 3.4 Human lower eyelid skin stained with picrosirius solution viewed under crossed polarizing filters at X20 magnification. Note the concentric pattern of thin weakly birefringent fibres surrounding a hair follicle (yellow arrow). Also note weak birefringence of hair shaft (pink arrow) and the birefringence of stratum corneum (blue arrow).

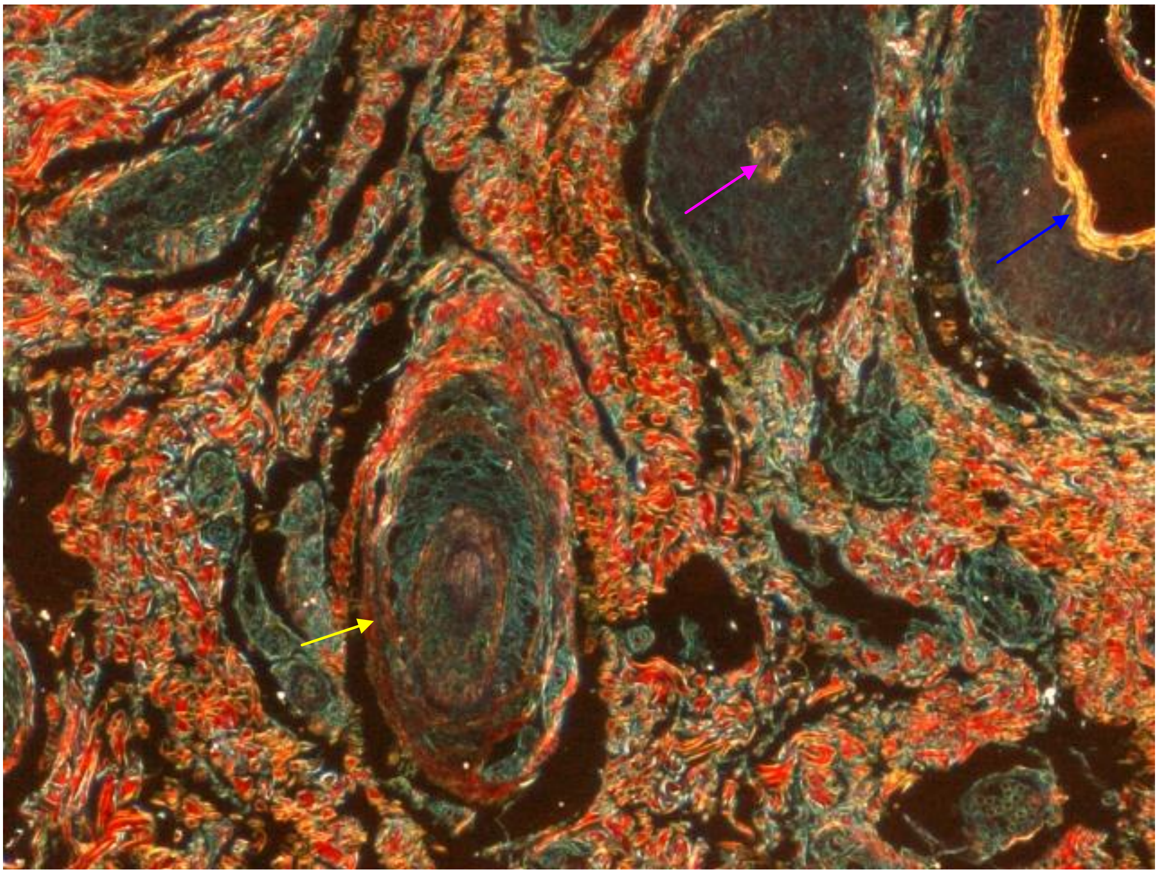

Eyelid skin

Thin red yellow and green weakly birefringent fibres were present in a random pattern. A number of thin fibres exhibited multiple colours. Occasional medium sized red strongly birefringent fibres were seen, but these were not as thick as the deep dermal fibres present in other areas of the body. Some of these red fibres also displayed yellow peripheries. The general appearance of the dermis was more uniform and did not display very different characteristics of the deep and superficial dermis as in other regions of the body. A concentric pattern of weakly birefringent fibres surrounded epidermal appendages (Fig 3.4).

Human scar tissue

Areas of normal skin were seen whose appearances were the same as previously reported. Human mature scar tissue appeared as thick red strongly birefringent fibres. They were arranged into compact parallel bundles. They exhibited much less colour variability than fibres in normal skin (Fig 3.5).

Fig 3.5 Human mature burn scar stained with picrosirius solution and viewed under crossed polarized filters at X20 magnification. Note the parallel appearance of the thick collagen fibres, and contrast this with the basket-weave arrangement seen in Fig 3.3.

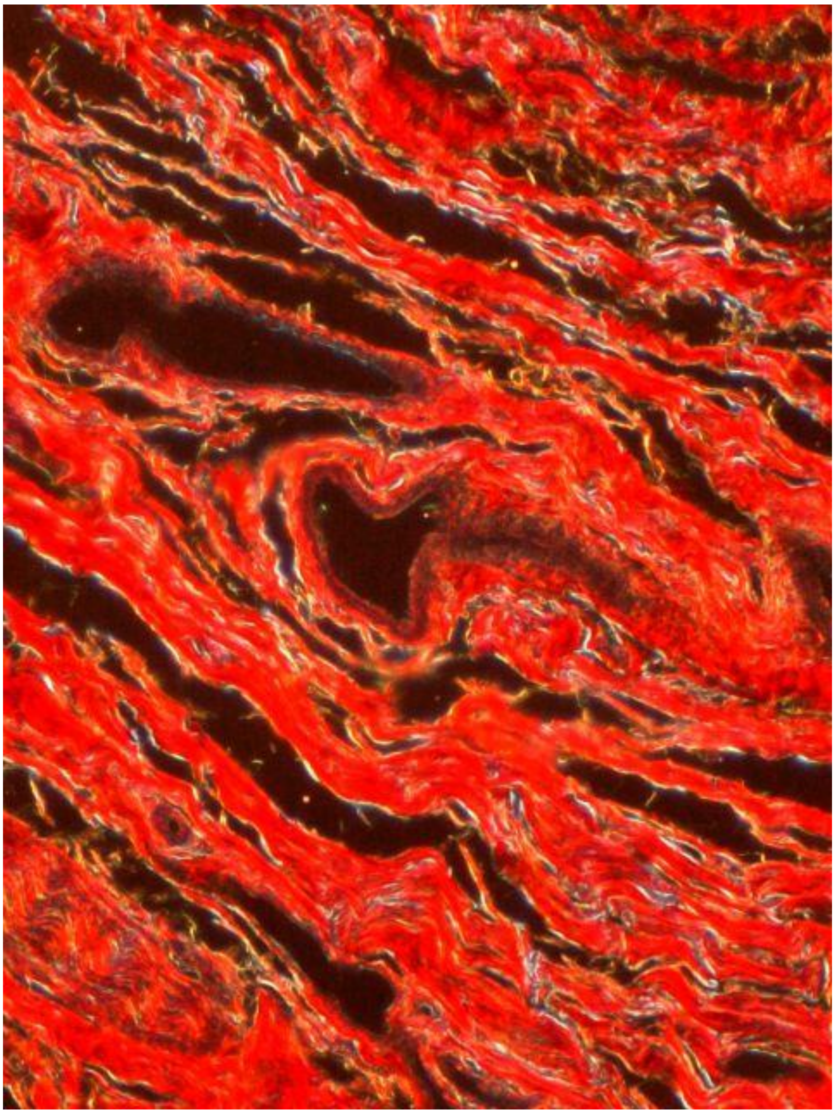

Additional comments

The stratum corneum displayed red, weakly birefringent fibres. Some hair shafts displayed a weak green birefringence (Fig 3.4).
When comparing slides viewed with and without crossed polarizers; less regions appeared to be stained under crossed polarizing filters in comparison to those seen with normal light microscopy. This can be seen comparing the granulation tissue in figs 3.1 and 3.2.

3.1.2 Picrosirius Polarization with Haematoxylin Counterstain

When viewed under normal light microscopy the collagen fibres in the dermis and granulation tissue were thick or thin deep red fibres. Cytoplasm and keratin was light purple and nuclei were dark purple (Fig 3.6).

Under crossed polarized filters the appearances were generally similar to the samples stained without haematoxylin except that the colour of the green and yellow fibres was less intense and there were fewer of these fibres visible. Birefringence was still evident in the stratum corneum. Colour variability within individual fibres was still present , but slightly less pronounced than samples stained without haematoxylin. Thick fibres sometimes appeared a deeper shade of red/ less orange (Fig 3.7).

The staining patterns seen both with and without crossed polarizing filters were consistent among all samples studied.

Fig 3.6 Human breast skin stained with picrosirius solution and a haematoxylin counterstain viewed under normal light microscopy at X10 magnification.

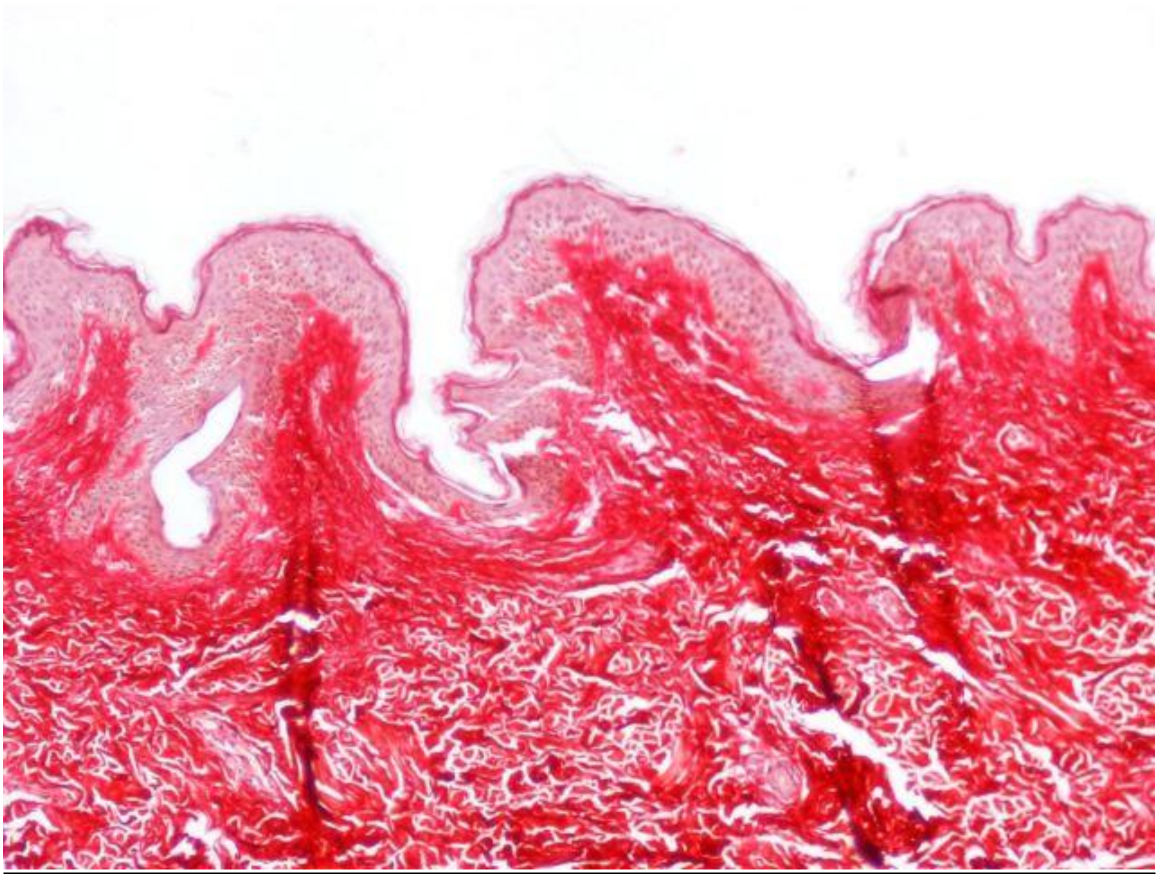

Fig 3.7 Human breast skin stained with picrosirius solution and a haematoxylin counterstain viewed under crossed polarizing filters at X10 magnification. Compared with figs 3.3 and 3.4 the thin green fibres are less intensely stained and numerous.

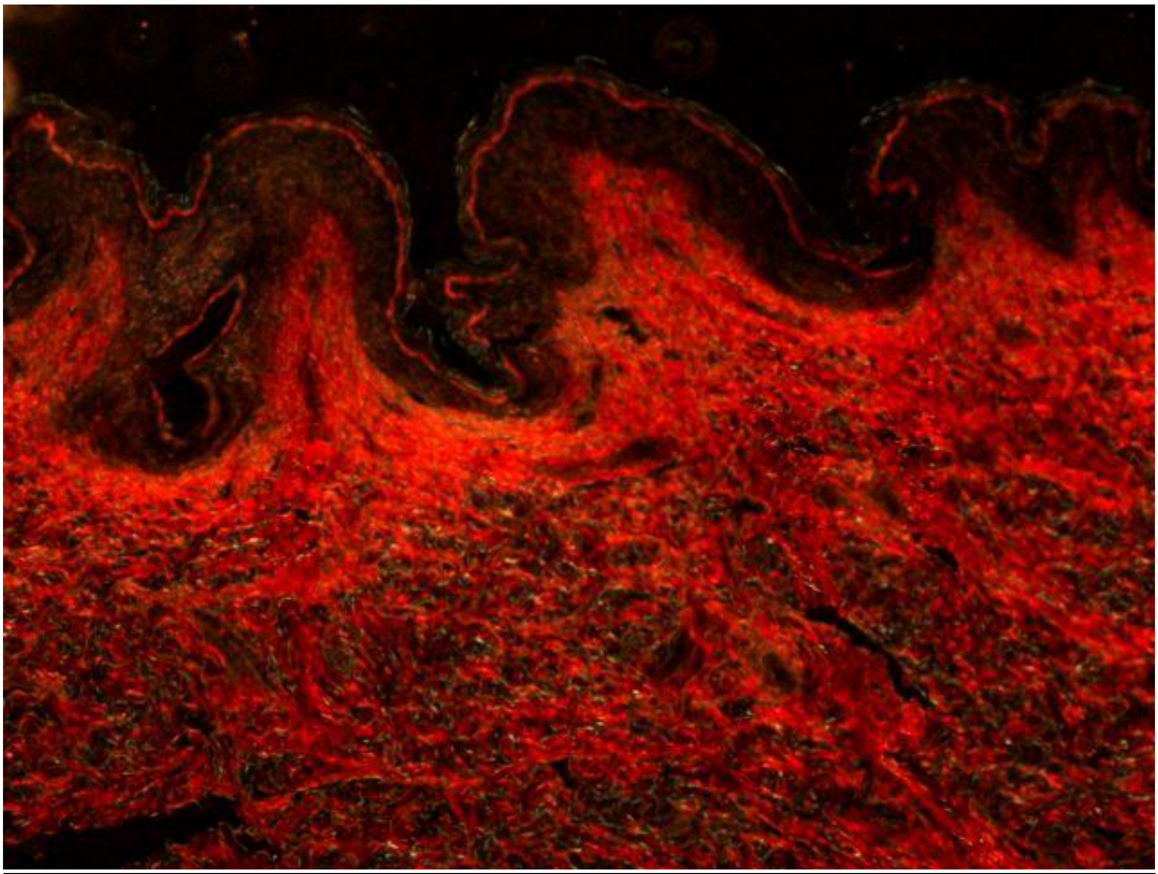

3.1.3 Picrosirius Polarization with Addition of 30 Minutes Acetic Acid

A number of samples (n=10) were stained with an additional step involving exposure for 30 minutes in acetic acid. Appearances were identical.

3.2 Herovici's Staining

General observations

All nuclei stained dark brown. All cytoplasm was greenish brown. Red blood cells and hair shafts appeared yellow (Fig 3.8).

Full skin thickness rat wounds

These sampled the full thickness dorsal skin through the entire width of the wound including edges of normal skin. 4 samples were studied. Within these tissues, there were distinct areas of normal dermis at the edges and between this, areas of granulation tissue. In addition numerous epidermal appendages particularly hair follicles and sebaceous glands were seen in the normal dermis, but not the granulation tissue (Fig 3.9).

Normal dermis consisted of a very thin superficial region beneath the epidermis and surrounding epidermal appendages that was of a very similar appearance to granulation tissue with fibres orientated parallel to the epidermis. As dermal depth increased an increasing amount of thicker red fibres coexisted with the blue fibres. The deeper dermis mainly comprised thick red fibres organized into a basket weave pattern. Some thin blue fibres were seen surrounding and parallel to epidermal appendages. The granulation tissue was visible as a network of thin blue fibres in which many blood vessels could be seen. All the collagen fibres were thin and blue.

Fig 3.8 Human abdominal skin stained with Herovici's technique (X20 magnification) demonstrating the classical staining pattern of normal skin. See main text for full details.

Fig 3.9 Rat wound stained with Herovici's technique (X10 magnification). Thin blue fibres of granulation tissue (G) can be contrasted with appearances of normal dermis (D).

Operative samples

Epidermis

Stratum corneum was seen as wavy greenish-brown fibres parallel to the skin's surface. The remainder of the epidermis was several cells deep with greenish brown cytoplasm and dark brown nuclei (Fig 3.8).

Sub-epidermal region

A narrow band of thin blue fibres forming a delicate network of randomly arranged fibres. The thickness of this region varied between samples (Fig 3.8).

Papillary dermis

The pattern seen in the immediate sub-epidermal region continues and generally these thin blue fibres predominate. Thin red fibres also become interwoven. As dermal depth increases the number and thickness of these red fibres also increases. The relative numbers of blue and red fibres varied between samples (Fig 3.8).

Reticular dermis

Mostly consists of thick red collagen fibres in a basket weave arrangement. Thin blue fibres can be seen at their periphery almost forming a sleeve around them. The transition between papillary and reticular dermis was gradual. The superficial vascular plexus appeared at different levels of this transistion in different samples (Fig 3.8).

Adnexal dermis

Thin blue and sometimes red fibres surround epidermal appendages in a concentric pattern. Thin blue fibres can be seen between the ducts of sweat glands.

Fig 3.10 Transverse section of abdominal skin through a hair follicle in the reticular dermis (X20 magnification). The adnexal dermis is clearly demonstrated surrounding the hair follicle and consists of a concentric pattern of thin, blue, type III collagen, followed by thin and then thick fibres of red type I collagen.

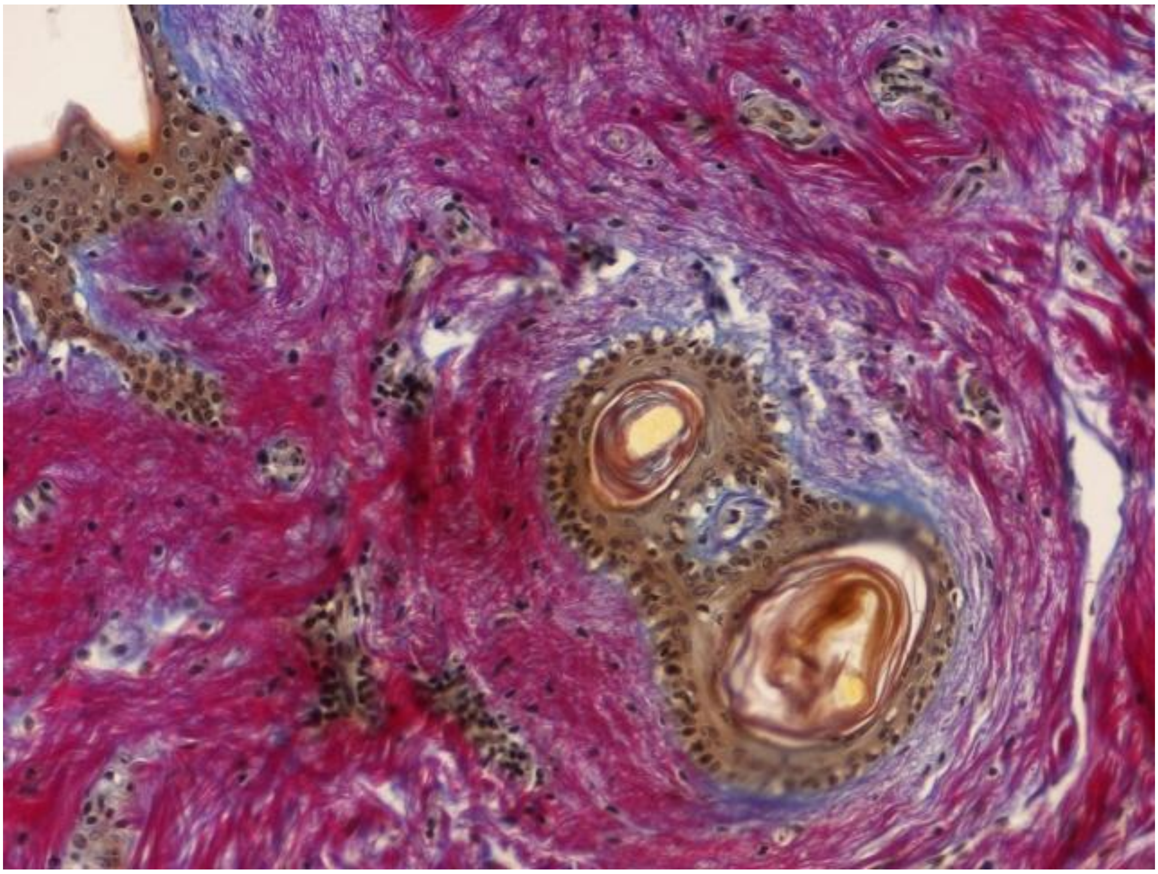

Other sites

Eyelid skin

The appearance of the epidermis and sub-epidermal regions was similar to other body sites. The superficial and deep dermis had a more uniform appearance than other sites. However the vast majority of fibres were thin and stained blue. Thin to medium sized red fibres were also present, but were not as numerous or dense as in other sites. The arrangement of the vascular plexus appeared different in eyelids compared to other regions studied owing to the number of hair follicles. Additionally the dermis appeared more vascular than other regions with vessels of increased diameter and number compared with other sites. The staining pattern around vessels and epidermal appendages was the same as in other body sites (Fig 3.11). The upper and lower eyelids appeared histologically identical.

Fig 3.11 Eyelid skin stained with Herovici's technique (X 20 magnification). See main text for details.

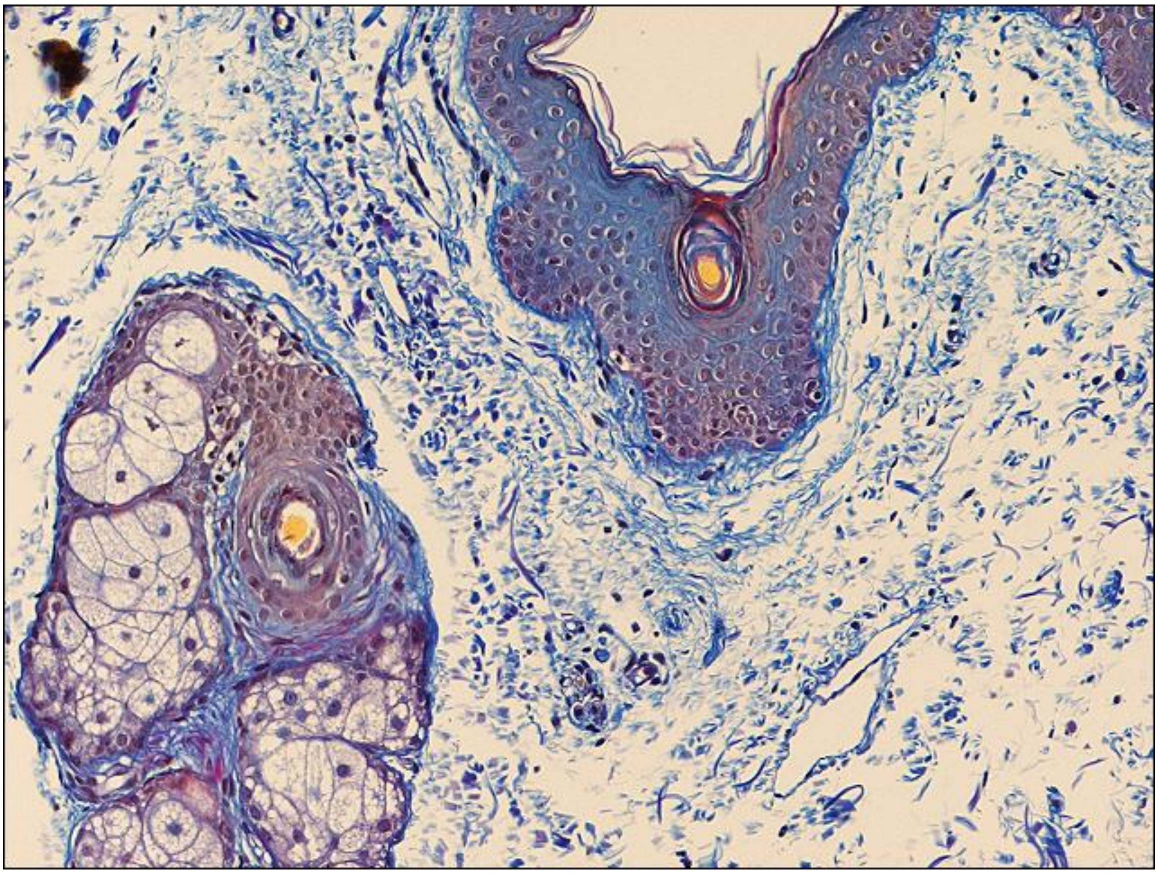

Cadaveric samples

Comparison with operative samples showed the pattern of staining was identical to that seen in operative specimens, in the eyelids and other body. Tissue preservation was excellent and fine detail was visible in both groups of samples. However, the epidermis appeared thinner and flatter and the rete ridges were less deep and pronounced. The presence and number of tissue processing artefacts was similar in both groups of samples.

Fig 3.12 Embalmed cadaveric deltoid skin stained with Herovici's technique. The staining pattern is identical to that seen in the fresh operative samples (X20 magnification).

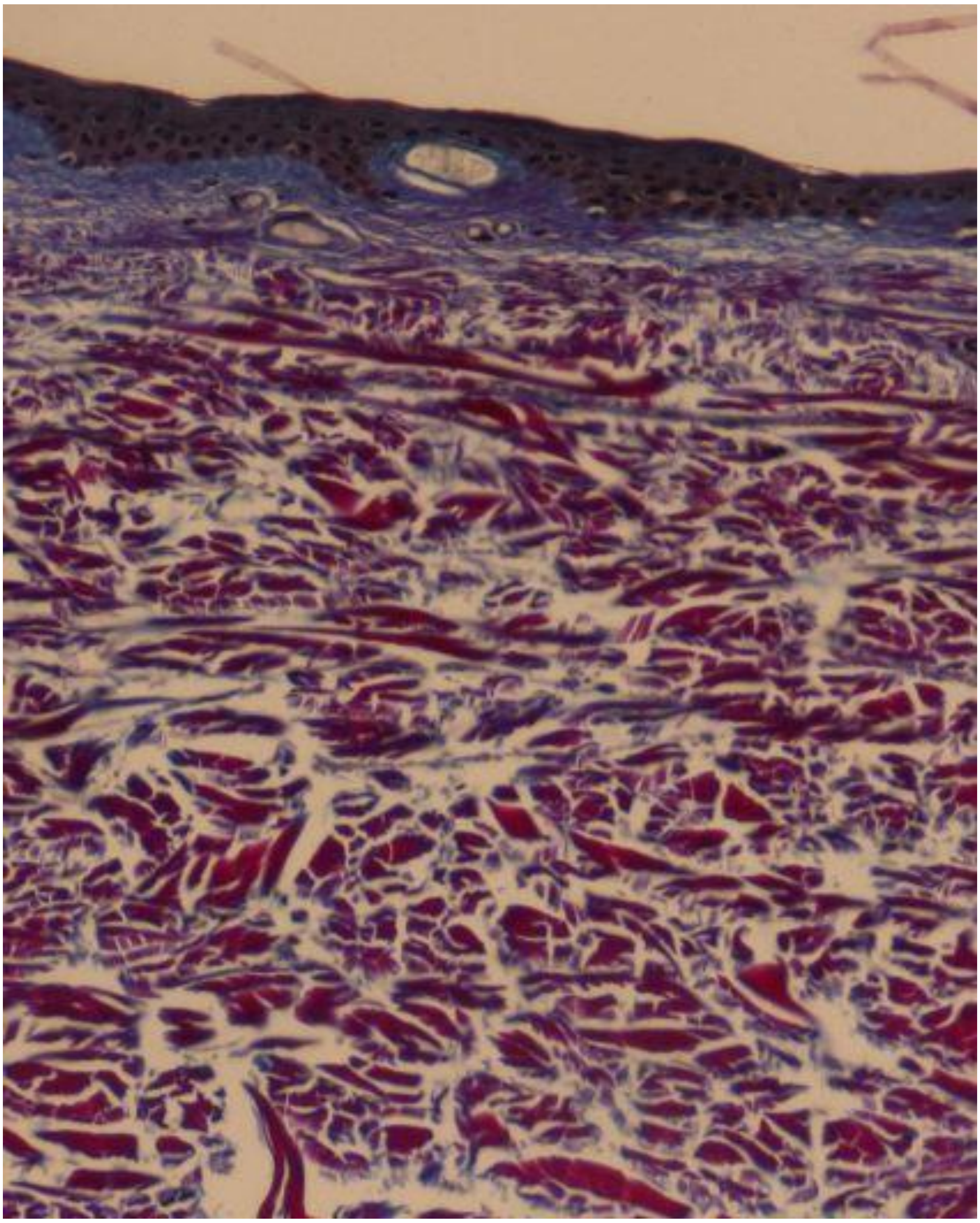

Fig 3.13 Embalmed cadaveric abdominal skin stained with Herovici's technique. The histological structure is similar to that seen in fig 3.12 (X20 magnification).

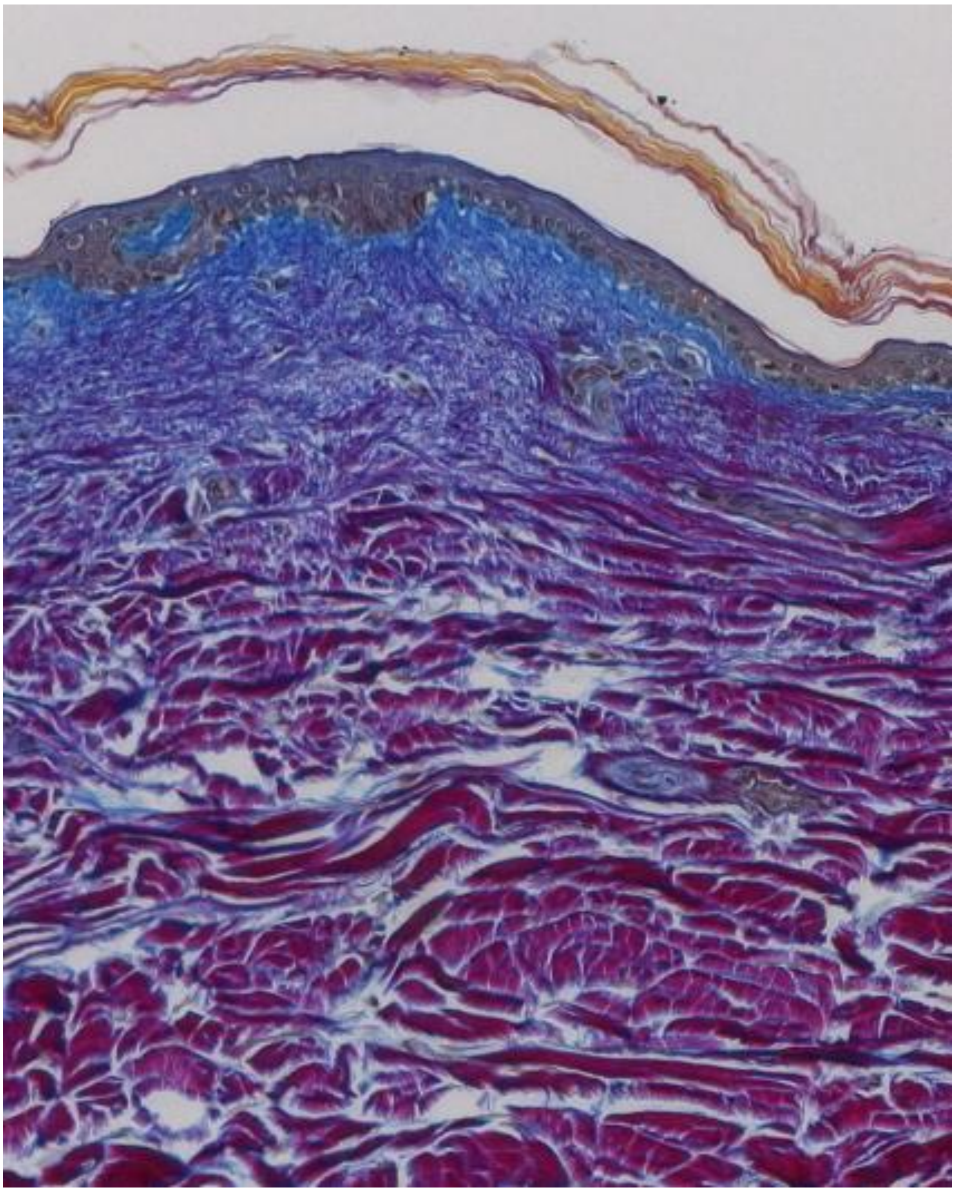

Fig 3.14 Embalmed cadaveric sternal skin stained with Herovici's technique. The histological structure is similar to that seen in figs 3.12 and 3.13 (X20 magnification).

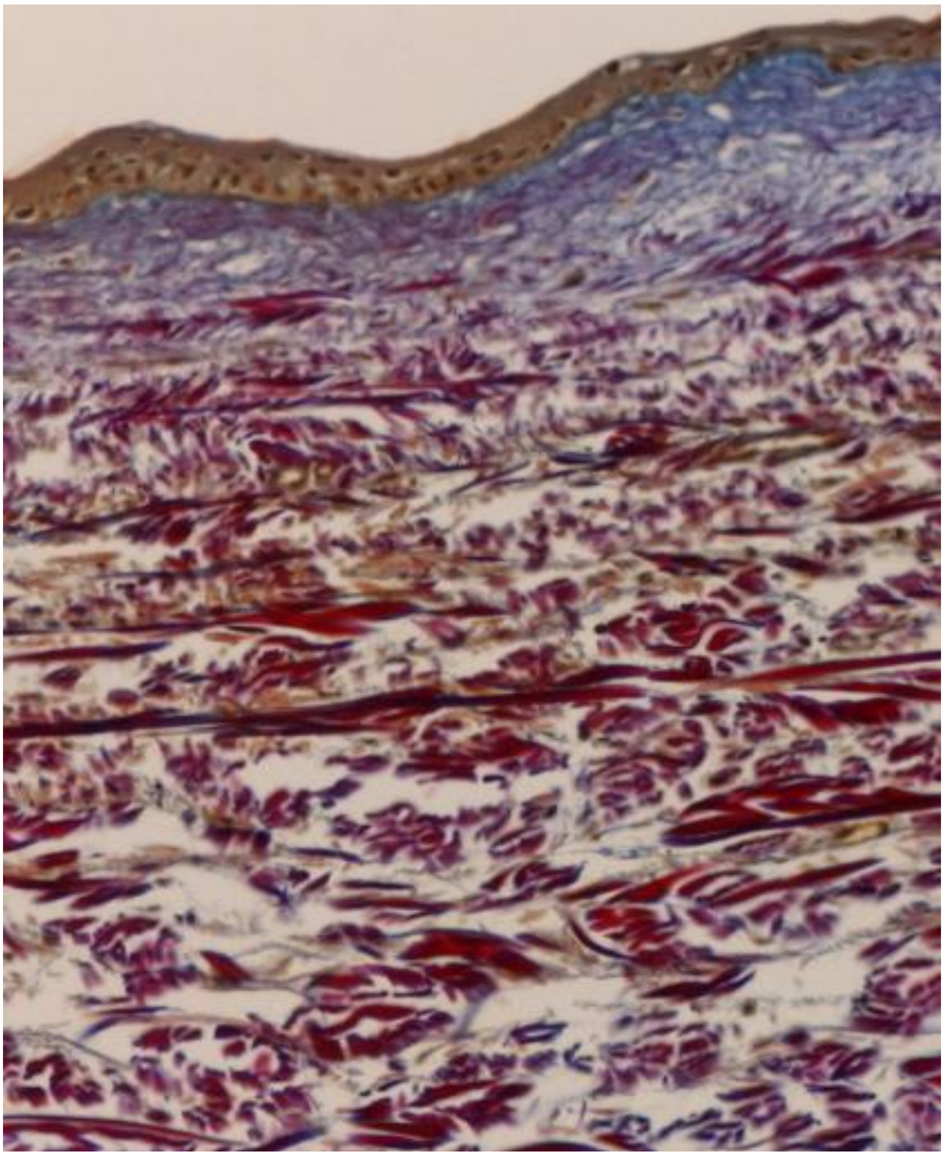

Fig 3.15 Embalmed cadaveric post-auricular skin stained with Herovici's technique. The histological structure is very different to that seen in figs 3.12, 3.13 and 3.14 (X20 magnification).

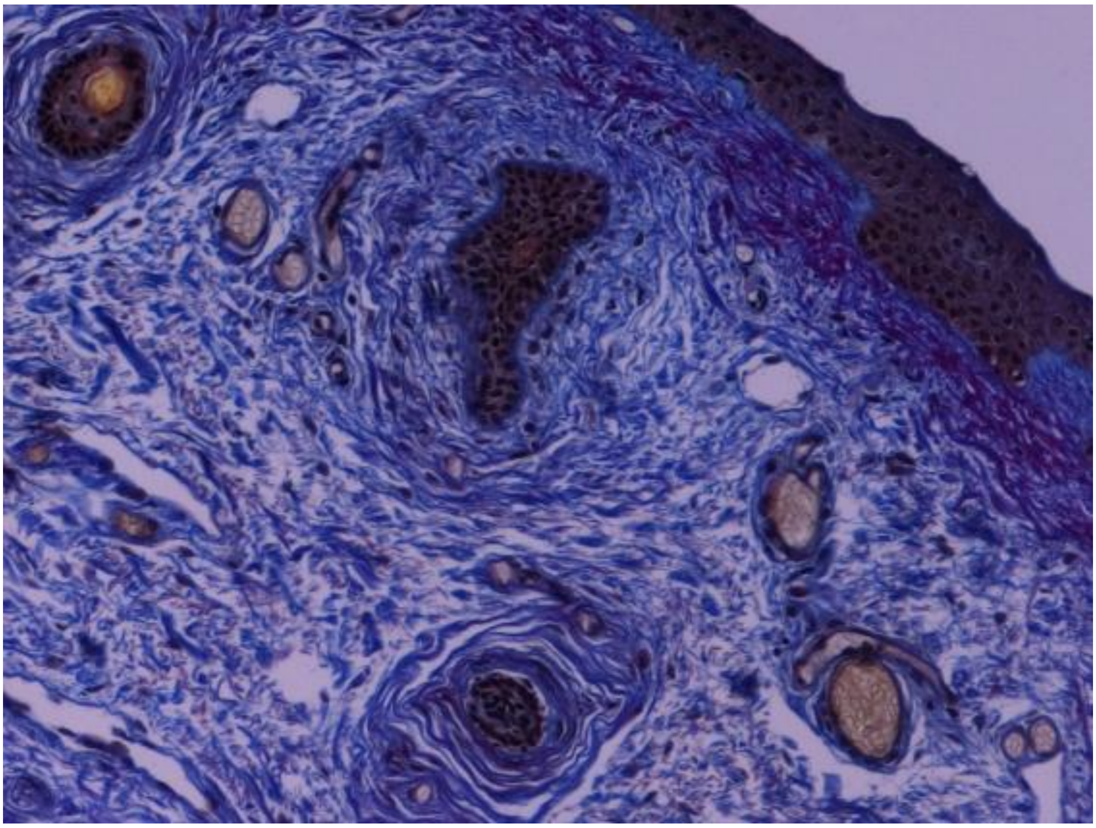

Fig 3.16 Embalmed cadaveric upper eyelid skin stained with Herovici's technique. The histological structure is identical to the operative specimen seen in fig 3.11 and similar to that seen in fig 3.15 (X20 magnification).

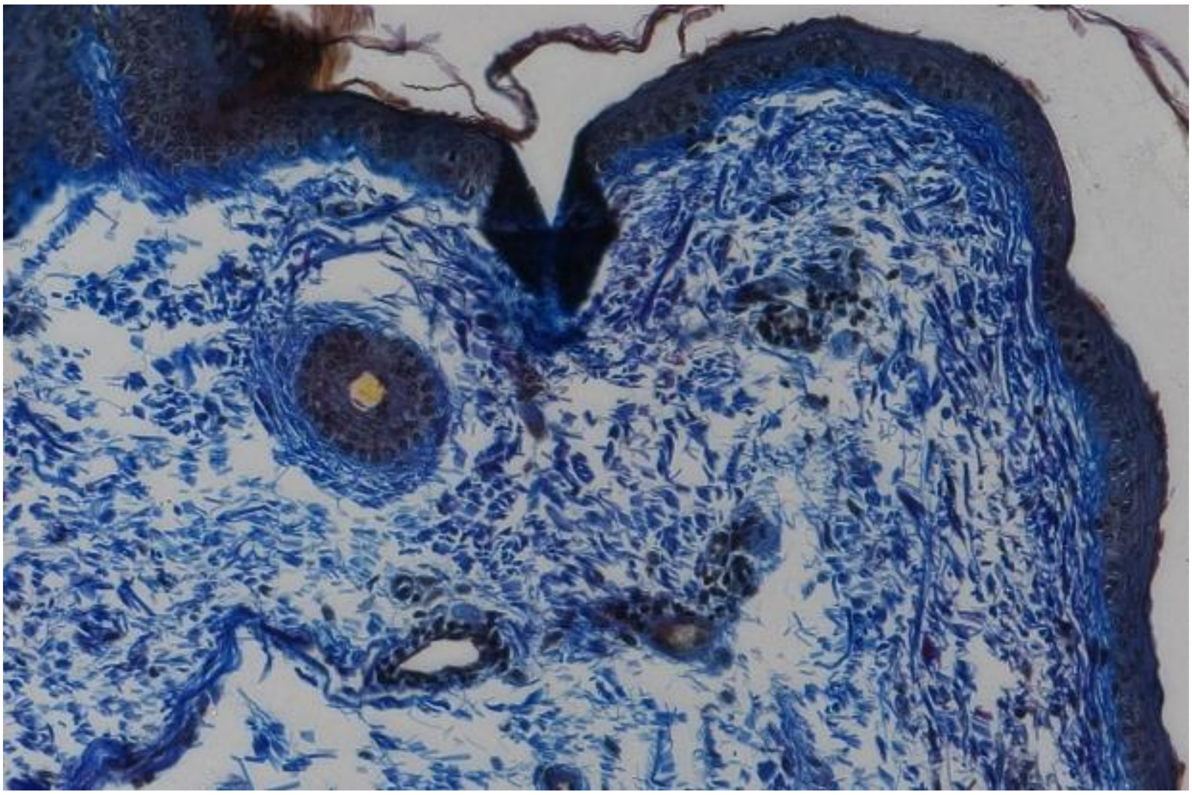

Fig 3.17 Embalmed cadaveric earlobe skin stained with Herovici's technique. The histological structure is very different to all other samples seen (X20 magnification).

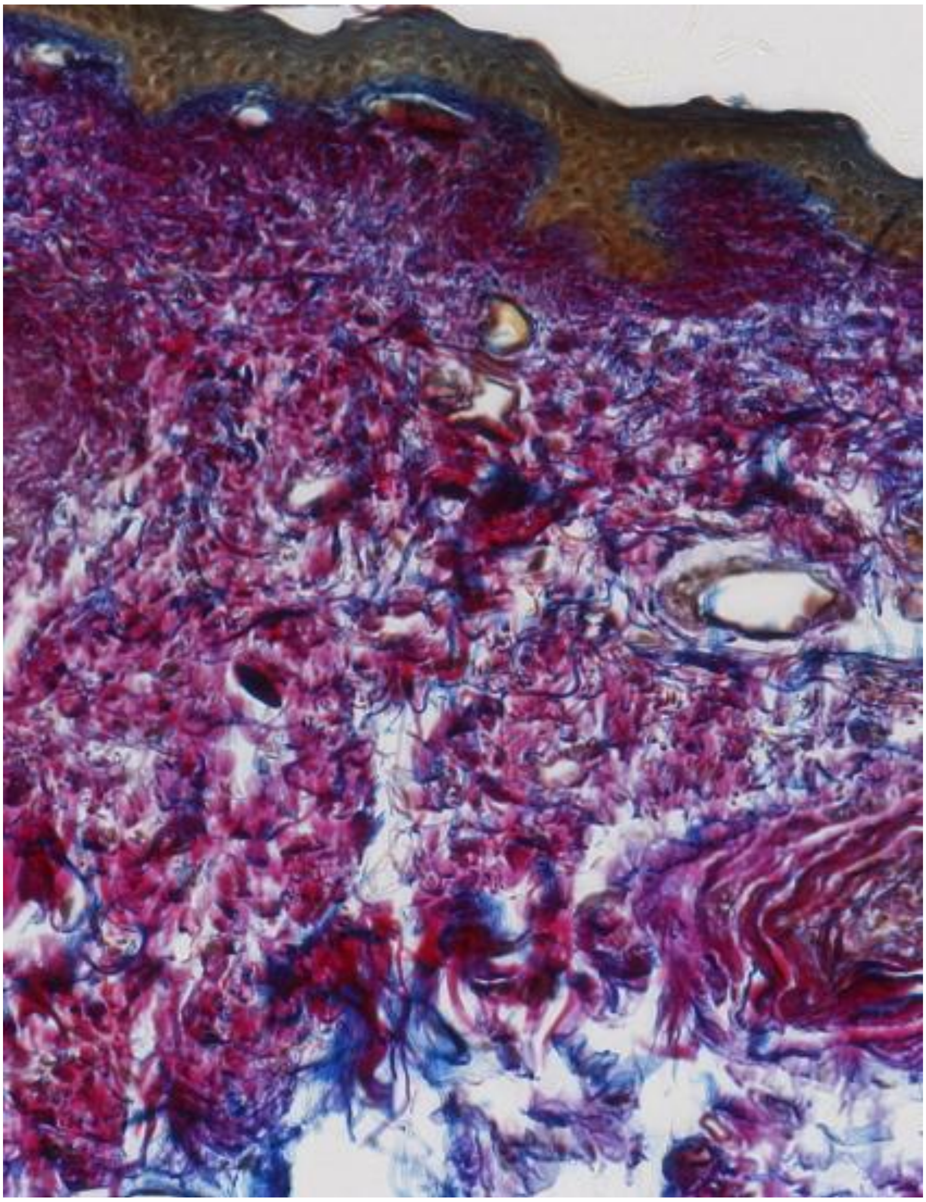

Scar tissue

Where normal skin was present on operative samples the appearances were identical to skin obtained from operations. Areas of mature scar tissue showed thick red staining fibres in a compact parallel arrangement. A small number of thin blue fibres were present on the peripheries of these fibres, but fewer compared with normal tissue. No epidermal appendages were present in areas of scar.

Fig 3.18 Mature burns scar stained with Herovici's technique (X 20 magnification). As in fig 3.5 parallel fibres of type I collagen predominate, contrasting with the basket-weave arrangement seen in the dermis of fig 3.8.

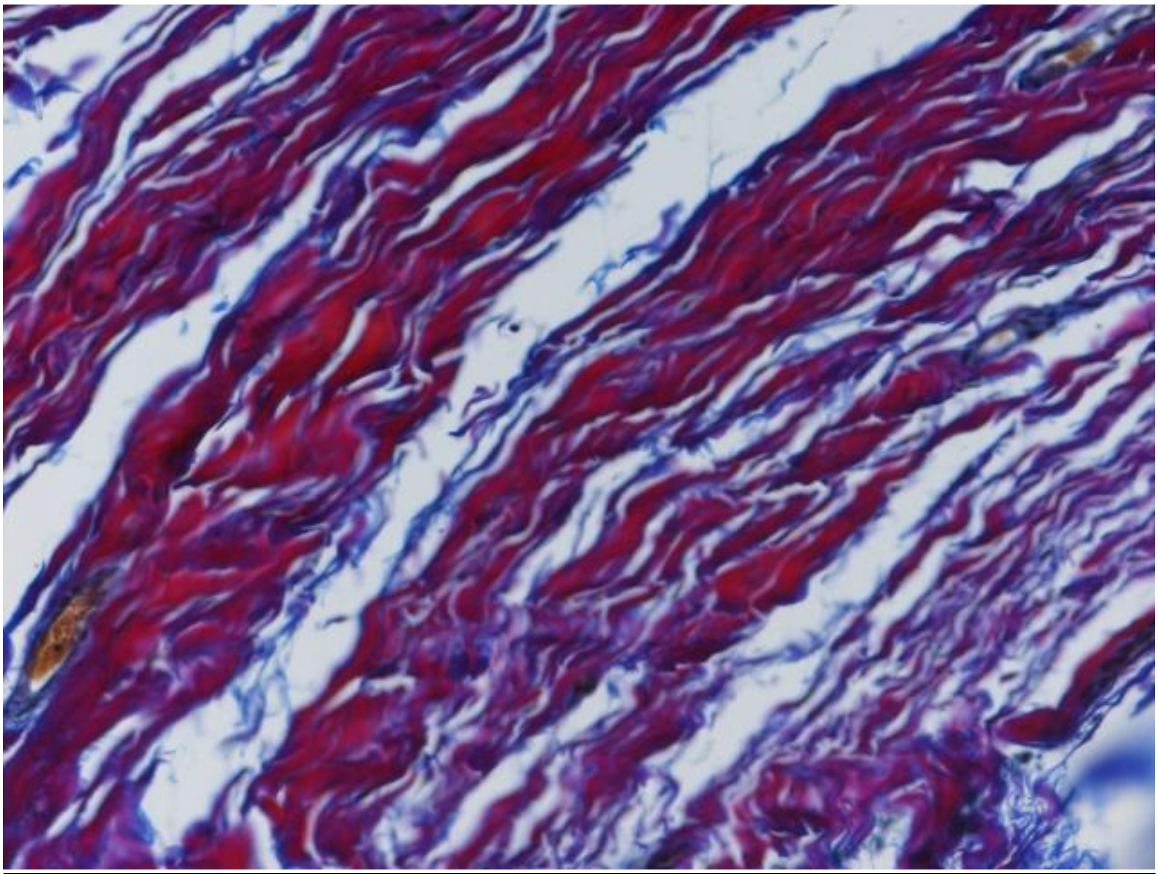

3.3 Tissue Preservation

The preservation of the embalmed cadaveric skin was comparable to that of the “fresh” operative specimens. The epidermis and dermal collagen were virtually identical fibres in both types of tissue. This is clearly shown when comparing figures 3.8 and 3.13. These show sections of human abdominal skin stained with Herovici’s technique. One is from an embalmed cadaver and one taken from surgery, yet their appearances are almost identical.

A similar situation is also seen with other structures. Figure 3.19 shows excellent preservation of a hair follicle. Figure 3.20 shows preservation of erythrocytes within a blood vessel.

Fig 3.19 Excellent preserervation of a hair follicle within embalmed cadaveric tissue stained with Herovici's technique (X40 magnification).

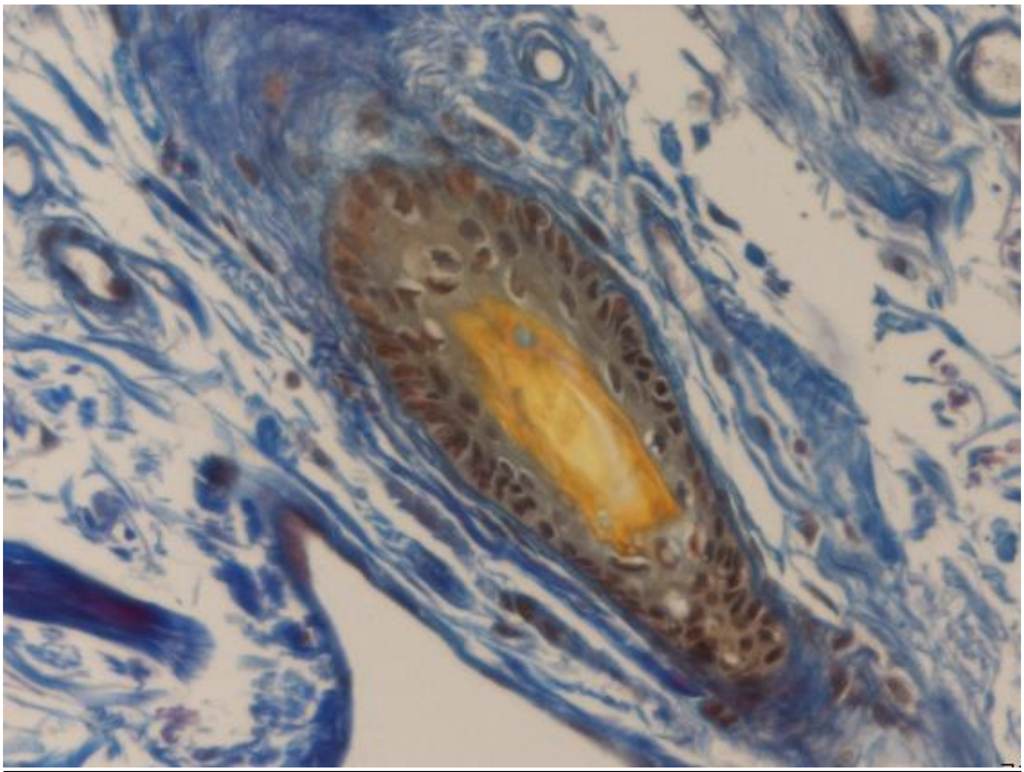

Fig 3.20 Erythrocytes clearly visible (arrow) within a blood vessel in embalmed cadaveric tissue stained with Herovici's technoque (X40 magnification)

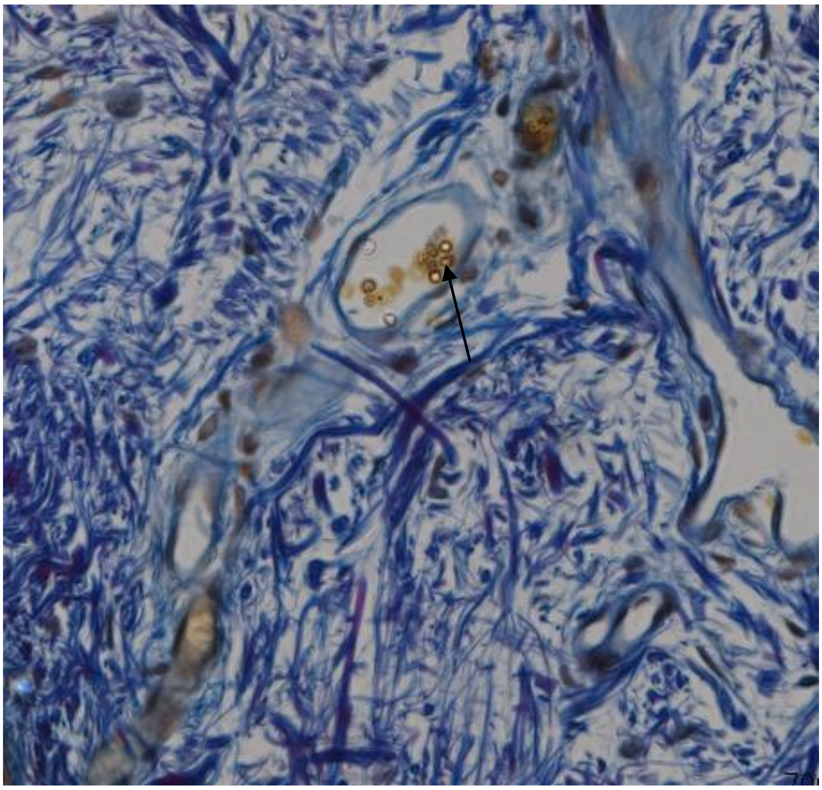

3.4 Transverse Sectioning

Sectioning the skin in a plane parallel to the epidermal surface as described in 2.1.6 allowed further views on the relationship of the type I and type III dermal collagen fibres. The relationship of these fibres and epidermal cells to epidermal appendages is clearly demonstrated in figure 3.10.

Using Herovici's technique, it can also be seen that the thin, blue type III fibres of the papillary dermis are gradually replaced by red type I collagen fibres. These are thinner at first, but their thickness increases with dermal depth. Both the intermingling of type I and type III fibres and the basket weave arrangement of the reticular dermis fibres are shown in figures 3.21-3.23.

Fig 3.21 Herovici's staining of a transverse section of human abdominal skin at X20 magnification. We see different levels of tissue present in the same section including epidermis (E), thin, blue and red type I and III collagen fibres of the papillary dermis, a hair shaft and follicle (H) and fibroblasts (F).

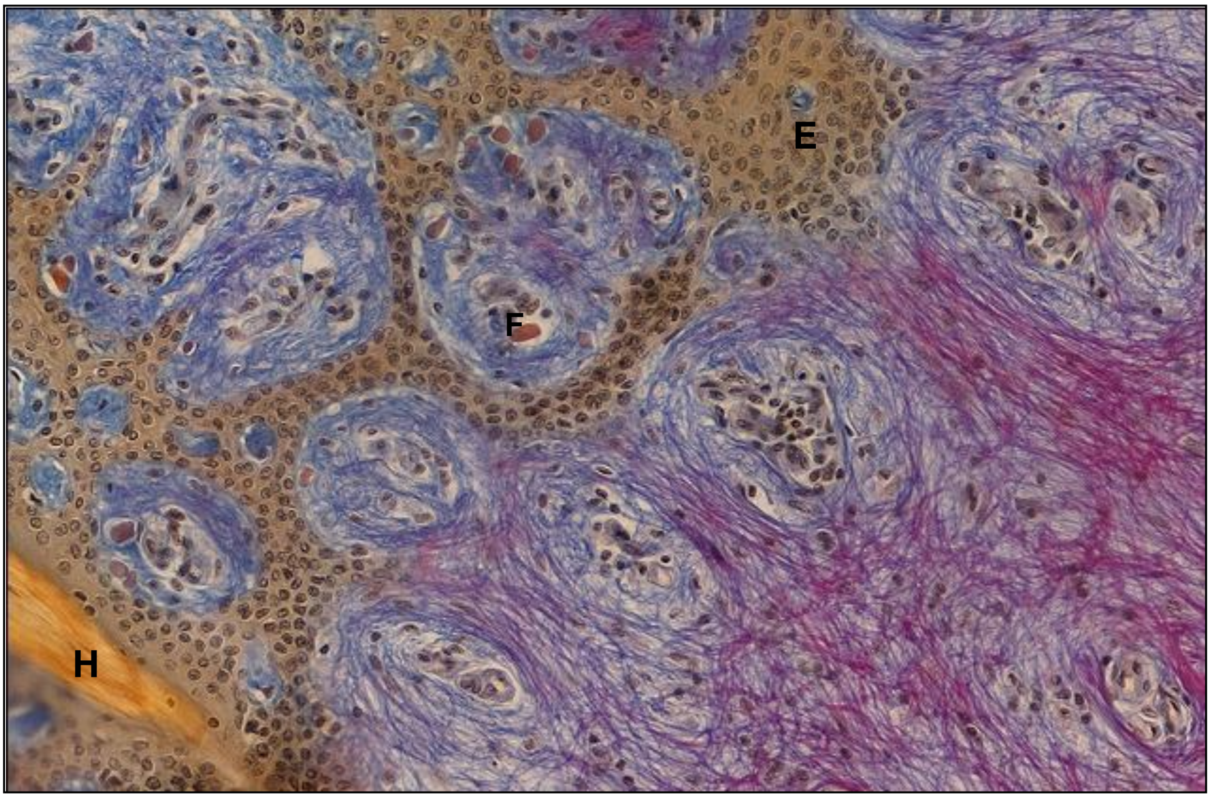

Fig 3.22 Deeper section of the same sample seen in Fig 4.4a. Note the intermixing of thin blue and red type I and III collagen fibres. A few thicker red type I collagen fibres are seen to the right of the picture.

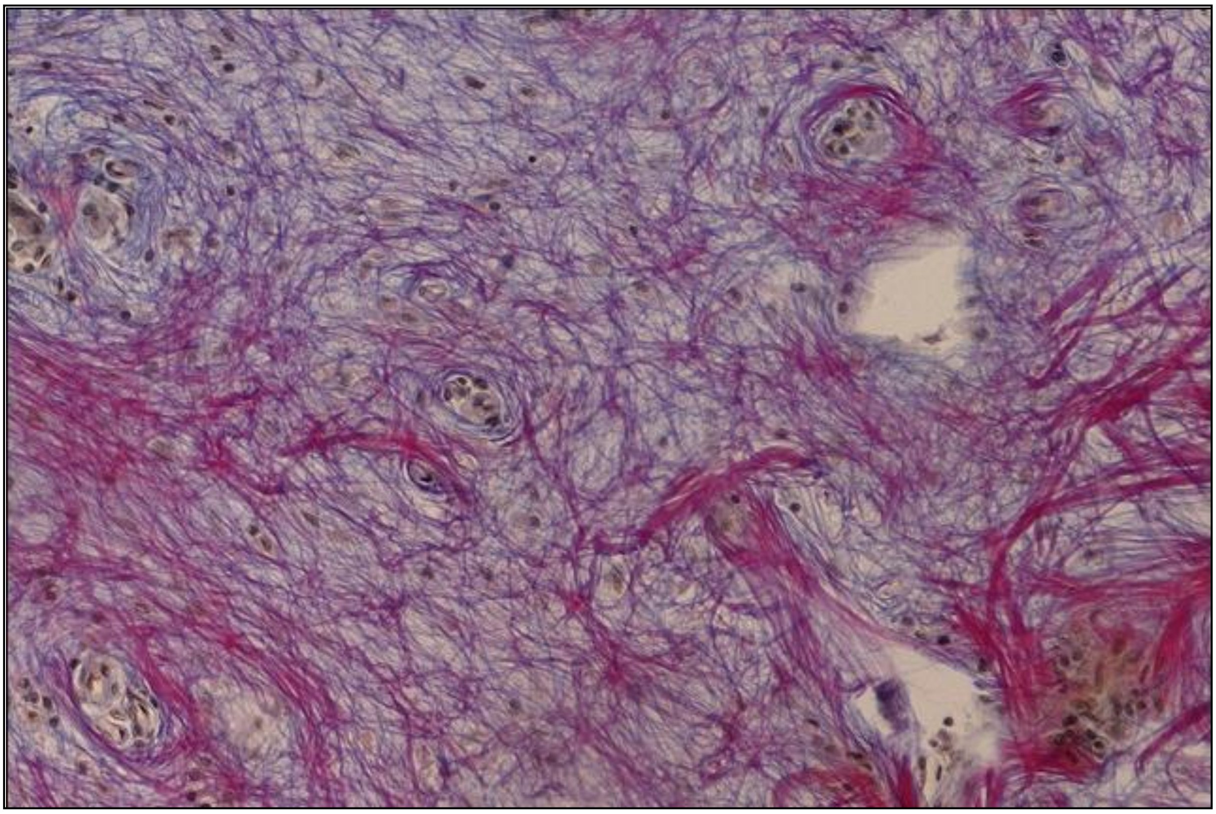

Fig 3.23 Deeper section of the same sample seen in Figs 4.4a and b. Here we see the classic basket-weave appearance of thick red type I collagen bundles of the reticular dermis. It is important to stress that this is a "bird's eye view" of tissue not normally seen in conventional histology and in conjunction with vertical tissue sections can aid our appreciation of the 3-dimensional dermal structure.

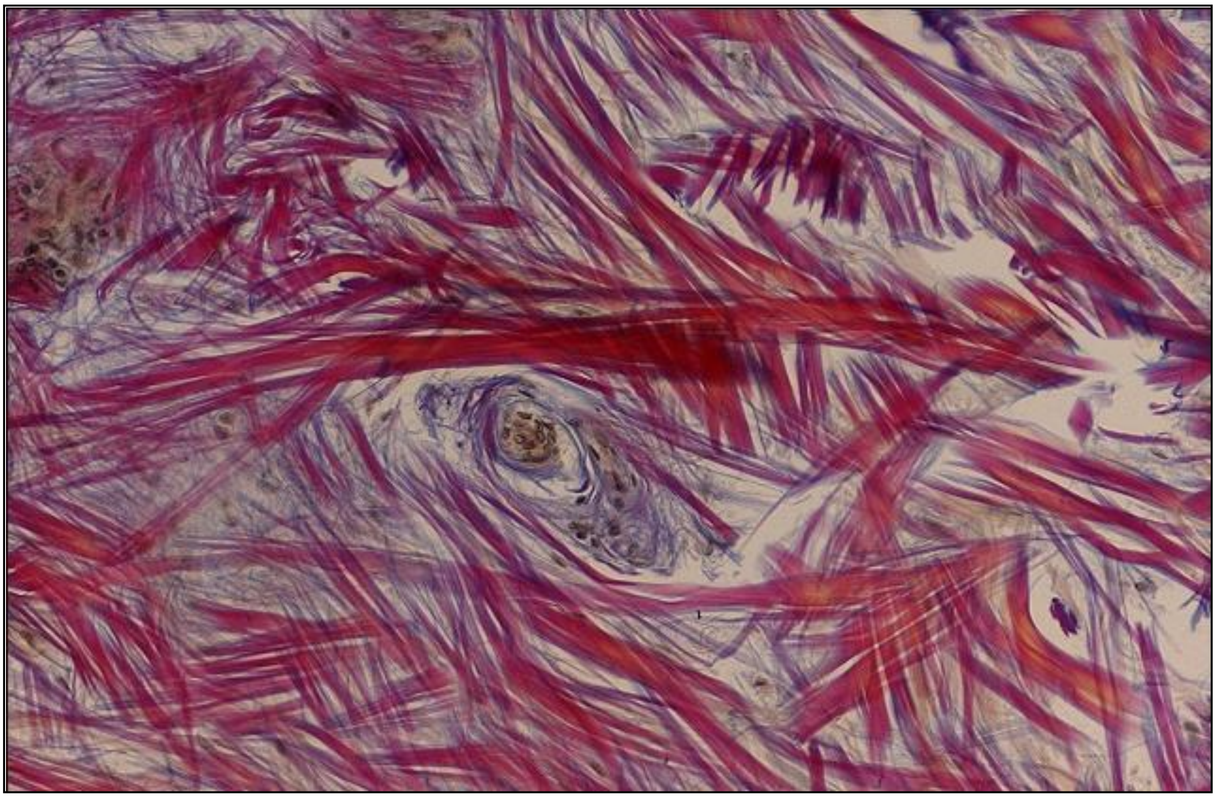

3.5 Variations of Herovici's Method

Variations of herovici's method were used as outlined in the methods section.

3.5.1 Methyl Blue and Water

Nuclei stained dark purple, all other structures were pale blue.

Fig 3.24 Abdominal skin stained with modification of Herovici's technique substituting methyl blue in water for solution F (X20 magnification). See main text for description.

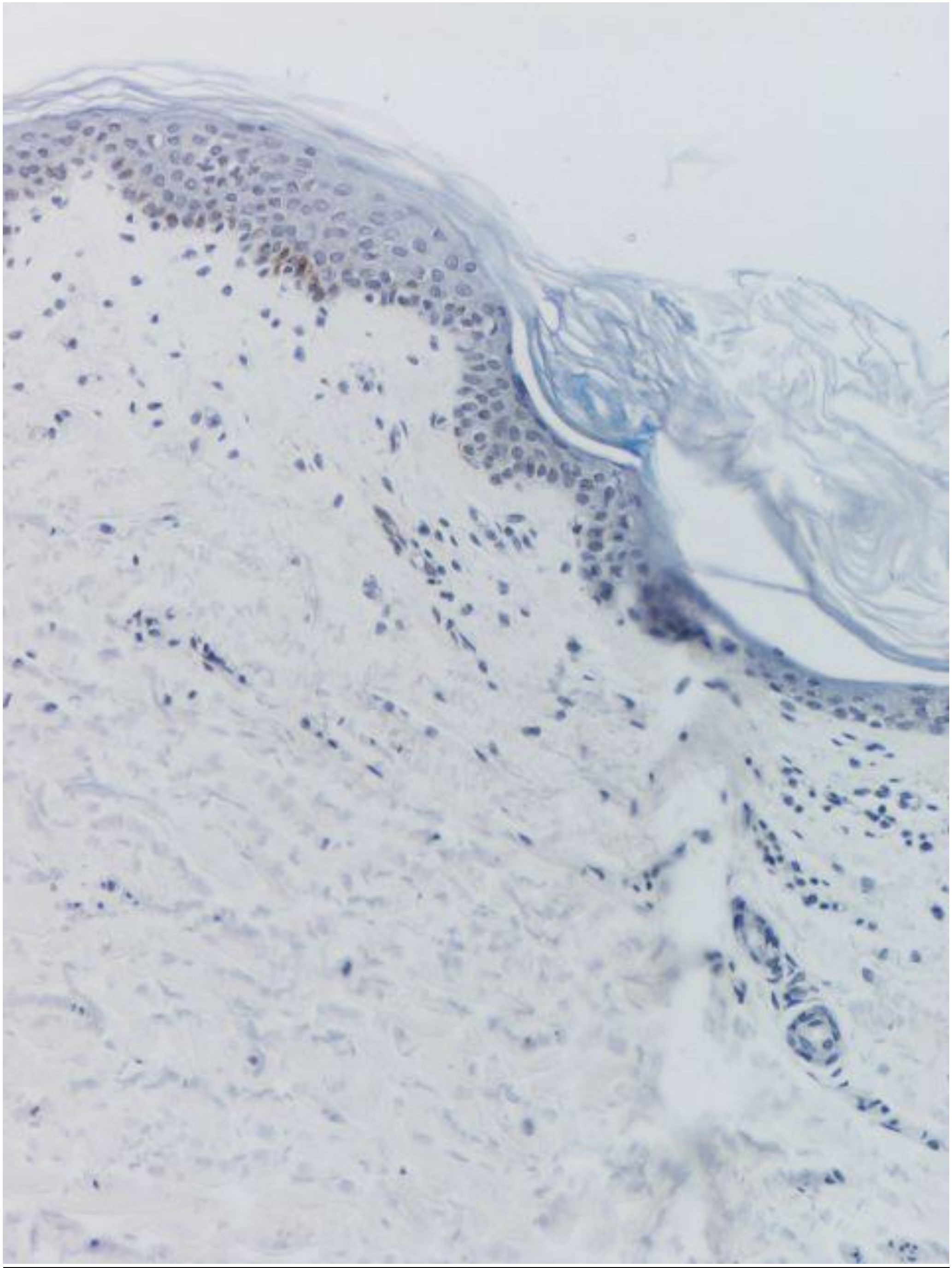

3.5.2 Methyl Blue and Picric Acid

Nuclei were dark purple, cytoplasm was green. Collagen showed as either thin blue fibres or thick green fibres with occasional blue fibres forming a sleeve around the thicker fibres.

Fig 3.25 Abdominal skin stained with modification of Herovici's technique substituting methyl blue in picric acid for solution F (X20 magnification). See main text for description.

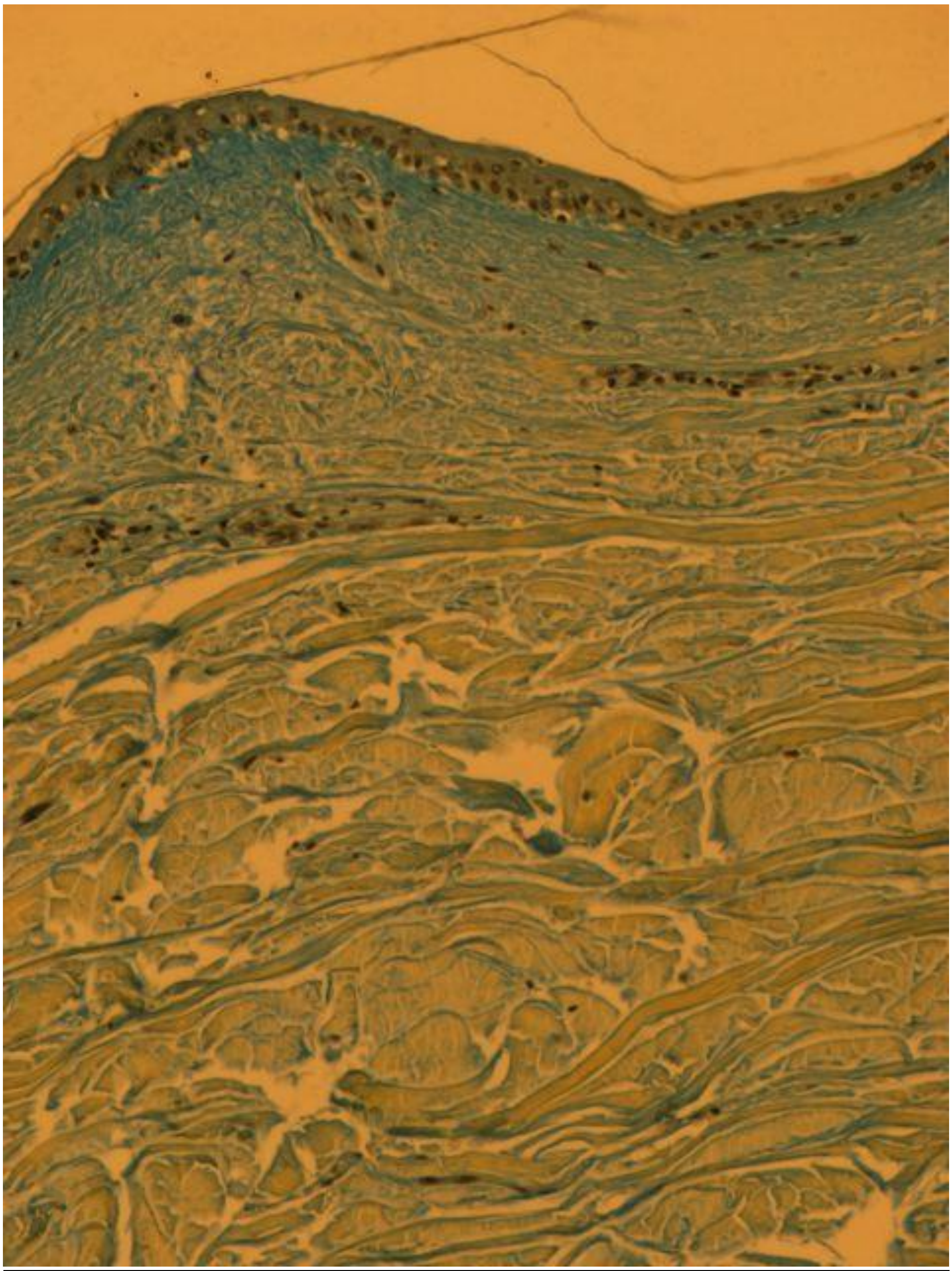

3.5.3 Methyl Blue and Picric Acid Followed by Sirius Red in Picric Acid

Nuclei were dark brown, cytoplasm was pale green and collagen fibres were red (Fig 3.26).

3.5.4 Sirius Red in Picric Acid Followed by Methyl Blue and Picric Acid

Nuclei were dark brown, cytoplasm was blue and green and collagen fibres were red (Fig 3.27).

Fig 3.26 Human breast skin stained with modification of Herovici's technique substituting methyl blue in picric acid and then picrosirius solution for solution F (X20 magnification). See main text for description.

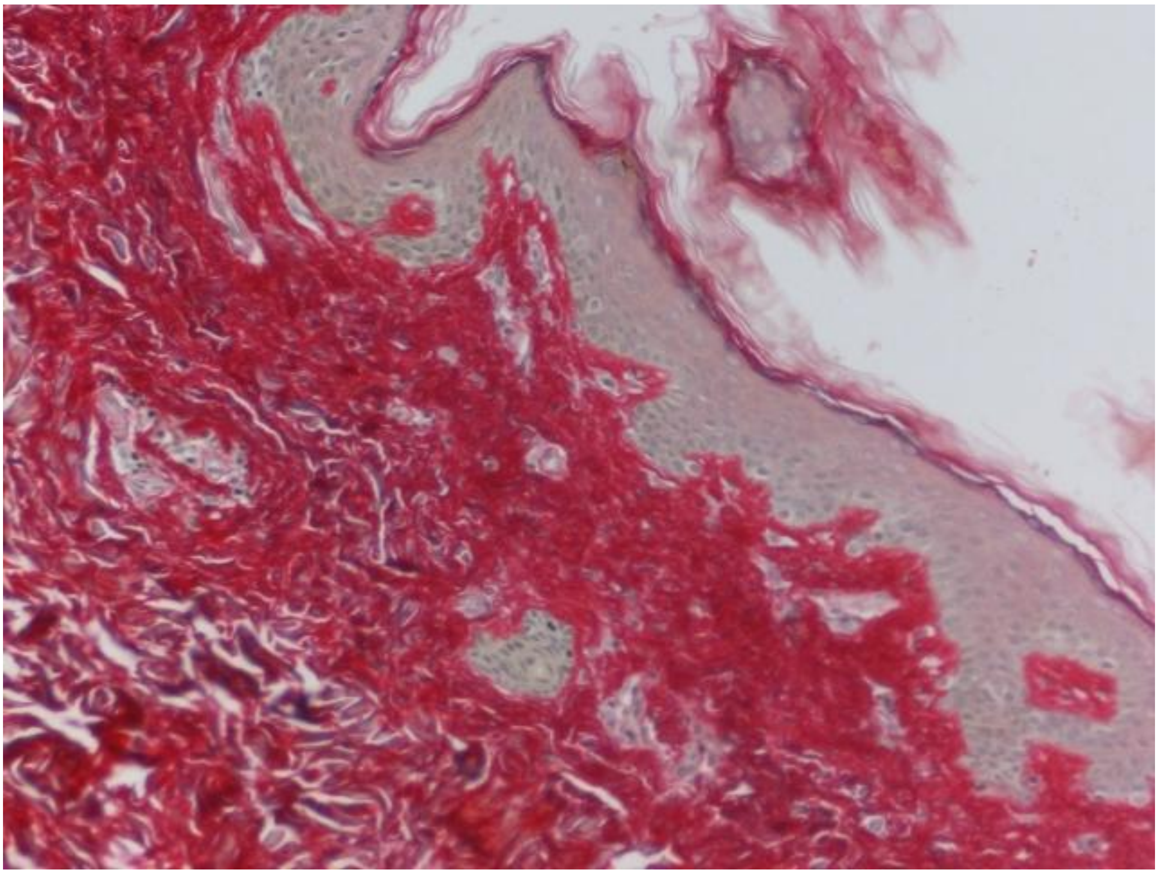

Fig 3.27 Human abdominal skin stained with modification of Herovici's technique substituting picrosirius solution and then methyl blue in picric acid for solution F (X20 magnification). See main text for description.

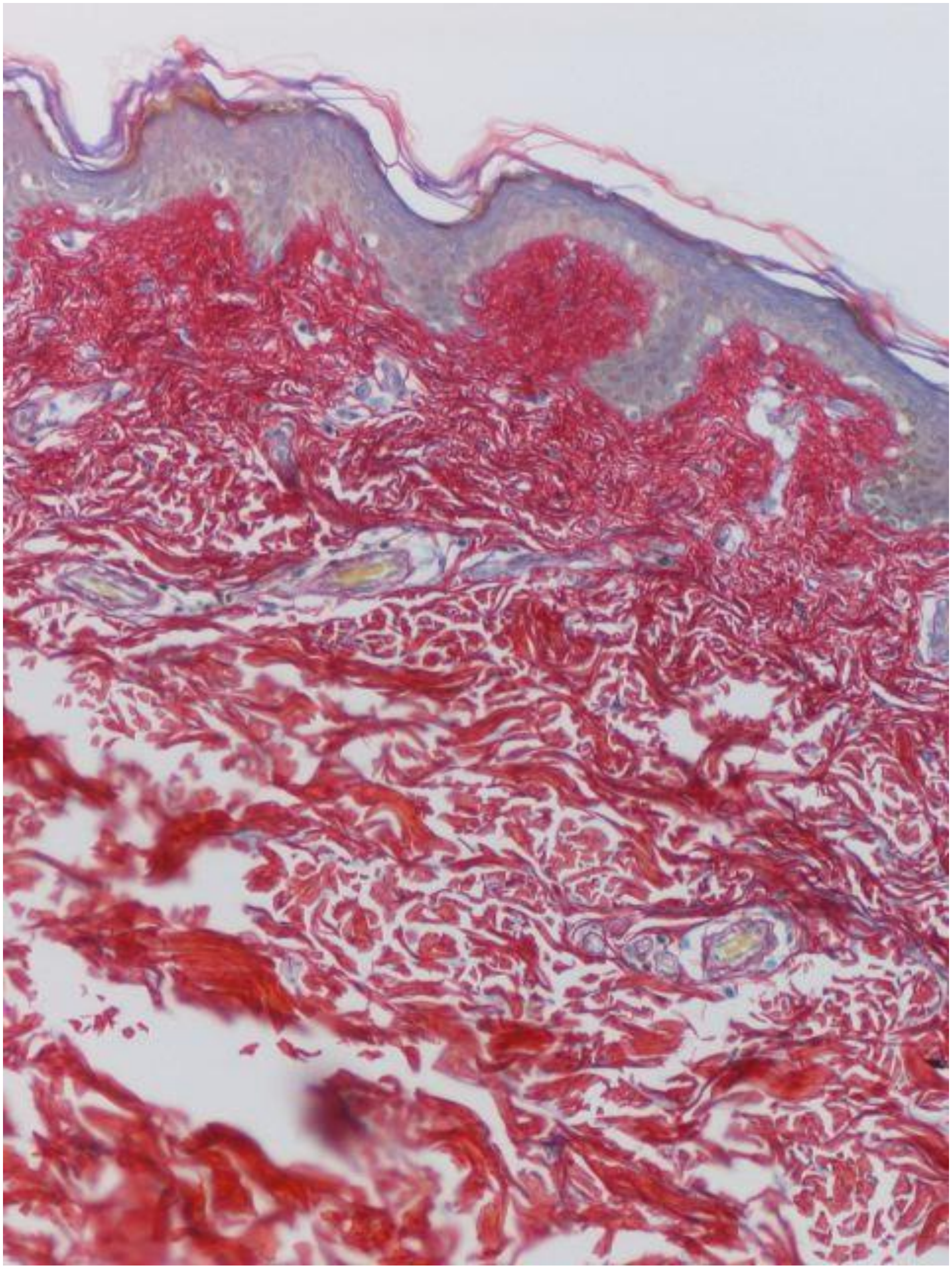

3.5.5 Substitution of Acid Fuschin with Sirius Red in Herovici's Stain

Normal kidneys from 4 rats and 17 normal human skin samples were tested. In the skin samples basement membranes were stained purple in 15 of 17 cases (Fig 3.28). In the remaining 2 samples the basement membrane stained turquoise. All cytoplasm was stained greenish-brown and nuclei dark brown. Collagen fibre colour displayed some heterogeneity, the majority of fibres were either thin and blue or thick and green. Basement membranes in all 4 rats' kidneys were purple (Fig 3.29). No increase in birefringence was seen when slides were viewed under crossed polarizing filters.

Fig 3.28 Human abdominal skin stained with modification of Herovici's technique substituting picrosirius solution for solution F (X40 magnification). See main text for full description. Purple staining of the dermo-epidermal junction basement membrane can clearly be seen (arrow).

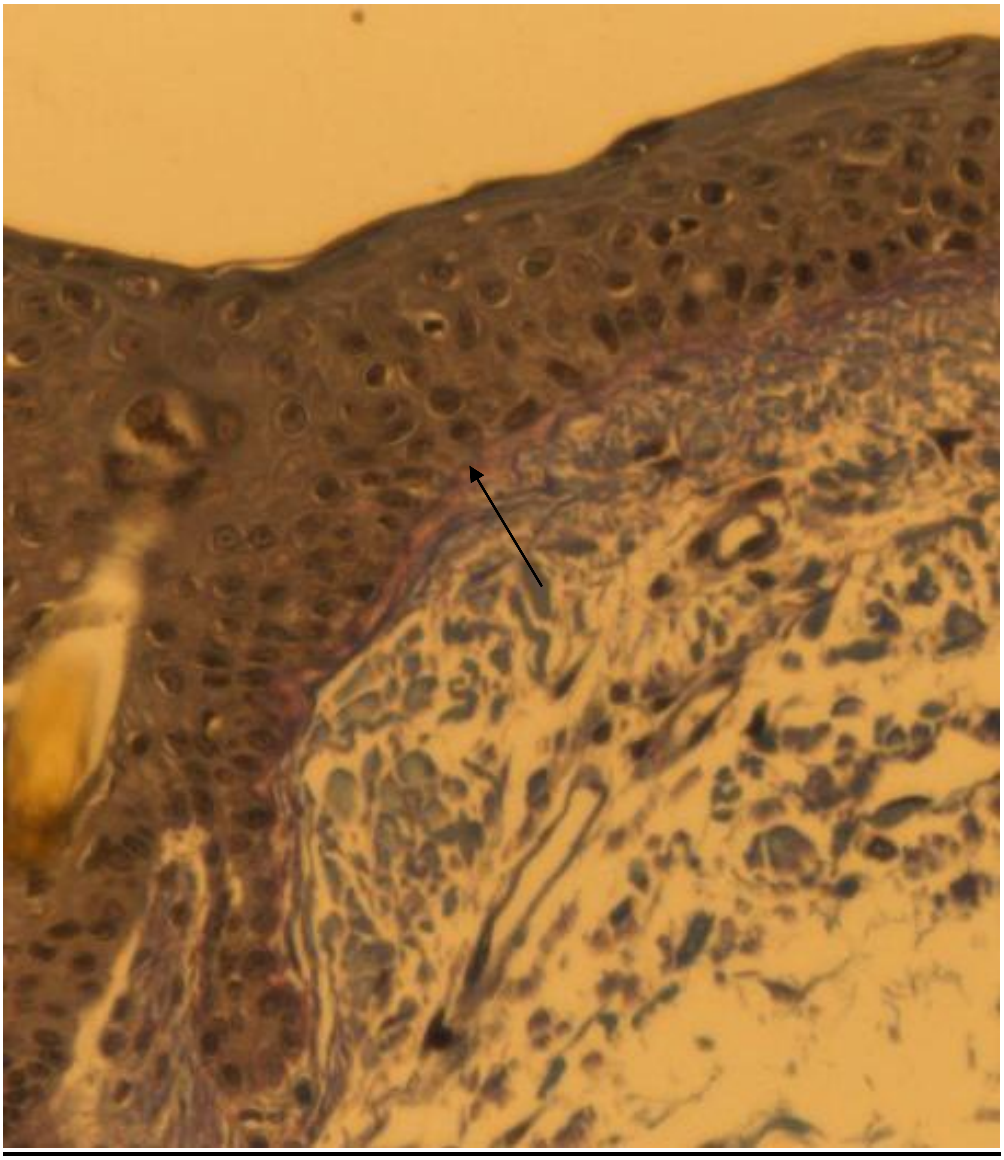

Fig 3.29 Rat kidney stained with modification of Herovici's technique substituting picrosirius solution for solution F (X40 magnification). See main text for full description. Purple staining of basement membranes can clearly be seen (arrows).

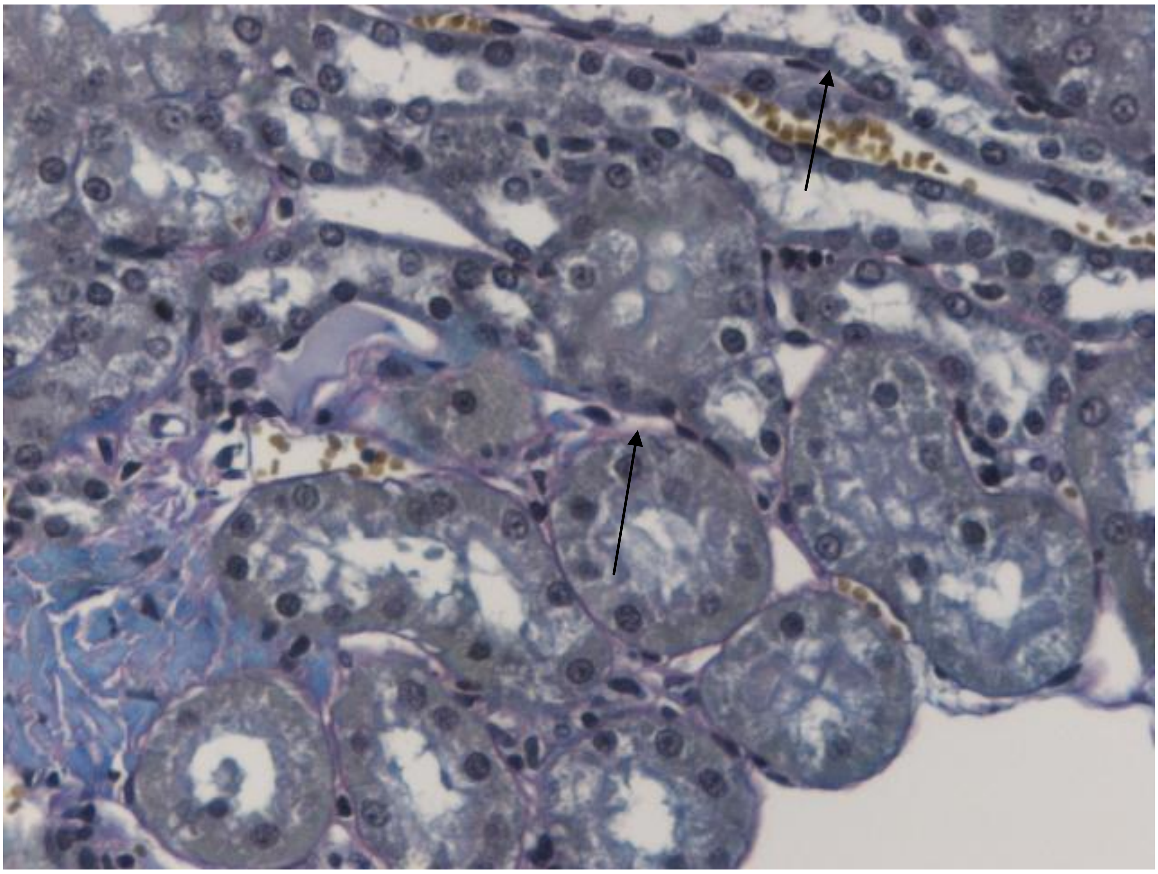

3.6 PAS Staining

Normal kidneys from 4 rats and 17 normal human skin samples were tested. In all samples studied basement membranes were stained a deep pink colour. All other structures were pale pink (Figs 3.30, 3.31).

Fig 3.30 PAS staining of human eyelid (X20 magnification). Purple staining of dermo-epidermal membrane can be seen (arrow) and corresponds to the purple staining region of fig 3.25.

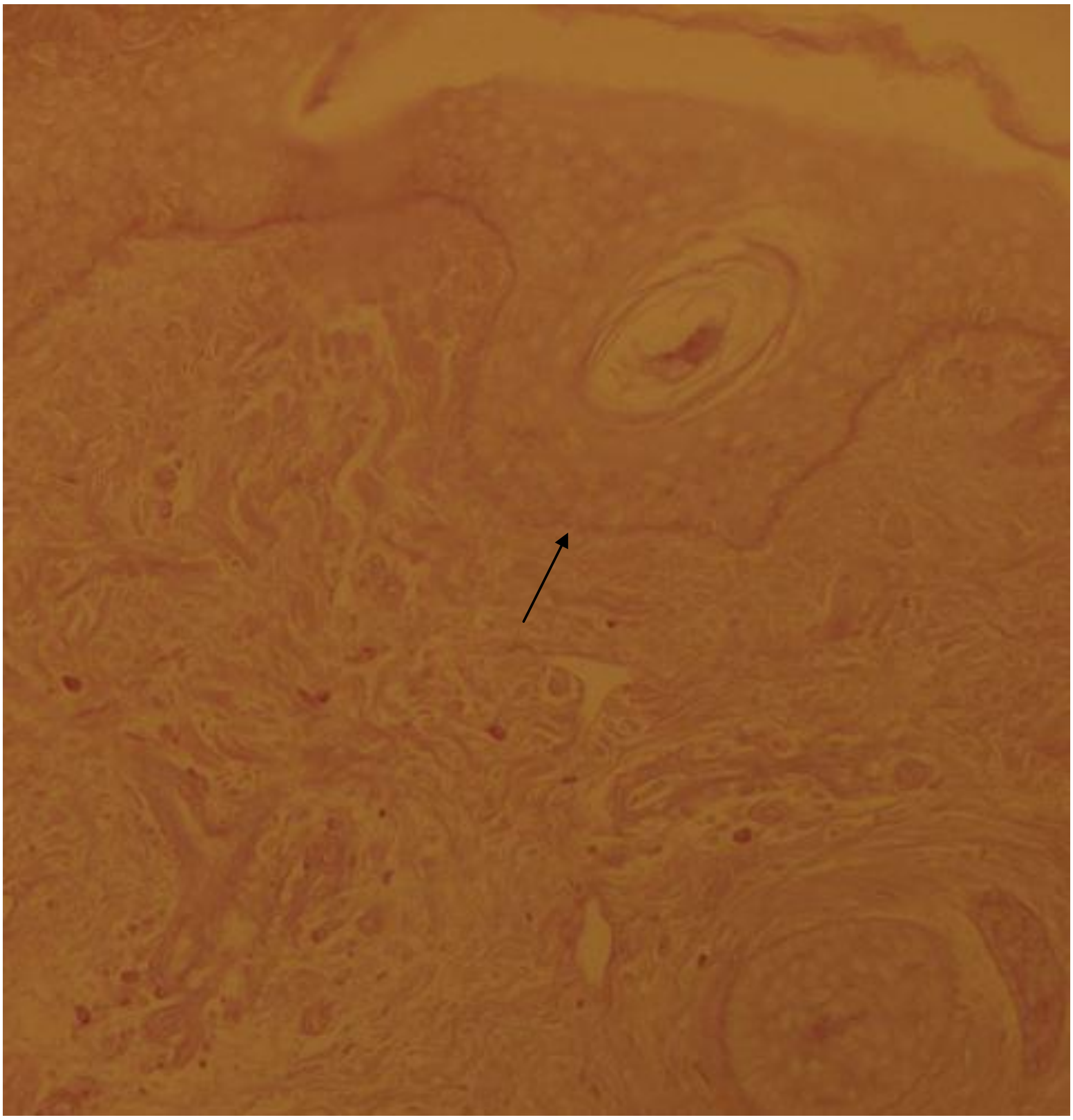

Fig 3.31 PAS staining of rat kidney (X40 magnification). Purple staining of dermo-epidermal membrane can be seen (arrow) and corresponds to the purple staining region of fig 3.26.

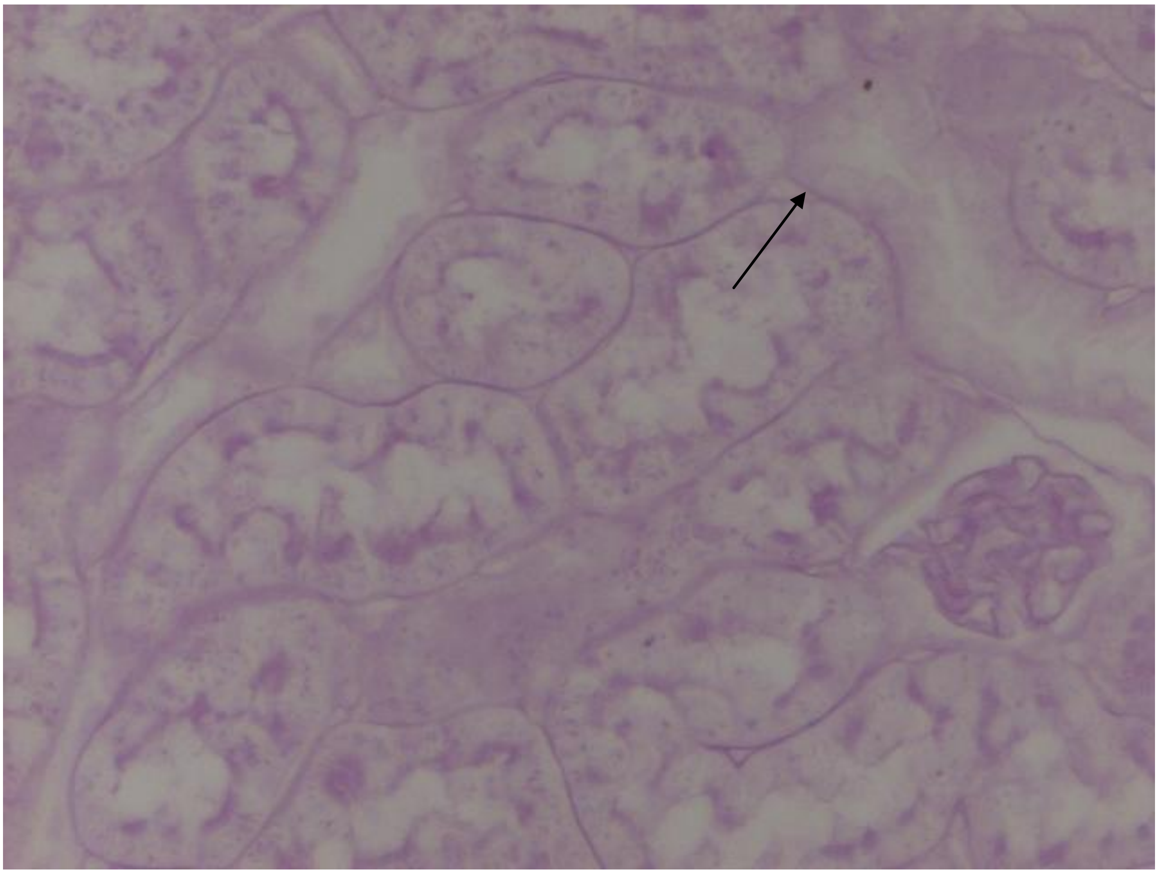

3.7 Epidermal Thickness

Table 3.1 Comparison of Random Sections of Epidermal Thickness Between Fresh Operative and Embalmed Cadaveric Samples Taken From a Variety of Body Regions

Sample	**Number**	**Mean thickness (μm)**	**Range (μm)**	**SD**
Operative	38	40.8	13.9-77.2	14.6
Cadaveric	58	27.4	11.7-67.8	9.11

The operative samples are 48.9% thicker than the cadaveric samples. This was found to be statistically significant using the Students t test. P value <0.001 (5.07×10^{-6})

For clarity and accuracy, all quantitative data shall be presented in 2 ways; as graphs and tables.

Graph 3.1 Comparison of epidermal thickness between cadaveric and operative tissue samples. Each value shown is the mean + SD. Cadaveric n=58, operative n=38. P<0.001.

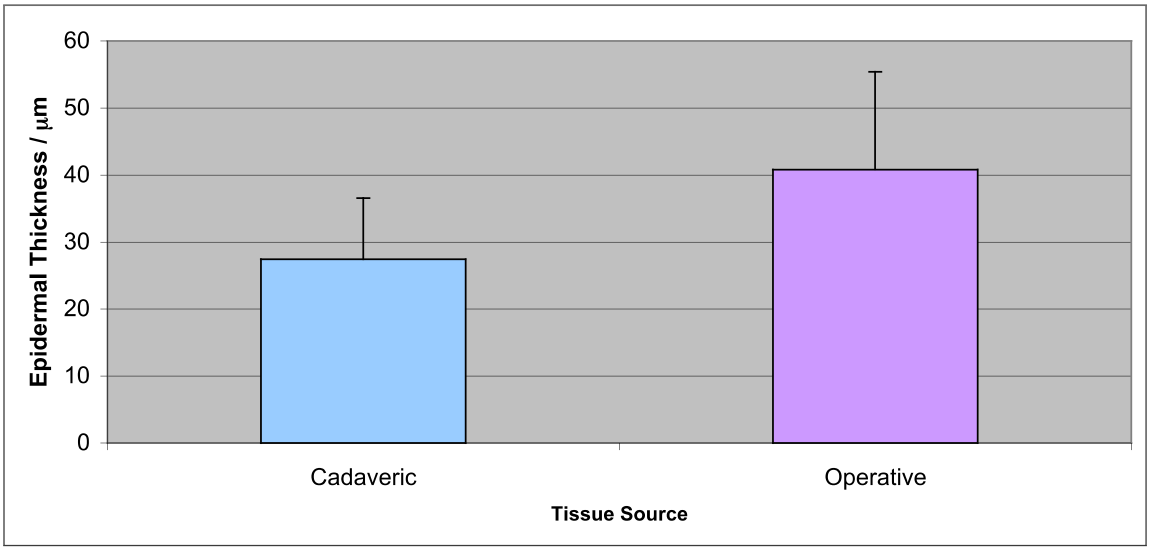

Table 3.2 Mean Epidermal Thickness for Each Body Region

Region	**Number**	**Mean Thickness (μm)**	**Range (μm)**	**SD**
Deltoid	9	27.41	22.5-38.3	6.1
Abdomen	13	24.02	11.7-40.6	7.86
Sternum	10	22.50	13.9-36.1	6.68
Post-auricular	5	38.33	23.9-67.8	17.1
Earlobe	12	30.69	13.9-43.9	8.40
Eyelid	9	27.47	20-35	5.41

Graph 3.2 Mean epidermal thickness for individual body regions of cadaveric samples. Each value shown is the mean + SD. Deltoid n=9, abdomen n=13, sternum n=10, post-auricular n=5, earlobe n=12, eyelid n=9.

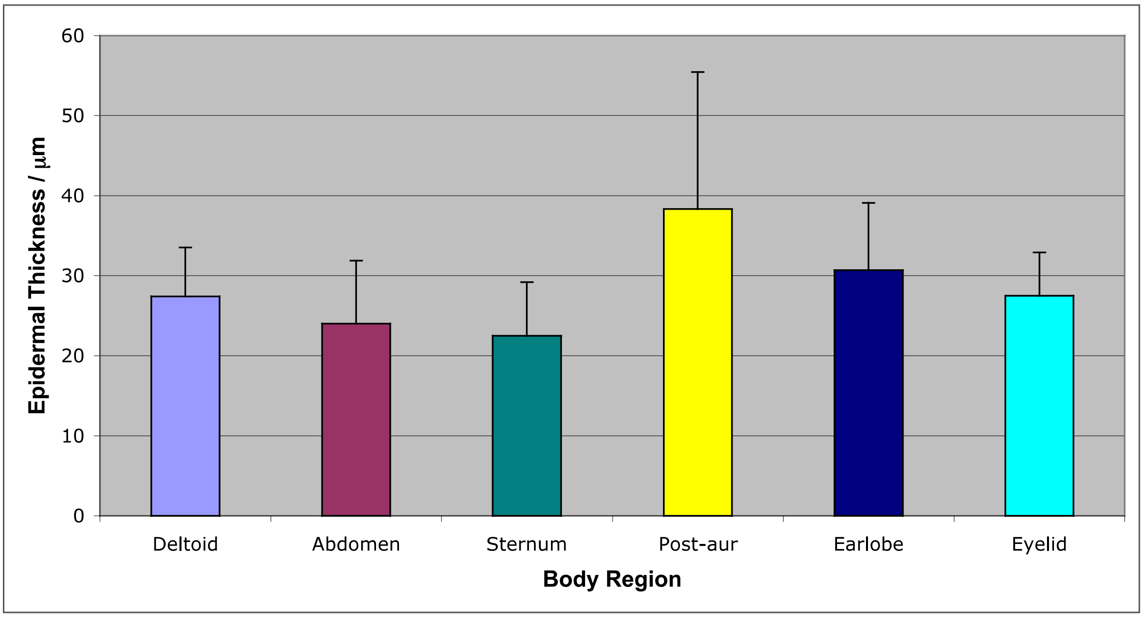

Table 3.3 Mean Epidermal Thickness for Body Regions Grouped by General Topographical Location

Region	**Number**	**Mean Thickness (μm)**	**Range (μm)**	**SD**
Trunk	32	24.50	11.7-40.6	7.09
Head	26	31.05	13.9-67.8	10.1

The samples obtained from the head are 26.5% thicker than samples obtained from the trunk. This was found to be statistically significant using the Students t-test. The p value is 0.008

Graph 3.3 Epidermal thickness of cadaveric samples grouped by general topographical location. Each value shown is the mean + SD. Trunk n=32, head n=26.

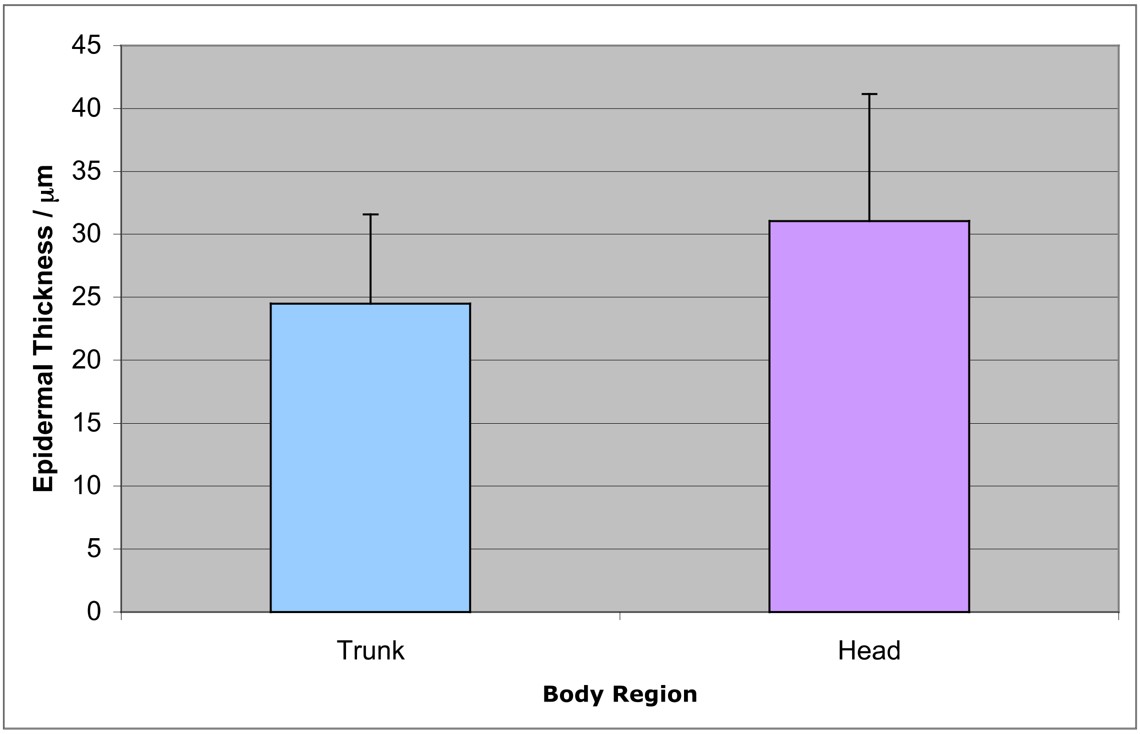

Table 3.4 Mean Epidermal Thickness for Body Regions Grouped by Scarring Potential

Region	**Number**	**Mean Thickness (μm)**	**Range (μm)**	**SD**
Good	22	25.43	11.7-40.6	7.03
Poor	36	28.66	13.9-67.8	10.1

Samples from potentially poor scarring regions were 13.0% thicker. Using Students t-test, this was found not to be statistically significant. The p value is 0.157.

Graph 3.4 Epidermal thickness of cadaveric samples grouped by scarring potential. Good scarring potential n=22, poor scarring potential n=36. P=0.157.

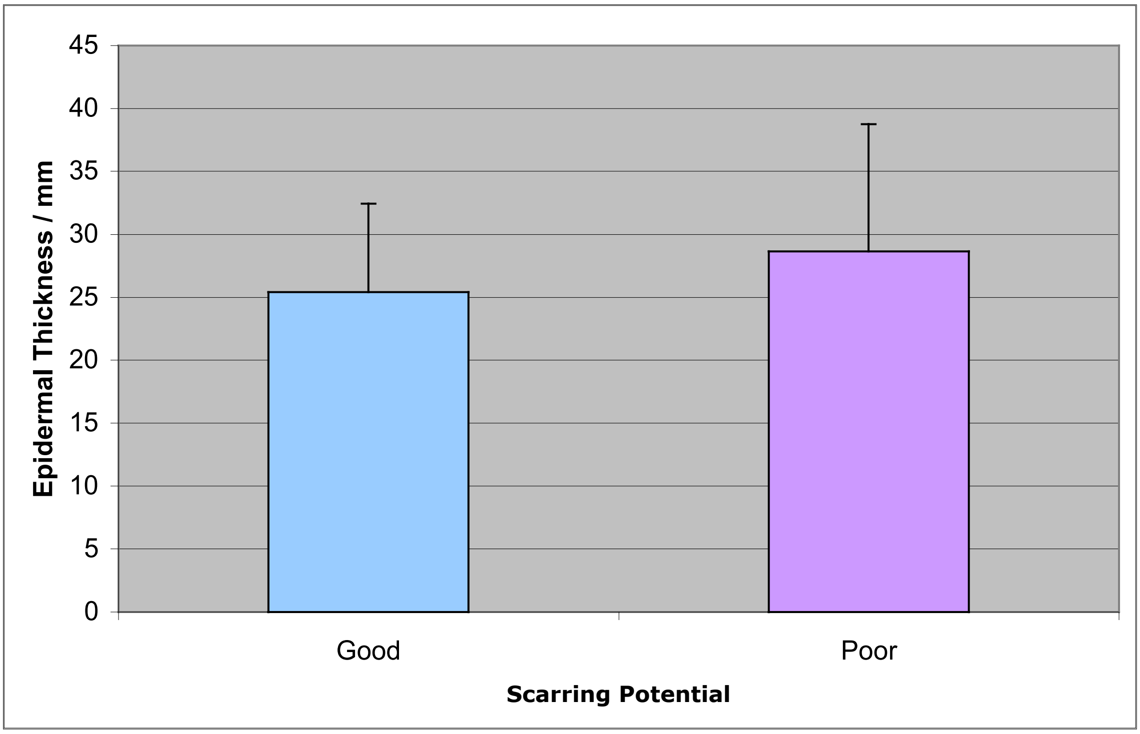

3.8 Epidermal Appendage Counts

Table 3.5 Epidermal Appendage Counts for Individual Body Regions

Region	Number	Sebaceous Glands	Sweat Glands	Hair Follicles	Total
Deltoid	9	0.178	0.444	0.689	1.31
Abdomen	13	0.015	0.323	0.277	0.615
Sternum	10	0.28	0.56	0.32	1.16
Post-auricular	5	1.60	0.00	3.56	5.16
Earlobe	12	1.05	0.033	3.02	4.10
Eyelid	9	0.711	0.244	2.18	3.13

Density of epidermal appendages (hair follicles, sebaceous glands, sweat glands) compared between different body regions. Mean counts per 5 random, low power fields (X20 magnification)

Graph 3.5 Subdivided epidermal appendage counts for individual body regions studied. Number of samples from each body region were as in table 3.2.

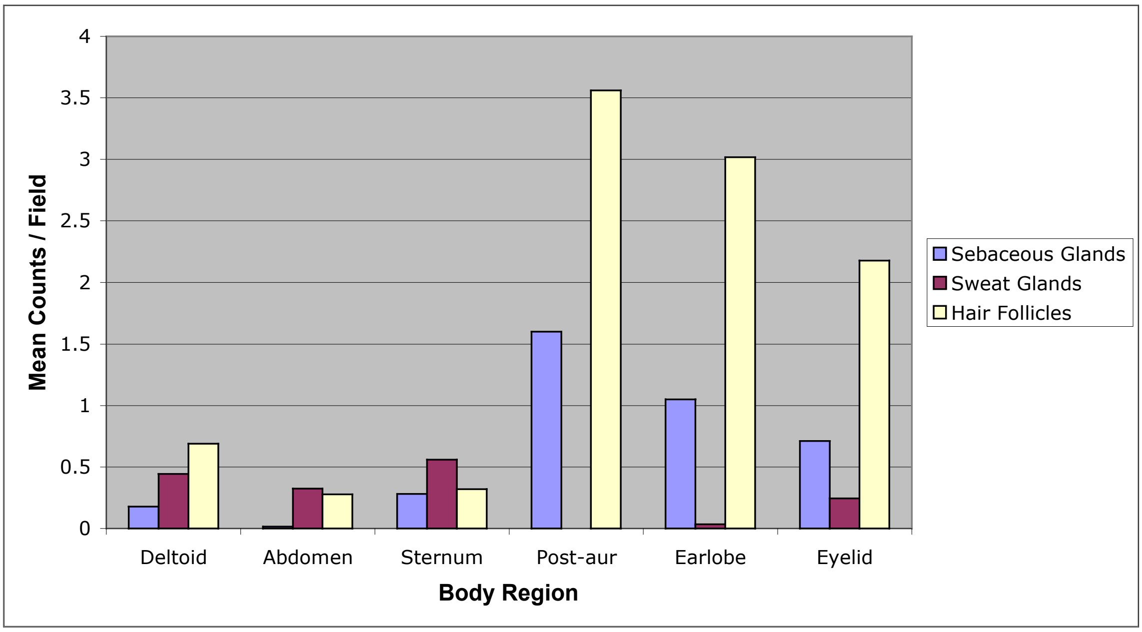

Table 3.6 Epidermal Appendage Counts for Body Regions Grouped by General Topographical Location.

Region	Number	Sebaceous Glands	Sweat Glands	Hair Follicles
Trunk	32	0.144	0.431	0.406
Head	26	1.038	0.100	2.83

The total appendage counts are 305% higher in regions sampled from the head compared with the trunk. Using Students t test the p value is 3.37×10^{-6}.

The total hair follicle counts are 597% higher in regions sampled from the head compared with the trunk. Using Students t test the p value is 2.36×10^{-6}.

The total sweat gland counts are 331% higher in regions sampled from the trunk compared with the head. Using Students t test the p value is 0.0004.

Table 3.7 Total Epidermal Appendage Counts for Body Regions Grouped by Topographical Location.

Region	Number	Total Appendage Counts	SD
Trunk	32	0.981	0.768
Head	26	3.97	2.56

The total sebaceous gland counts are 639% higher in regions sampled from the head compared with the trunk. Using Students t test the p value is 3.54 X 10^{-5}.

Graph 3.6 Mean total epidermal appendage counts for body regions grouped by topographical location. The mean + SD is shown. Number of samples from each region are as in table 3.3. P < 0.001.

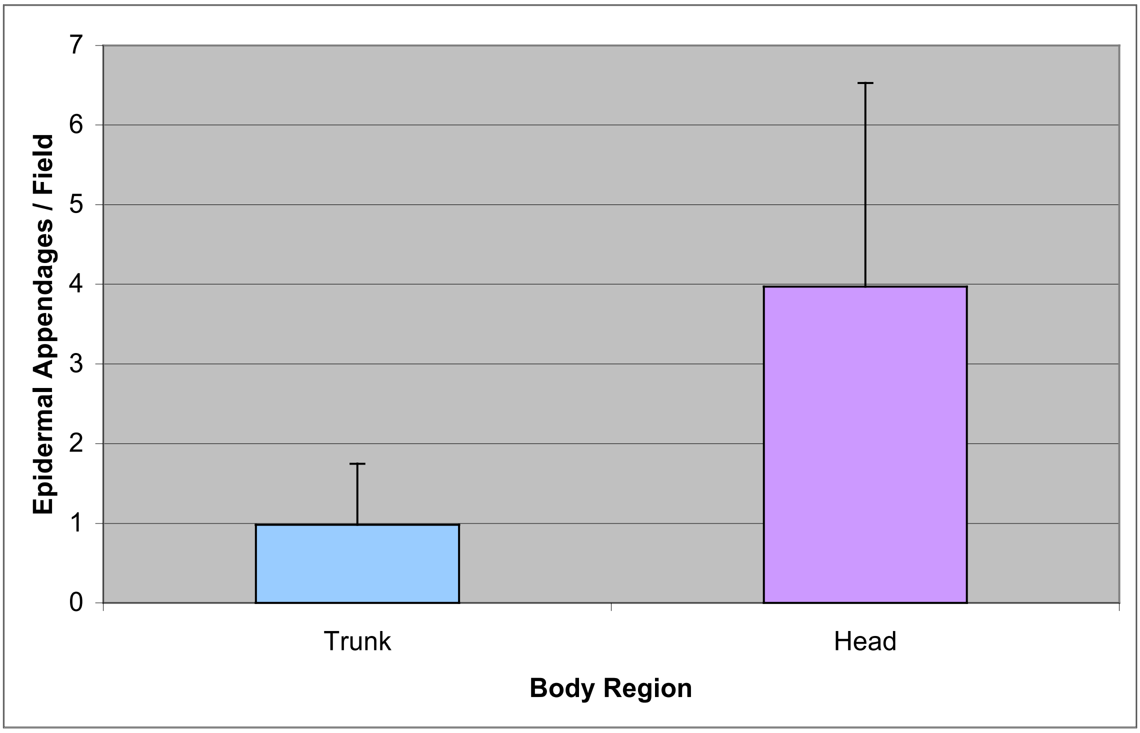

Table 3.8 Subdivided Epidermal Appendage Counts for Body Regions Grouped by Scarring Potential

Region	Number	Sebaceous Glands	Sweat Glands	Hair Follicles
Good	22	0.300	0.291	1.05
Poor	36	0.514	0.290	1.37

Table 3.9 Total epidermal Appendage Counts for Body Regions Grouped by Scarring Potential

Region	Number	Total Appendage Counts	SD
Good	22	1.65	1.80
Poor	36	2.17	2.39

Comparison of the density of epidermal appendages between samples taken from the good and poor scarring regions. Mean counts per low power field (X20 magnification)

None of the above parameters showed any statistically significant differences between regions that form good or bad scars. Using Students t test p values were 0.309 for total appendage counts; 0.193 for sebaceous glands; 0.990 for sweat glands; and 0.429 for hair follicles.

Graph 3.7 Mean total epidermal appendage counts for body regions grouped by scarring potential. The values shown are mean + SD. The number of samples are as in table 3.4. P > 0.05.

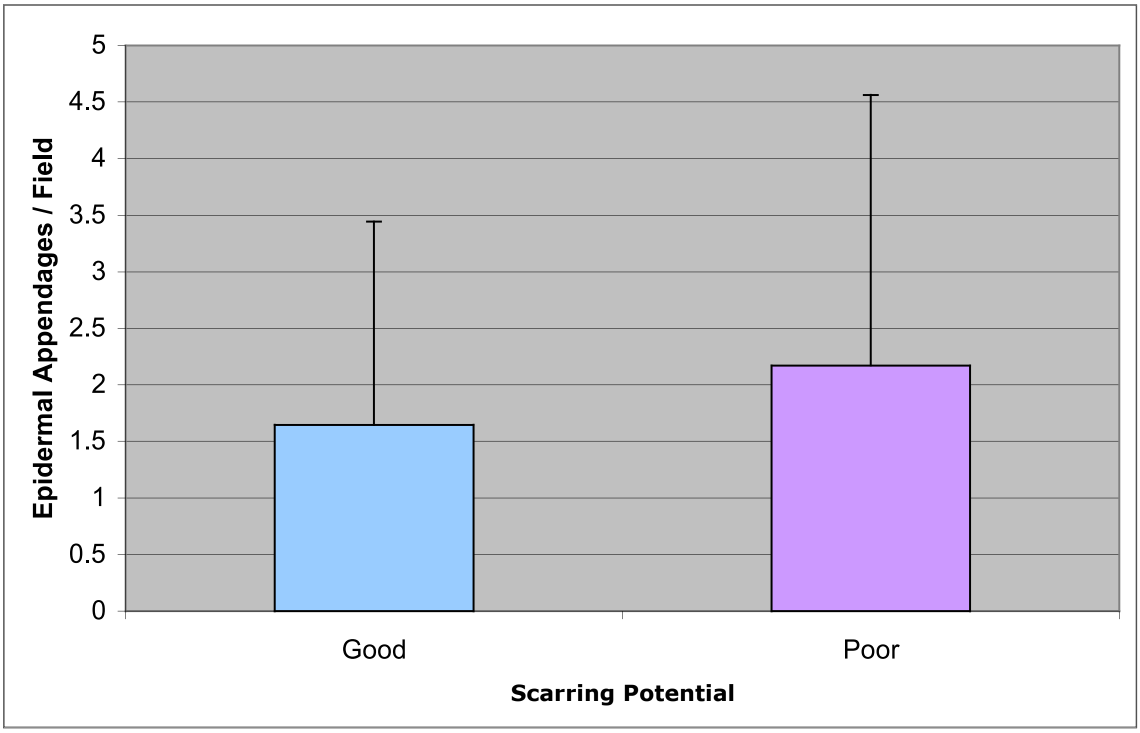

3.9 Collagen Fibre Orientation

Counts of collagen fibres with orientations parallel, oblique and perpendicular to the coronal plane per low power field were made and the relative proportion of each determined.

Table 3.10 Collagen Fibre Orientation for Each Body Region

Region	Number	Parallel fibres (%)	Oblique fibres (%)	Perpendicular fibres (%)
Deltoid	9	36.3	36.0	27.8
Abdomen	13	49.2	26.3	24.5
Sternum	10	44.2	23.9	31.9
Post-auricular	5	23.8	53.2	23.0
Earlobe	15	27.2	49.2	23.6
Eyelid	9	42.3	33.6	24.0

Graph 3.8 Relative proportions of collagen fibre orientation for individual body regions. The number of samples from each body region are as in table 3.5. The percentage of fibres in each orientation is shown.

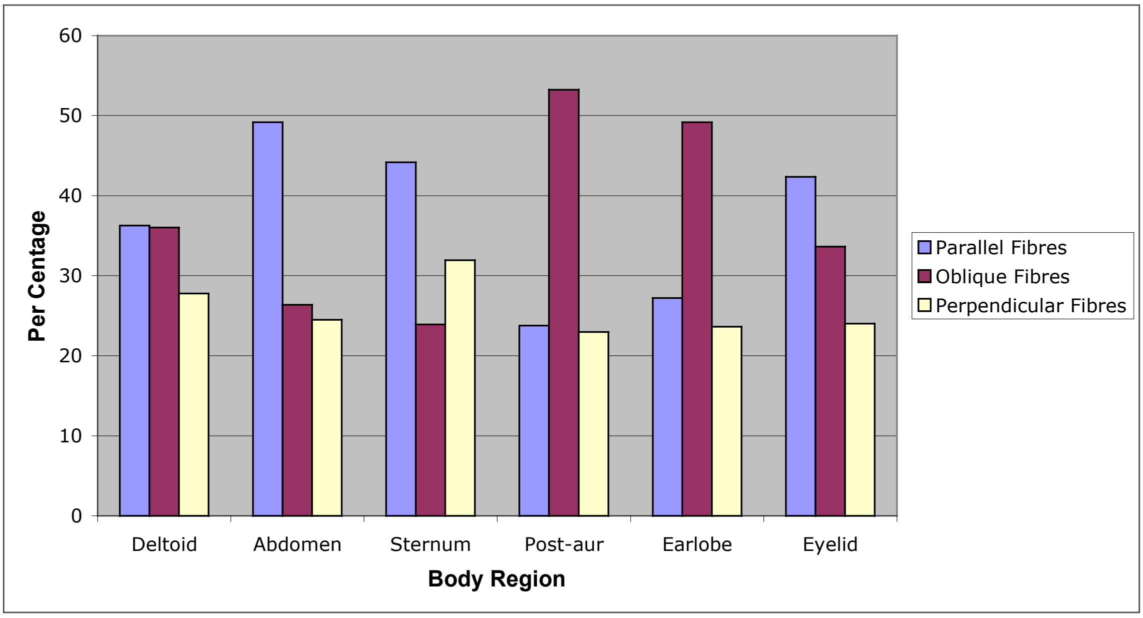

Table 3.11 Collagen Fibre Orientation for Body Regions Grouped by Topographical Location

Region	Number	Parallel fibres (%)	Oblique fibres (%)	Perpendicular fibres (%)
Head	26	30.7	45.7	23.6
Trunk	32	42.8	29.1	28.1

The proportion of parallel fibres was 39.4% higher in the skin samples from the trunk compared to those from the head. Using Students t test this was shown to be statistically significant with a p value of 0.003.

The proportion of oblique fibres was 57.0% higher in the skin samples from the head compared to those from the trunk. Using Students t test this was shown to be statistically significant with a p value of 8.4×10^{-5}.

The proportion of perpendicular fibres was 19.1% higher in the skin samples from the trunk compared to those from the head. Using Students t test this was not shown to be statistically significant with a p value of 0.077.

Graph 3.9 Collagen fibre orientation for body Regions grouped by topographical location. The number of samples from each location are as in table 3.3. Please refer to text on the previous page for p values.

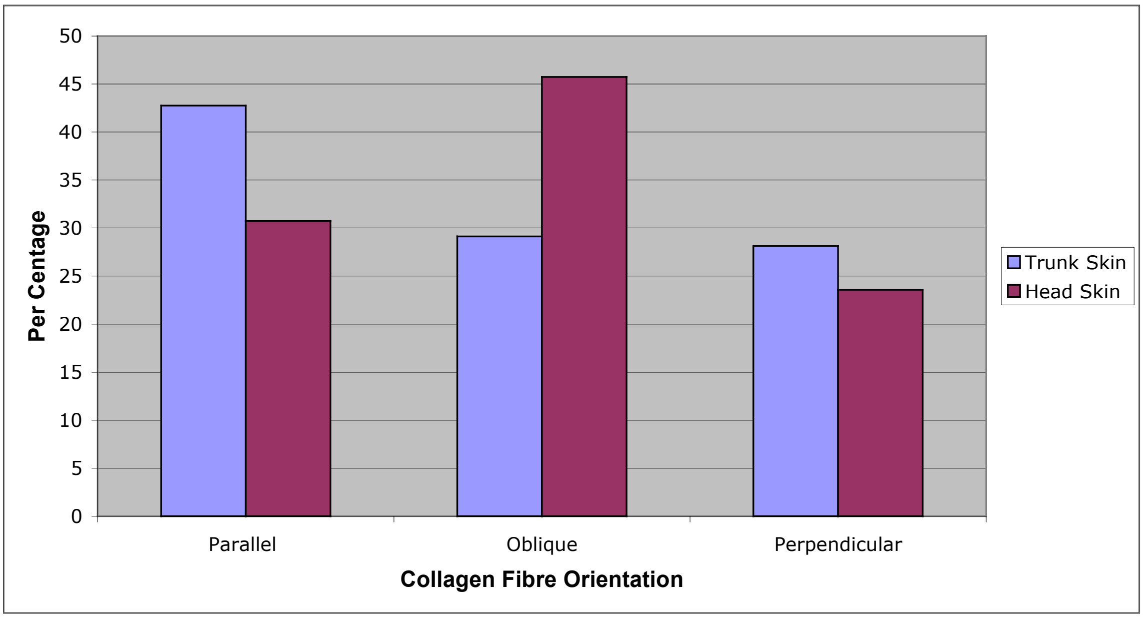

Table 3.12 Collagen Fibre Orientation for Body Regions Grouped by Scarring Potential

Region	**Number**	**Parallel fibres (%)**	**Oblique fibres (%)**	**Perpendicular fibres (%)**
Good	22	45.1	30.6	24.2
Poor	36	31.5	42.5	26.0

The proportion of parallel fibres was 43.2% higher in the skin samples from regions with better scarring potential. Using students t test this was shown to be statistically significant with a p value of 0.0001.

The proportion of oblique fibres was 38.9% higher in the skin samples from regions with poorer scarring potential. Using students t test this was shown to be statistically significant with a p value of 0.01.

The proportion of perpendicular fibres was 7.44% higher in the skin samples from regions with poorer scarring potential. Using students t test this was not shown to be statistically significant with a p value of 0.118.

Graph 3.10 Collagen Fibre Orientation for Body Regions Grouped by Scarring Potential. The number of samples from each location are as in table 3.4. Please refer to text on the previous page for p values.

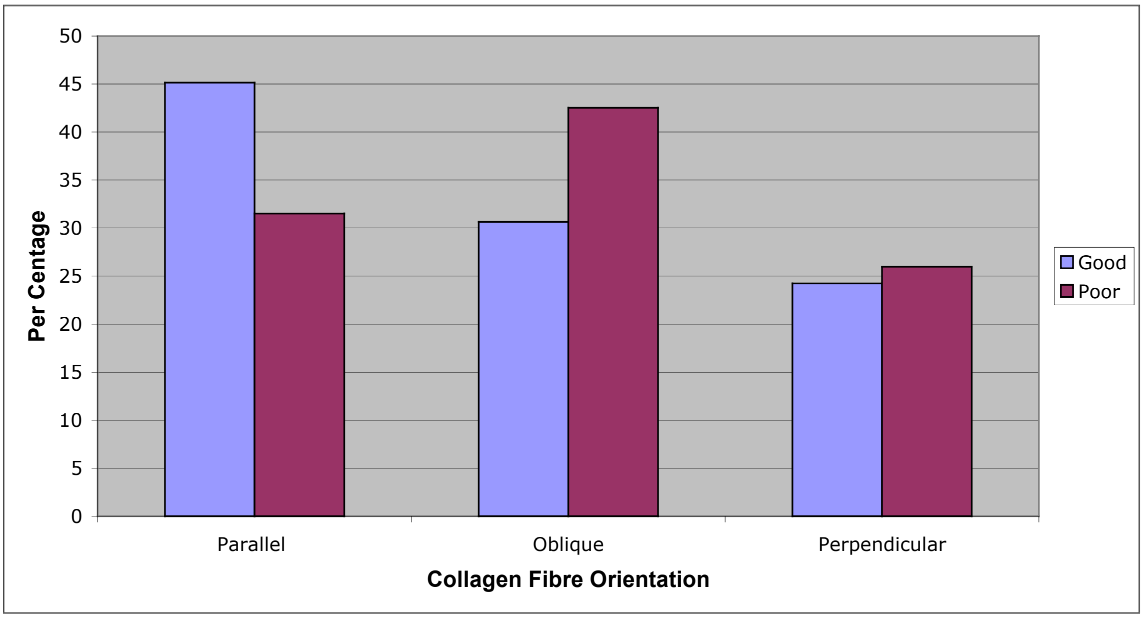

3.10 Ratio of Parallel to Oblique Collagen Fibres

Table 3.13 Ratio of Parallel:Oblique Collagen Fibres for Individual Body Regions

Region	Number	Parallel:Oblique Fibre Ratio
Deltoid	9	1.23
Abdomen	13	0.552
Sternum	10	0.585
Post-auricular	5	4.37
Earlobe	12	2.42
Eyelid	9	0.880

Graph 3.11 Ratio of parallel:oblique collagen fibres for individual body regions. The mean values of this ratio + SD are shown. The number of samples from each region are as in table 3.2.

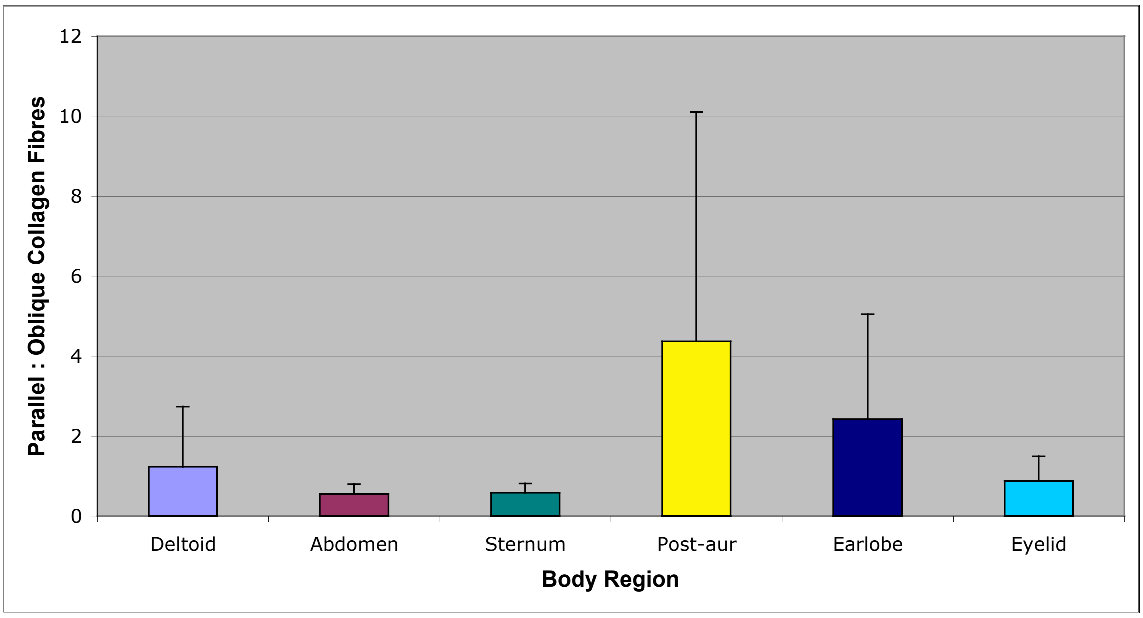

Table 3.14 Ratio of Parallel:Oblique Collagen Fibres for Body Regions Grouped by Topographical Location

Region	Number	Parallel:Oblique Fibre Ratio	SD
Head	26	2.32	3.21
Trunk	32	0.754	0.847

The ratio of parallel to oblique fibres is higher in the skin samples obtained from the head by 208%. Using Students t test this was statistically significant with a p value of 0.025.

Graph 3.12 Ratio of parallel:oblique collagen fibres for body regions grouped by topographical location. The mean values + SD are shown. The number of samples from each location are as in table 3.3. P value =0.025.

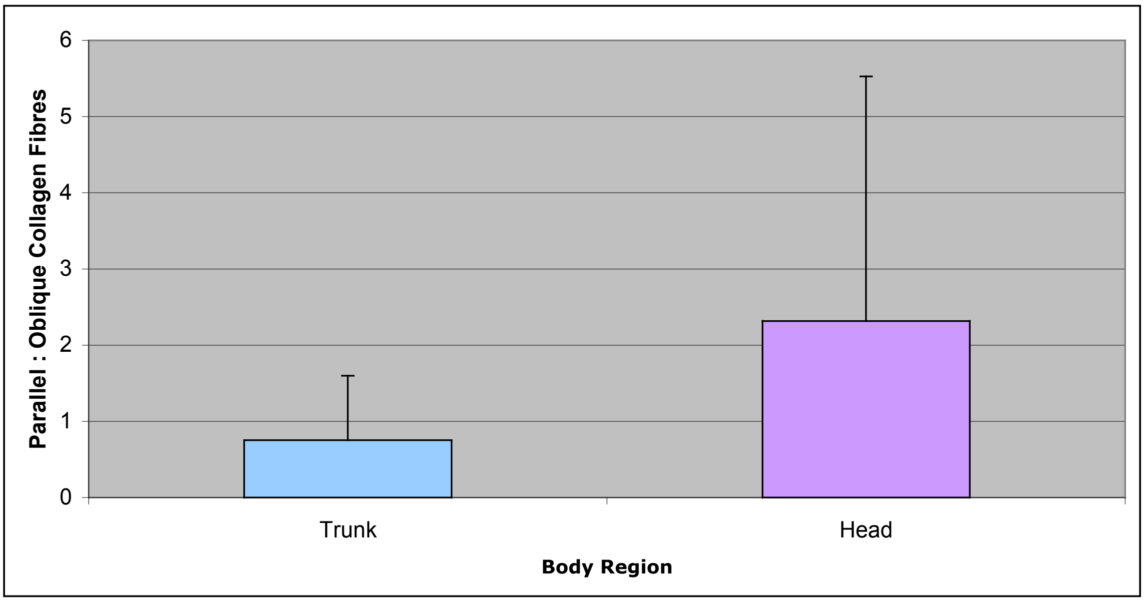

Table 3.15 Ratio of Parallel:Oblique Collagen Fibres for Body Regions Grouped by Scarring Potential

Region	**Number**	**Parallel:Oblique Fibre Ratio**	**SD**
Good	22	0.676	0.441
Poor	36	1.88	2.83

The ratio of parallel to oblique fibres is higher in those regions with better scarring potential by 64.2%. Using students t test this was statistically significant with a p value of 0.005.

Graph 3.13 Ratio of parallel:oblique collagen fibres for body regions grouped by scarring potential. The mean values + SD are shown. The number of samples from each location are as in table 3.4. P =0.005.

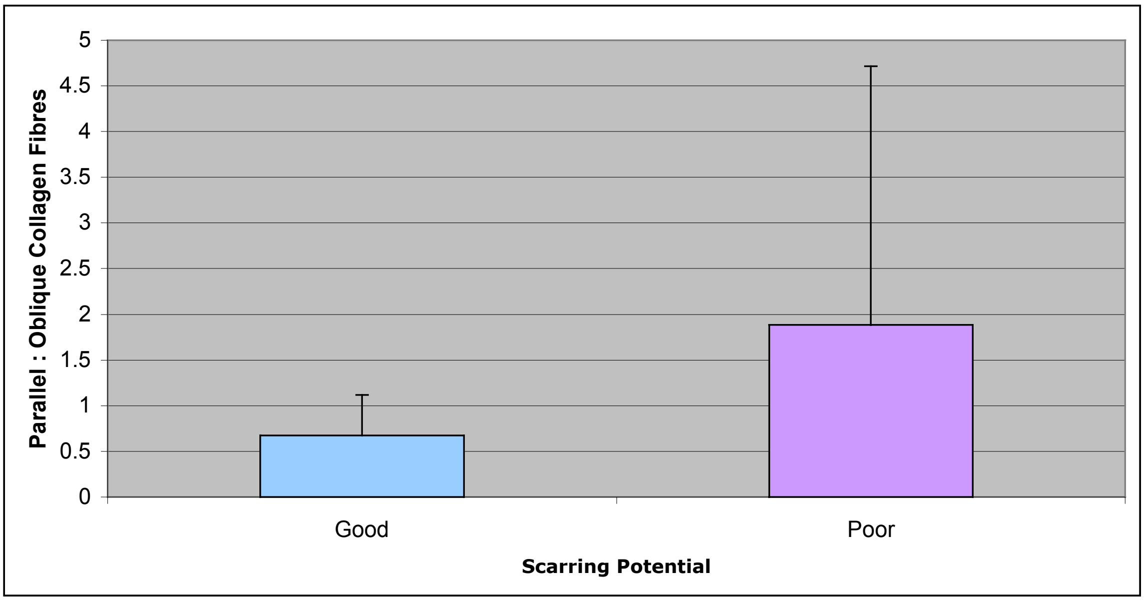

3.11 Subdivision of Scarring Potential by Topographical Location

Table 3.16 Ratio of Parallel:Oblique Collagen Fibres from Head Skin Samples Grouped by Scarring Potential

Region	Number	Parallel:Oblique Fibre Ratio	SD
Good	9	0.880	0.612
Poor	17	2.99	3.71

There was a statistically significantly lower ratio of parallel to oblique fibres in the skin with good scarring potential sampled from the head. Using Student's t test the p value was 0.03.

Graph 3.14 Ratio of parallel:oblique collagen fibres from head skin samples grouped by scarring potential. The mean values + SD are shown. There are 9 samples from regions with good scarring potential and 17 samples from regions with poor scarring potential. P value =0.03.

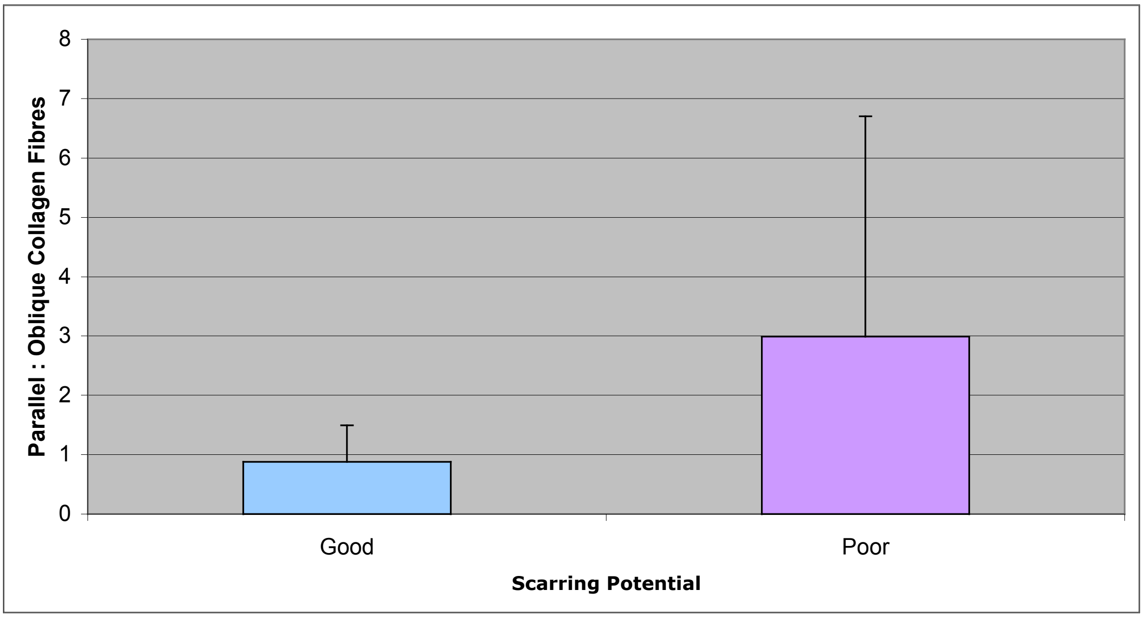

Table 3.17 Ratio of Parallel:Oblique Collagen Fibres from Trunk Skin Samples Grouped by Scarring Potential

Region	Number	Parallel:Oblique Fibre Ratio	SD
Good	13	0.552	0.248
Poor	19	0.892	1.07

There was no statistically significant difference in the ratio of parallel to oblique fibres in terms of scarring potential in skin sampled from the trunk. Using Student's t test the p value was 0.20.

Graph 3.15 Ratio of parallel:oblique collagen fibres from trunk skin samples grouped by scarring potential. There are 13 samples from regions with good scarring potential and 19 samples from regions with poor scarring potential. P value =0.20.

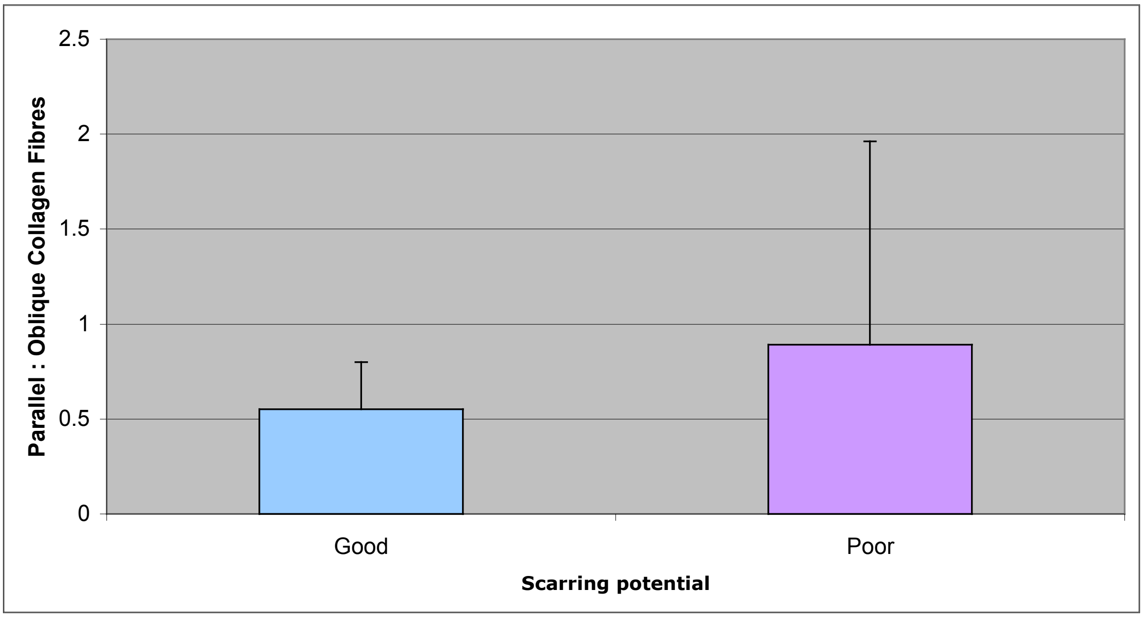

Chapter 4 Discussion

4.1 Histological Stains

Haematoxylin and eosin staining is used on a daily basis for both diagnosis and research. It can be automated, is cheap and easily reproducible. Its usage in the study of connective tissues has been famously questioned. It is worth quoting verbatim a passage from the comprehensive textbook of histology Gabe; he wrote:

"That has been outmoded since long ago and should have disappeared, but most authors seem to cling to it with a tenacity that is hard to understand; it is the hemalum-eosin technique. It may appear unnecessary to put this technique on trial again. P Masson has emphasised its sketchy nature at length in trying to convince his pathologist colleagues that resorting to a stain that makes guesswork of the distinction between different fibrous structures and ground substances, that does not bring out any tinctorial affinity, in short, that shows really nothing, amounts to voluntarily depriving oneself of much information easily obtainable by other techniques as sure as the indiscriminate smearing of eosin over sections whose nuclei have been stained with hemalum…But such authoritative opinion has not prevented the hemalum-eosin technique from pursuing a career far too brilliant for what it deserves…It is really due to an indifference for

histological technique and the force of habit that this method owes a triumph as undoubted as it is undeserved." (Gabe 1976)

So what of the conventional connective tissue stains? Whilst they may allow better distinction of connective tissue fibres compared to other structures, can they differentiate between different fibre types? Noorlander *et al* (2002) wrote,

"The Giemsa and H&E methods were not specific enough for collagen. Collagen fibres could barely be discriminated. The Shoobridge, Mallory and van Gieson methods were far better in that aspect. It was possible to discriminate collagen fibres in the sections. Unfortunately, these staining methods had the disadvantage that too low a contrast was obtained between collagen fibres and other structures in the sections. In addition to collagen fibres, glands and muscles were also stained, so that no specific segmentation of collagen fibres could be performed."

Against this background of relatively poor staining potential of routinely used techniques, are there any methods that are more specific for collagen and can be used on a routine basis?

The two most commonly used histological stains that are thought to provide reliable contrast between collagen types are picrosirius-polarization and Herovici's stain. In order to assess if one stain is clearer or more reliable I compared serial sections of tissue stained with each method. I shall consider each in turn.

4.1.1 Picrosirius-Polarization

The pattern of human dermal staining observed with this method for these studies is consistent with that reported in previous studies. (Constantine *et al* 1968, Junqueira *et al* 1983). Junqueira *et al* reported that **"*a finely woven meshwork of thin weakly birefringent greenish reticulin fibres (characteristic of collagen type III) in the adventitial dermis can be distinctly differentiated from the coarse collagen fibres present in deeper layers and that this was consistent among all the species of vertebrates studied*."** This pattern was seen in areas of normal rat skin, which would agree with Junqueira's observation about other vertebrate species. Surprisingly, in many of these studies the number of tissues that were studied is never clearly stated. This makes establishing the reproducibility of the method very difficult, if not impossible to assess.

The inclusion of rat wounds in this study was intended as a further control of the method. The greenish weakly birefringent fibres in areas of early granulation tissue was consistent with the pattern of staining observed in an experimental model of wound healing in mice (Hiss *et al* 1988). It also provided an opportunity to observe larger discrete areas of a high quantity of type III collagen and so establish the clear staining pattern of this collagen type.

When viewing slides under normal light microscopy, Sirius red stained most structures red, albeit with more intense staining of collagen fibres. The distinction between collagenous and non-collagenous fibres occurs only when slides are viewed under crossed polarized filters, as Sirius red does not impart birefringence to structures that do not naturally possess it (Junqueira *et al* 1979). However I observed that weak birefringence of the stratum corneum was displayed in a number of samples. The selectivity of this stain is also further questioned by the report that the picrosirius polarization method may also stain abnormal elastin fibres (Pierard 1989).

Furthermore not all fibres that were morphologically collagen fibres when viewed under light microscopy were still visible when crossed polarizing filters were applied. This occurred more commonly in the thin, more randomly orientated fibres particularly in the papillary dermis. It may be that when fibres are not aligned parallel to the slide their birefringence cannot be observed. Pierard (1989) indeed reported that this method might mask some dermal collagen fibres.

It is of great interest to note that each paper that uses picrosirius polarization exhibits slight variations in technique. They are however all based on one of two techniques, namely Junqueira *et al* (1979) or Dayan *et al* (1989). The key difference is an additional step of 30 minutes 1% acetic acid (Dayan *et al* 1989). Justification of this extra step is difficult to find as those authors using Dayan's method appear to do so unquestioningly (Koren *et al* 2001). Dayan *et al* (1989) reported that, "***longer periods of staining and differentiation allow more accurate standardization of the procedure.***" Having processed serial sections in an identical manner and either included or omitted this step as a verification, I could find no difference in the appearance of samples stained with either method. This step appeared unnecessary for staining formalin-fixed samples of both human and rat skin and in consequence was then omitted from the further histological studies which were undertaken.

Most histological studies of the picrosirius polarization method employed a haematoxylin counterstain. The addition of this stain improved discrimination of nuclei, cytoplasm and keratin when orientating slides under normal light microscopy prior to viewing under polarized filters. However it resulted in reduced visibility of thin, green and yellow, weakly birefringent, collagen fibres both in terms of numbers seen and colour intensity. In one of the original papers on this method Junqueira *et al* (1978) reported "***the green colour is observable only when intense illumination is used.***" My experience has been that these fibres were only visible when using a 100W mercury lamp. A possible explanation is that the haematoxylin absorbs some of the light, thereby reducing the intensity of illumination available to view slides with, analogous to using a weaker lamp. It could be argued that one does not need to use haematoxylin, but if this not done then positive identification of cellular structures is made much more difficult if not impossible.

It appears generally acceptable that collagen fibres studied with the picrosirius polarization method exhibit two distinct entities. Type III fibres are thin, greenish and weakly birefringent. Whereas type I fibres are thick, yellow or red and strongly birefringent (Montes *et al* 1980). However comparing the colours reported by different authors shows that assigning colours to different collagen types is not universally agreed.

A study exposing samples of liver tissue to collagenase in order to study collagen degradation (Perez-Tamayo *et al* 1980) found that as collagen fibre thickness reduced there was a concomitant reduction in intensity of birefringence and a colour-shift towards decreasing wavelengths from red to yellow to green.

The effect of tissue thickness on colour and intensity of birefringence was studied (Junqueira *et al* 1982) by subjecting dermal collagen samples of thicknesses ranging from 0.25 to 11 μm to the picrosirius–polarization method. A gradual shift from a weak greenish birefringence in thinner sections to a yellow birefringence in medium sized sections to a strong red birefringence in thicker sections. In my own study tissue section thickness was standard at 5 μm, as used in most conventional studies of any tissue. However in areas where there was a fold in the tissue section the intensity of birefringence increased accordingly and the fibres appeared brighter.

In a study of twelve purified collagens that varied in type and were classified as thin (0.8μm or less) or thick fibres (1.6-2.4 μm) and submitted to routine histological processing and picrosirius staining (Dayan *et al* 1989). It was found that thin collagen fibres displayed colours more in the green to yellow end of the spectrum and thicker fibres displayed colours with longer wavelengths in the yellow to orange end of the spectrum. In these isolated, purified collagen samples, fibre thickness determined the colour more than the collagen type. The authors concluded that fibre thickness could not be the only determinant of colour and the arrangement of fibres was important as tightly packed, better aligned fibres would show a shift to longer wavelengths.

Further evidence of the difficulties in ascribing colours to specific collagen types can be found by reviewing the colours reported by different authors in the literature.

Table 4.1 Polarization Colours of Thin Fibres (0.8 μm or less)

Each + represents 20% of the examined fibres. Reproduced from Dayan *et al* 1989

Type of collagen Colour	I 0.15 NaCl	I 0.1 Hac	I 0.5 HAc	I Ins	I 0.15 NaCl Lath	P-N-I 0.15 NaCl	P-N-I 0.1 HAc	II Pepsin	III sol	III Pepsin	P-N-III 0.15 NaCl	V sol
Green	++				+++	+++	+++				+++	
Bright Green	++	+++	++	+	++	++	++	++		+++	++	+++
Greenish Yellow	+	++	++	++				++	+++	++		++
Yellow			+	+				+	++			
Yellowish orange				+								
Orange												
Red												

Table 4.2 Polarization Colours of Thick Fibres (1.6-2.48 μm)

Each + represents 20% of the examined fibres. Reproduced from Dayan *et al* 1989

Type of collagen / Colour	I 0.15 NaCl	I 0.1 HAc	I 0.5 HAc	I Ins	I 0.15 NaCl Lath	P-N-I 0.15 NaCl	P-N-I 0.1 HAc	II Pepsin	III sol	III Pepsin	P-N-III 0.15 NaCl	V sol
Green					+						+	
Bright Green	+				++	+	+				+	
Greenish Yellow	+++				++	++	++				++	
Yellow	+			+		+	+	++			+	
Yellowish orange			+++	++		+	+	+++				
Orange		+++	++	++					+++	+++		+++
Red		++							++	++		++

Table 4.3 Varied Descriptions of Picrosirius-Polarization Staining Patterns by Different Authors.

Paper	Tissue Types	Colours Reported
Sweat 1964	Human liver, kidney, lung spleen	Connective tissue deep red. All other tissue bright yellow. Reticulum fibre "intensely stained"
Constantine 1968	Human skin	Yellow birefringence
Junqueira 1978	Multiple organs from humans and other vertebrates	Collagen type I- Brilliant orange, yellow or red Collagen type II-Blue or light yellow Collagen type III- Thin green fibres
Montes 1980	As above	Reticular fibres- thin, weakly birefringent greenish fibres. Collagen-thick strongly birefringent yellow or red fibres
Hiss 1988	Mouse cutaneous wounds	Spectrum of blue, green, yellow, orange and red with shades in between
Dayan 1989	Purified collagens of different sub-types	Variable spectrum from green, yellow, orange, and red with shades in between
Canham 1991	Human arteries	Type III collagen-yellow-green
Montes 1991	As Montes 1980	Collagen I- Thick, strongly birefringent red and yellow fibres. Collagen III-Thin, weakly birefringent greenish fibres
Trau 1991	Connective tissue nevi	Normal dermis-orange to red. Nevi: Thin fibres-green to yellow, thick fibres-green to greenish yellow to yellow
Rabau 1994	Rat intestine	Thin fibres-green, greenish yellow, yellow, yellowish orange, Thick fibres-yellow and yellowish orange
Noorlander 2002	Piglet skin	Thin yellow or green fibres Thick mostly red fibres
Madruga de Melo 2003	Human vocal fold	Type I collagen-Thick yellow or red, strongly birefringent fibres Type III collagen-green, fine, weakly birefringent fibres
Har-Shai 2003	Human keloids	Thick red (mature) collagen fibres. Thin, green collagen fibres (young)

While it has never been claimed that a specific interaction occurs between Sirius red and collagen to result in differential staining of collagen subtypes (Junqueira *et al* 1979) the importance of their physical arrangement and fibre thickness is said to play an important role (Dayan *et al* 1989). The variability of descriptions seen for each collagen subtype indicates that a spectrum of colours is actually observed. This makes a reproducible study extremely difficult.

In my own study I noticed that both thick and thin fibres displayed considerable variability of colours. This manifests itself in two ways. Firstly, either fibres that were yellow, red, orange or green and of similar thickness co-existed in the same area of a slide (Fig 4.1). Secondly different areas on the same fibre displayed different colours for example a thick red fibre may be yellow at its peripheries, or different areas of the same thin fibre may be green or yellow (Fig 4.2). Although less colour variability was seen in mature scar tissue. This may be due to its more orderly parallel arrangement compared with the basket weave pattern of normal reticular dermis. Pierard (1989) found that the colours could further change when the slide was rotated on the stage of the polarizing microscope and also noted this colour variability. This may explain why fibres are termed greenish instead of green. It may further be suggested that the differences in colour that are reported are not caused by actual differences of method or results, but are the subjective reporting of the same colour spectrum by different individuals. In view of this variability of colour reporting and the overlap in colour by different collagen types (Dayan *et al* 1989) and given that serial sections comparing immunohistochemistry and picrosirius polarization have never been undertaken I would agree with those authors who feel that collagen type cannot be ascribed by the picrosirius polarization method. (Pierard 1989, Canham *et al* 1991).

Fig 4.1 Section of human abdominal skin stained with picrosirius solution. Viewed at X20 magnification under crossed polarized filters. Note the yellow and occasionally green colours at the edge of the thick red collagen fibres.

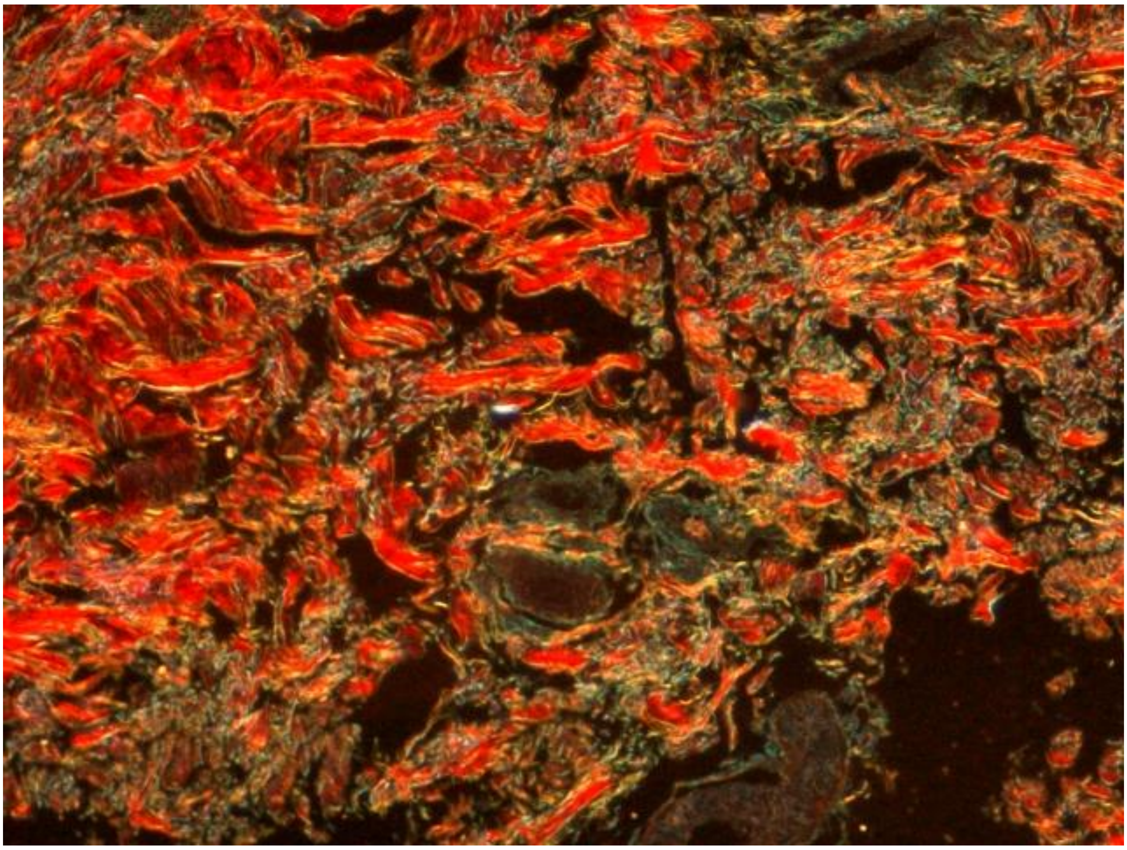

Fig 4.2 Section of human breast skin stained with picrosirius solution. Viewed at X20 magnification under crossed polarized filters. Thin yellow, green, orange and red collagen fibres all co-exist in close proximity in the upper dermis.

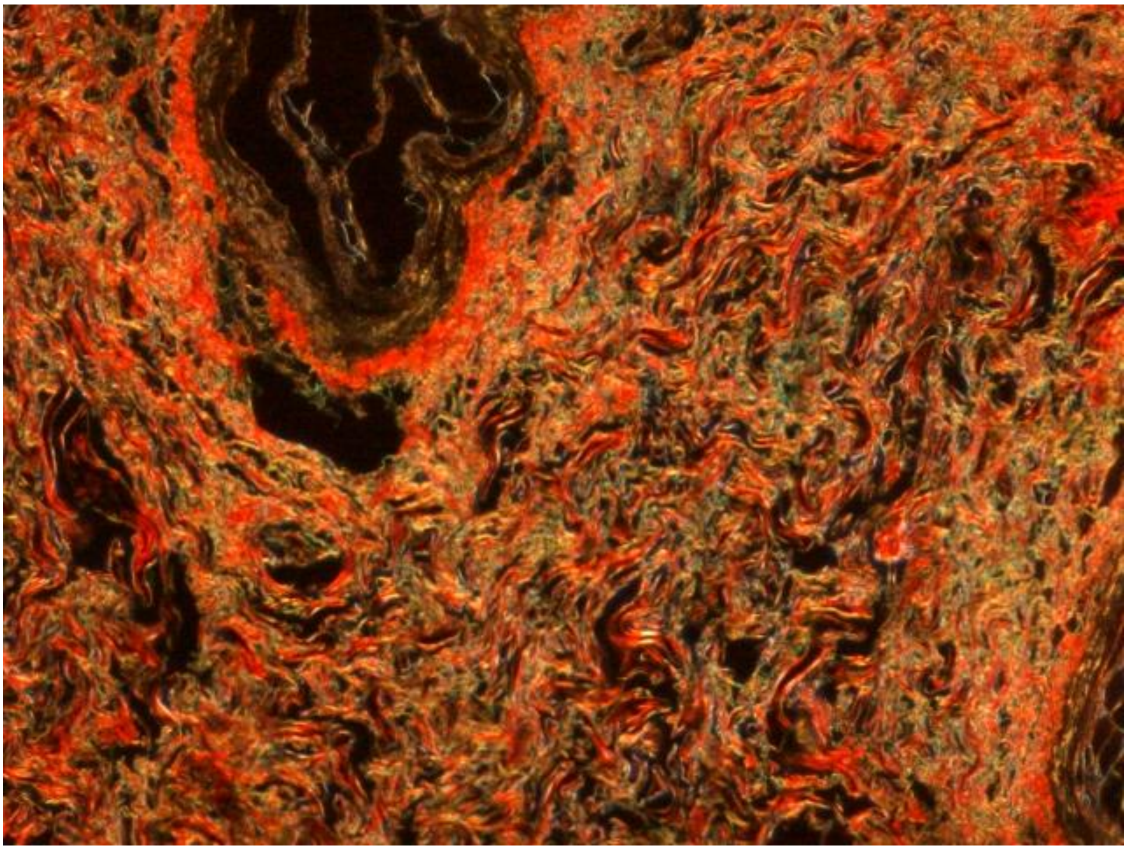

After picrosirius staining it is now appropriate to consider the second method which was extensively used in this study, namely Herovici's technique.

4.1.2 Herovici's Staining

The colours and patterns observed when staining were easily reproducible and consistent with those reported by other authors. Nuclei appeared dark brown, cytoplasm stained greenish brown, red blood cells and hair shafts were stained yellow, and collagen fibres displayed a consistent differential staining pattern of red and blue. (Herovici 1963) The blue fibres were thin and the red fibres were usually thick, though some thin and medium red fibres were also seen. In addition blue fibres were found to form a sleeve around thick red fibres (Fitzgerald *et al* 1996). This pattern was repeated in the adnexal dermis with thin blue fibres surrounding blood vessels and epidermal appendages in a concentric manner, thin and medium sized red fibres in turn surrounded this before merging with thick red fibres of the surrounding dermis. The pattern of dermal collagen staining, with a sub-epidermal layer of thin blue fibres, and thicker red fibres in the deeper dermis surrounded by blue fibres is consistent with work reported by Levame *et al* (1987) and Fitzgerald *et al* (1996). Serial sections comparing Herovici's stain in skin to immunohistochemical staining have shown that the blue fibres correspond to type III collagen and the red fibres to type I collagen (Levame *et al* 1987 and Fitzgerald 1997).

Although red and blue fibres exist in close proximity to each other they are easily distinguished using standard optical microscopy even at low powers of magnification. Thus Herovici's stain provides a cheap, reproducible and simple technique that has been used to examine the relationship of collagen fibres of types I and III in the healing processes of various tissues (Mackay *et al* 1972, Griffioen *et al* 1987, Lamme *et al* 1998, Furuzawa-Carballeda *et al* 2002).

The network of thin fibres of type III collagen characteristic of the papillary dermis are quite distinct from the basket-weave of thick bundles of type I collagen in the reticular dermis (Elder *et al* 2004). The boundary between these two regions is much less clear. There is some debate regarding where and how exactly to draw the line between papillary and reticular dermis. Some authors refer to this area as a junction, implying a discrete change in structure, while others refer to an interface, suggesting a more gradual mixing of fibres. Montagna (1962) states that in many mammals the distinction between papillary and reticular layers is not clear. He later (1974) referred to the division of the dermis into an upper papillary layer and lower reticular layer as "arbitrary". It is accepted that the superficial dermal vascular plexus is located somewhere between the papillary and reticular dermis. However, it has been stated that this interface is usually identified by the position of the superficial vascular plexus (Fig 4.3) (Royal College Pathologists 2002). Although many authors do not attempt to define its exact level (Elder *et al* 2004 Gray *et al* 1995), or will simply state that the papillary dermis accounts for 10% of the dermis and the remaining 90% is reticular (Ebling *et al* 1992).

Fig 4.3a Herovici's staining of abdominal skin at X20 magnification. Note the superficial vascular plexus (indicated by arrow) appears to lie surperficially within an area of thin red, type I collagen fibres.

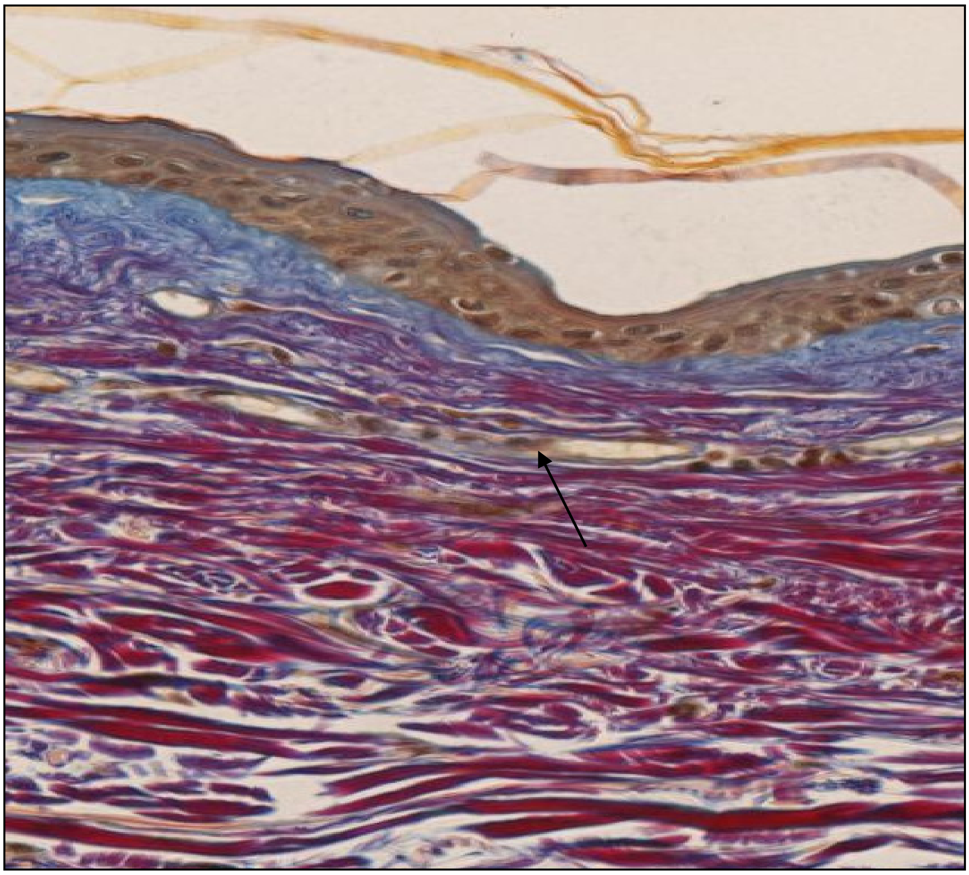

Fig 4.3b Herovici's staining of abdominal skin at X20 magnification. Compare the location of the superficial vascular plexus (shown by arrow) with Fig 4.3a. It is slightly deeper, but still within thin red type I collagen fibres.

Fig 4.3c Herovici's staining of abdominal skin at X20 magnification. Compared with Figs 4.3a and b, the superficial vascular plexus (shown by arrow) is at a deeper dermal level and appears to rest on thicker type I collagen fibres.

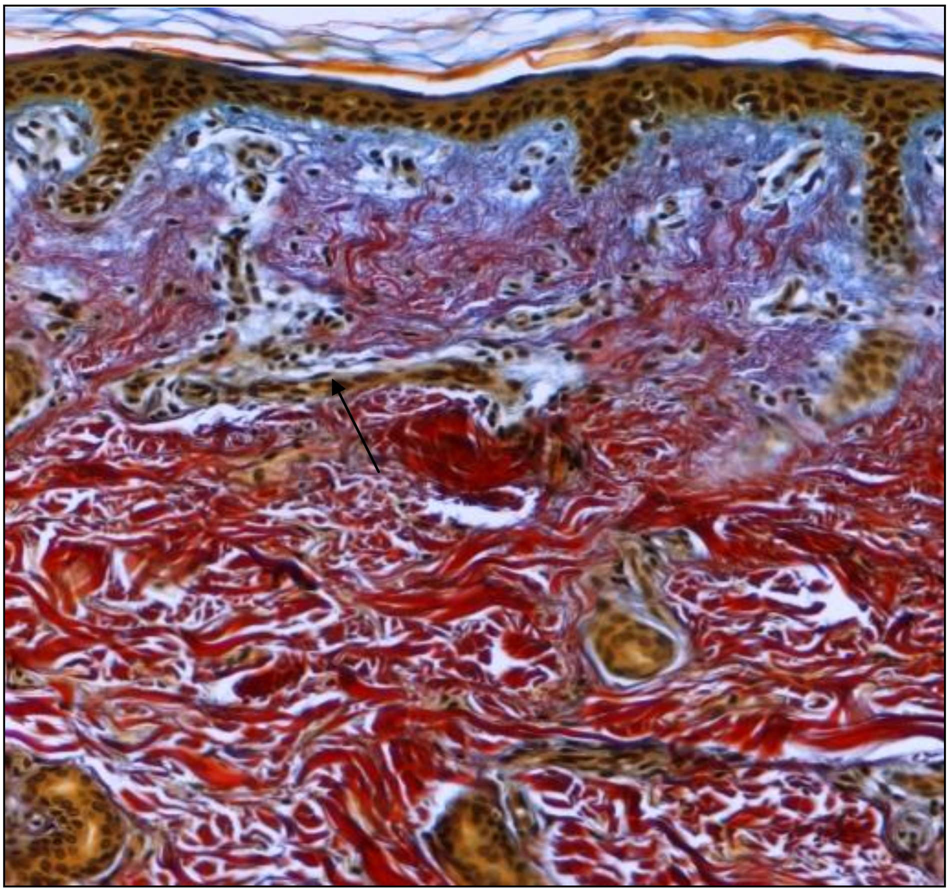

This is of clinical importance in the staging of malignant melanoma. Clark *et al* (1969) reported that the prognosis of melanomas was directly related the anatomical level of their invasion. He described five levels.

Level I: All tumour cells are above the basement membrane.
Level II: Neoplastic cells have broken through the basement membrane and extended into the papillary dermis, but not the reticular dermis.
Level III: The interface between papillary and reticular dermis.
Level IV: Extension of neoplastic cells between collagen bundles characteristic of the reticular dermis.
Level V: Tumours have invaded into subcutaneous tissue.

In this paper he describes the papillary-reticular dermal interface as somewhat ill defined, where collagen begins to be organized into bundles. Level III exists as, ***"a number of melanomas where the base of the tumour seemed to form an almost straight line and impinge upon the upper part of the reticular dermis without showing any significant invasion of the reticular dermis. Our statistical studies suggest it is justified to use level III as a separate category."*** (Clark *et al* 1969).

Breslow (1970) reported that tumour thickness was an important prognostic indicator in malignant melanoma. It has been shown that tumour thickness may be a more important determinant of survival than depth of invasion in the majority of cases. However Clark's levels are still of prognostic importance in thin melanomas that have invaded deeply into the dermis, despite their size. (Morton *et al* 1993, Buttner *et al* 1995). It is still recommended that they are included in histopathology reports (Marghoob *et al* 2000, Royal College of Pathologists 2002). Clark's levels may also be of prognostic value in squamous cell carcinoma (Royal College of Pathologists 2002).

4.1.3 Transverse Tissue Sections

Herovici's stain was used on sections of skin cut at 90 degrees to the conventional procedure for orientating specimens as described in 2.1.6. These are referred to as transverse sections in this study. This was performed as it was thought that it may shed further light on how collagen fibres were distributed within the skin.

However from the very beginning, transverse sectioning of tissue presented great practical difficulties. When sectioning the paraffin blocks it is not possible to know the precise dermal level being cut. Different levels of tissue appear on the same section. This is because the epidermis is never perfectly flat, different areas within the same sample will be of different thicknesses, as well as the difficulty in orientating the tissue block precisely parallel to the microtome blade. Despite this, these sections offered a further dimension to the histological study of skin structure. It showed in more detail the intermingling of collagen types at the papillary-reticular dermal boundary. Thin, blue type III collagen fibres were seen, however these are clearly seen intermingling with red type I collagen fibres that were initially thin and then medium sized with increasing dermal depth before becoming thick bundles characteristic of the reticular dermis (Figs 3.21-3.23). This information is consistent with and expands upon the pattern seen with conventional vertical tissue sections; namely that in the sub-epidermal region all fibres were thin and blue, corresponding to type III collagen. As dermal depth increased so did the size and quantity of red type I collagen fibres. This change in the nature of dermal connective tissue is gradual and supports the idea that the change between papillary and reticular dermis does not exist as a junction. Perhaps it should be regarded as an “interzone” and defined as the band of dermis where the greatest intermixing of type I and type III collagen fibres occurs. The superficial vascular plexus is located in this region, but at a variable level.

This method of sectioning produced some very unusual views of human skin. The technique shows the very delicate fibre arrangement and orientation which conventional sections simply do not. This may be a useful technique for other workers to consider in the future.

At either end of the dermis it may be straightforward to distinguish the papillary and reticular dermis with H&E or more conventional connective tissue stains. However these are less discriminating at their boundary. The enhanced contrast of collagen fibres that Herovici’s stain offers may add a further dimension to histological assessment of this area. Herovici's stain may be of help in cases where a malignant melanoma's level of invasion of is uncertain between Clark's levels II and III or III and IV using conventional staining. The pattern of dermal collagen distribution observed with Herovici's stain agrees with Becker *et al* (1976) and Meigal *et al* (1977) who showed that type III collagen was the main collagen in the papillary dermis and adnexal dermis. It is also compatible with Tajima and Nagai's (1980) findings in a biochemical analysis of calf skin that type III collagen decreases with depth. It agrees with the findings of Junqueira *et al* (1983) using picrosirius polarization, silver staining and electron microscopy, where he found that the thin, argyrophilic, green and weakly birefringent fibres of the papillary dermis were likely to be type III collagen and distinct from the thick, red type I collagen fibres of the reticular dermis. My findings disagree with the work of Epstein and Munderloch (1978) who used biochemical analysis Pieraggi *et al* (1984) using immunochemical techniques to study type I and III collagen at different depths of dermis found that the ratio of both collagen subtypes was constant irrespective of depth. The latter seriously questions the specificity and value of immunological techniques to study collagen.

4.1.4 Comparison of Herovici's Stain and Picrosirius Polarization

Cumulatively both techniques have been used in numerous different settings, as reported earlier, showing the usefulness of a histological stain that can differentiate collagen subtypes. Picrosirius polarization has been used significantly more than Herovici's stain in the past, but does this mean it is the superior stain?

Both stains make a distinction between the thin fibres of the papillary dermis and the thick fibres of the reticular dermis. Both show the thin fibres of the adnexal dermis. Both are thought to distinguish between collagen I and III. Picrosirius polarization has never been compared to immunohistochemistry on serial sections, but Herovici's stain has (Levame *et al* 1987, Fitzgerald 1997). The difficulties in reporting colour variability of picrosirius polarization do not occur with Herovici's stain, suggesting that is the clearer of the two. Picrosirius polarization requires a microscope with crossed polarizing filters and a powerful (100W) light source, whereas any optical microscope will suffice for studying Herovici's stain again suggests that Herovici's stain is perhaps more appropriate as it requires less demanding apparatus. When examining tissues stained with Herovici's technique one has clear distinction between collagen subtypes, nuclei and cytoplasm at the same time. In studying tissue with picrosirius-polarization the collagen subtypes are distinguished only when viewed through crossed polarizing filters, eclipsing any nuclear staining, which is visible only when the birefringence of collagen fibres is not. Therefore Herovici's is the more informative of the two stains. Owing to the additional information and clarity offered by Herovici's stain, it was decided that it was unnecessary to continue using picrosirius polarization for the remainder of the study.

4.1.5 Variations of Herovici's Method

Herovici's method comprises several steps employing different reagents to stain different tissue components. Celstine blue, iron alum, and haematoxylin stain nuclei. Metanil yellow stains cytoplasm. The connective tissues are stained by methyl blue and acid fuschin in picric acid (Herovici 1963). It has been observed that acid fuschin may fade after a few months and this was the motivation behind the discovery of Sirius red in picric acid as a connective tissue stain (Constantine *et al* 1968). I have not observed any fading on slides stained with Herovici's method that are over a year old, although that does not mean they may not fade in the future.

I performed several variations of Herovici's method that were designed to examine the possibility of substituting Sirius red for acid fuschin with the aim of imparting a red colour to type I collagen fibres, while retaining the blue staining of type III fibres without the potential problem of sections fading with time. All the initial steps of the staining protocol were identical to Herovici's method described earlier, only the constituents of solution F were altered.

The combination of Sirius red, methyl blue, picric acid and glycerol produced interesting results in normal human skin. The nuclei were dark brown, cytoplasm greenish brown and hair shafts and red blood cells were yellow as with Herovici's stain. However the collagen fibres stained very differently; there were thin, blue fibres and thick, green fibres. The fibres that had stained red with Herovici's now appeared green. Additionally the wrapping of these fibres with thin blue fibres was now more evident. The other major difference with Herovici's stain was that there was purple staining at the basement membrane of the dermo-epidermal junction. This was present in 15 of the 17 skin samples tested with the technique. It is important to note that in 3 of the samples there was also some purple staining of collagen fibres in the superficial dermis. The purple staining of the basement membrane corresponded to the purple regions stained with PAS reaction.

As a control, sections of normal rat kidney were stained with this method to further examine the staining of basement membranes. Nuclei and cytoplasm stained as before. Purple staining of the tubular basement membranes was evident in all samples and corresponded with positive regions on PAS staining.

Removing Sirius red from the modified solution F resulted in an identical staining pattern, without the purple basement membrane zone, consistent with the findings of Fitzgerald (1997).

Substituting methyl blue in water for solution F for resulted in dark purple nuclei with non-specific pale blue staining of all other structures. This finding was unsurprising given that a number of connective tissue stains rely on competition between two acidic dyes.

From these reactions it seems that methyl blue in picric acid is responsible for the differential staining of collagen seen in Herovici's stain, as has been previously reported (Fitzgerald 1997). When acid fuschin is substituted for Sirius red in solution F a competition occurs between the dyes, with picric acid and methyl blue diffusing into the dermal collagen fibres; perhaps this leaves Sirius red to diffuse into and attach to the type IV collagen in the basement membrane. The basement membrane staining corresponds to that of PAS staining, but offers potentially more information. Two other collagen stains have been shown to produce a similar purple staining at the dermo-epidermal junction. Hale's luxol fast blue stained connective tissues blue and basement membranes purple. This staining is due to the PAS reaction as these are some of the reagents used in this stain. (Hale *et al* 1960). Lillie's allochrome stain (Lillie 1951) also shows a similar staining pattern and employs Schiff's reagent. This variation on Herovici's stain offers potentially more information than these stains. Whilst it may be too complicated for routine diagnostic use it may be of use for future research on skin or perhaps in wound healing studies where the role of the epidermal basement membrane remains controversial.

4.2 Tissue Sample Orientation

The idea of carefully orientating tissues samples prior to histology is not a new one. However little attention is given to this prior to study. An example of histological research where this has been used to good effect was in a study of the infra-mammary fold (Boutros *et al* 1998). There has been debate as to whether the infra-mammary fold is maintained by ligaments or by a specialized dermal structure. Ten breast tissue dissections were performed on female cadavers, the tissue was orientated and marked. Control sections of skin from the upper chest and abdomen were taken for comparison. Picrosirius polarization was used to study the orientated dermal sections. No ligamentous structures were found on gross dissection. On microscopic examination, collagen bundles were packed densely and orientated in parallel to the long axis of the infra-mammary fold at all levels of the dermis. This pattern was not seen in control tissue. The authors concluded that the infra-mammary fold was maintained by modification of the dermis and not by a ligamentous structure. These conclusions would not have been valid without careful orientation of the tissue studied.

Attempts have been made to determine the orientation of dermal collagen fibres elsewhere in the body, particularly in reference to relaxed skin tension lines. Pierard *et al* (1987) used optical and scanning electron microscopy to study skin samples where the tension was preserved during excision and those where it was not. To preserve skin tension, firstly relaxed skin tension lines were determined by pinching the skin as described by Borges (1962). Plastic rings were glued onto skin prior to excision to maintain skin tension. Other areas of skin that were allowed to retract during excision were also studied for comparison. Samples were sectioned either in parallel to or perpendicular to the relaxed skin tension lines. No preferential orientation of the largest collagen bundles was seen, however the thinnest collagen bundles and elastic fibres were straightened and ran in the direction of relaxed skin tension lines. In skin samples that were allowed to retract on biopsy the collagen bundles were interwoven and orientated multidirectionally. This paper shows some association between collagen fibre orientation and relaxed skin tension lines. It also shows that it is necessary to preserve this tension when sampling tissue to preserve valuable information. Unfortunately the information for this study was gained from only two specimens of wide excision for malignant melanoma.

Cox (1941) explored the relationship between skin tension and collagen fibre orientation. He made 22,600 puncture wounds with a round, metal, marline-spike in 28 cadavers and observed the direction of tension, which he termed cleavage lines. He also studied histological samples of skin orientated in parallel to and perpendicular to the long axis of the cleavage lines and found “the majority” of collagen fibres ran in parallel to them, with the remaining fibres “interlacing.” Unfortunately no quantification or statistical analysis was performed to support this statement. He suggested that this pattern of collagen orientation was an adaptive response to increased skin tension.

Further support to the idea that collagen fibres align themselves along lines of tension comes from Gibson *et al* (1965) who applied stretching forces to samples of skin. He found that when skin was stretched as length increased there was a corresponding reduction in width at right angles to the stretching force. He noted that in the relaxed state collagen fibres were not orientated in a particular direction. However when subjected to stretching forces collagen fibres become increasingly aligned in the direction of force. He found that these changes occurred in the reticular dermis. He concluded that dermal collagen fibres form an intertwined meshwork that moves and changes with the stretching and relaxation of skin.

When working with embalmed cadaveric tissue there was an absence of tissue retraction as the skin samples were excised. It would appear that during the embalming process the skin is fixed under tension, thus preserving any alignment of collagen fibres with lines of tension. As an extra precaution to prevent any further tissue retraction and loss of this orientation that samples were pinned out to length onto thick card prior to secondary formalin fixation upon removal from the cadaver as described in section 2.1.3.

There has been no standard accepted method to determine the orientation of collagen. I have attempted to count the direction of fibres in the reticular dermis marked on photographs of light microscopy samples of known orientation. Whilst this method may be time consuming it is quantitative and does not rely on any assumptions about the collagen structure. Determination of collagen orientation has been attempted in the past. Van Zuijlen *et al* (2002) states that**, "*an optimal technique for assessing collagen orientation has not been established*."** Inter-observer assessment of histological images with Fourier analysis of computer-generated images was compared. A five-step scale was used for describing the orientation of fibres: extremely parallel, predominately parallel, mixed organization, extremely random, predominately random. However the orientation of the tissue specimens relative to the body sampled from was not known. This was compared to computer-generated images composed of multiple ellipses of varying widths. This generated an orientation ratio that ranged from 0 (perfectly parallel) to 1 (perfectly random). It was found that Fourier analysis was more reliable than the histological scale used. This is not surprising since a qualitative method was compared to a quantitative method.

There have been many attempts to describe lines of skin tension (Borges 1984). Since this study used cadaveric tissue it would be more appropriate to consider Langer's lines, which were determined on cadavers (Gibson 1978). All tissue samples were orientated in the same direction. This allowed direct comparisons between body sites to be made. Whilst we found an intermixing of reticular dermis collagen bundles in different directions as previously described (Gibson 1965, Van Zuijlen *et al* 2002) there were statistically significant differences in the relative proportions of fibres in each direction. The proportion of fibres orientated perpendicular to the coronal plane was similar in all regions. Gibson (1978) organized a translation of Langer's original papers on various properties of skin, including Langer's lines. The direction of Langer's lines indicated on the paper corresponded to the majority direction of the collagen bundles in only two regions, the eyelid and abdomen, Interestingly these are the regions in the study that we have regarded as having good scarring potential. The direction of Langer's lines on post-auricular skin was not clearly indicated on the original paper.

It was not possible to fully assess the direction of the thin collagen fibres using light microscopy. A separate study using electron microscopy would be necessary to take the observations of Pierard *et al* (1987) further and compare and quantify the direction of these to Langer's or skin tension lines.

4.3 Tissue preservation

The use of cadaveric tissue offers the benefit of studying skin from regions not normally available during routine surgical operations. However few studies have performed histology on embalmed cadaveric tissue. At the outset of this project, the suitability of this tissue was not known. Changes may occur post-mortem and histological detail may not be adequately preserved. Encouraging evidence from the literature included one study (MacBride 1998) that examined embalmed medical school cadavers for the presence of mast cells on histology commented that this potential source of human tissue was "virtually untapped". Using alcian blue and avidin conjugated to fluorscein isothiocyanate they were able to detect the presence of mast cell granules equally well in embalmed cadaveric, unembalmed cadaveric and fresh surgical tissue samples. This suggested that "delicate" cells could be preserved in such tissue. Other studies on more extreme forms of preserved tissue such as mummies have found encouraging results. Perrin *et al* (1994) studied skin from two Egyptian mummies embalmed between 150 BC and 90 AD. Transmission electron microscopy was performed on material that had dried out and shrunk. The epidermis was reported to be well preserved with different cell layers, desmosomes and intercellular connections observable. Collagen fibrils formed thick bundles and demonstrated axial periodicity. Elastic fibres were also recognizable, as were some bacterial spores. Similar findings were reported by Hino (1982) using transmission and scanning electron microscopy to examine the skin of an Egyptian mummy embalmed between 100 and 300 AD. Montes *et al* (1985) observed that collagenous structures in an Egyptian mummy displayed increased birefringence when studied with picrosirius polarization, showing that preservation of these structures in mummified tissue was similar to that in fresh controls. Stucker *et al* (2001) studied skin samples from six 1600-2300 year old bog bodies from North Germany. Dermal collagen bundles were observed and appeared similar to more recently stained samples. However epidermis was not preserved and no cellular elements could be found. Histological study of the Tyrolean ice man (Hess *et al* 1998) a 5200 year old glacier mummy showed skeletal and connective tissues and the nervous system were well preserved, however epithelial, muscle and reticular connective tissue had disintegrated. By their nature these studies can only be performed on a small number of samples. They show that dermal collagen can be well preserved even after thousands of years. Other cutaneous structures are less resistant to decay, but in the case of Egyptian mummies where volatile oils are used preservation is still possible. In comparison there appeared to be a strong chance that cutaneous structures would be suitably preserved in bodies that have been embalmed within 48 hours post-mortem and carefully stored.

Brzezinski *et al* (2002) studied post mortem changes in human epidermis. It was found that keratinocytes in the spinous layer developed a hollow space around nuclei. The number of these cells increased up to day 8 post-mortem. From the second day post-mortem, nuclei in the spinous layer became crescent shaped. From the third day post mortem, groups of cells in basal layer with pale cytoplasm and shrunken nuclei grouped together and separated from the underlying dermis. In conjunction with a number of other histological changes these allow time since death to be estimated. The cadaveric samples show an increased number of the cells in the spinous layer with a hollow area surrounding the nuclei compared with operative samples. None of the other changes reported are seen, showing that the cadavers were preserved within two days of death and that the embalming process arrests any further structural changes at the microscopic level.

The preservation of collagenous structures was very similar between operative and embalmed cadaveric samples. The epidermis was similarly preserved with the exceptions described above. The appearance of epidermal appendages and blood vessels was identical in both groups of samples (Fig 4.5). The level of preservation of cadaveric tissue included erythrocytes visible within vessels fig 4.6). The degree of histological preservation is therefore suitable for tissues to be used for further study. However some differences in the two groups of specimens were observed. The epidermis of cadaveric specimens was significantly thinner than that of the fresh operative samples. In some, though not all, cases the dermal collagen fibres appeared more closely packed together in the cadaveric tissue. These small variations as a result of the embalming process must be taken into account when studying this type of tissue. However the ability to study areas of skin not normally available through routine operations compensates amply for this and is surprising that this tissue has not been utilised more in the past.

4.4 Skin Aging

A potential confounding factor in the study of embalmed medical school cadavers is the subject's age. The mean age of the cadavers was 83.2 years. Clinical signs of skin aging are fine and coarse wrinkles, mottled colouration and skin laxity (Bosset *et al* 2003). How are these changes manifested microscopically?

Montagna *et al* (1990) described a series of changes in aged skin. These could occur at different times in different individuals. Epidermal changes included flattening of the underside of the epidermis, a reduction in the number of Langerhans cells and decreased pigmentation from reduced numbers of melanocytes. Dermal changes included a reduction in the number of fibroblasts, mast cells, macrophages and hair follicles and a dilation of lymphatic channels.

Other studies have examined changes in skin thickness with age. Tan *et al* (1982) measured skin thickness on the flexor aspect of the forearm of 261 healthy volunteers with a pulsed ultrasound technique and found that skin thickness increased up to age 20 and then gradually decreased thereafter. It was not possible to state whether this alternation in thickness was due to the epidermis, dermis, or both. Additionally it was suggested that in vitro measurements of thickness were larger than with in vivo methods, probably due to release of skin tension during excision of the samples.

Escoffier *et al* (1989) also used ultrasonic echography to measure the thickness of skin on the volar aspect of the forearm of 123 healthy volunteers. However very little variation in skin thickness was found between ages 10 and 70. It was found to decrease after the seventh decade.

De Rigal *et al* (1989) used B-scan ultrasonic echography to study the thickness of skin on the dorsal and volar forearms of 142 women. Dorsal skin was 17% thicker than volar skin up to age 70, after which both were similar. Volar skin was of a similarly thick between the first and seventh decades, with atrophy occurring after the eighth decade. In dorsal skin atrophy begins in the seventh decade. These findings also contradict those of Tan *et al* (1982). The authors suggest that their technique is more accurate at studying the dermis-hypodermis interface, which can be difficult to delineate. They also found that the dermis was composed of two areas with different echogenic qualities. With the technique used homogeneous media do not generate echoes and appear dark. Heterogeneous media generate numerous echoes and appear light. A sub-epidermal non-echogenic band (SENEB) and a dermal echogenic band (DEB) were seen. The SENEB was thought to correlate with the adventitial dermis and the

DEB with the reticular dermis. A progressive increase in the SENEB was seen with increasing age and this mirrored a decrease in the DEB. This would suggest an increase in the relative proportion of thin collagen fibres with age.

Hwang *et al* (2006) measured upper eyelid skin in 61 Korean women using H&E staining and measurements using microscopy. Subjects were divided into 10-year age groups and found no statistically significant difference in skin thickness related to age.

Lovell *et al* (1987) studied abdominal skin from 30 subjects to determine the changes in total collagen content and types I and III with age. Several techniques including SDS page electrophoresis and hydroxyproline estimation. The total collagen content of the skin did not vary with age. However a higher proportion of type III collagen was found in subjects age 65 or over. This relative increase in type III collagen would be compatible with the findings of De Rigal *et al* (1989) that the volume of thin collagen fibres increases with age.

It appears that there is no consensus in the literature regarding how skin thickness alters with age. Three of the studies described compared identical body sites using a similar method, but obtained different results. Clearly more study is needed to answer this question. The epidermis was thinner in cadaveric tissue compared with the operative samples. This may be due partly to the embalming, but may reflect age related thinning. The underside of the epidermis certainly appeared flatter than that of the operative samples in the majority of cases. However all cadaveric subjects were of similar age and this acts as an internal control against age related skin changes when considering comparisons between subjects and regions.

4.5 Regional Variability

"There is considerable regional variation in structure, making a knowledge of the normal anatomy of skin at its varying sites essential for the accurate diagnosis of skin biopsies." (McKee *et al* 1996)

Most texts draw an important distinction between thin, hairy skin that covers most of the body and thick hairless, glabrous skin covering the palms and soles. Even this simple system has problems as minor areas of specialized skin at mucocutaneous junctions such as the lips and outer rim of the anal canal have also to be placed in a class of their own (Gray *et al* 1995).

Consequently, it is recognized that the structure of skin at different anatomical sites does vary, little has been written on the subject. One feature that has been commented on is epidermal thickness. Epidermal thickness is reported as measuring 50μm on the eyelids to 1mm on the palms. Dermal thickness also varies, being thicker on the back or palms and soles than on the eyelids (Kanitakis 2002). However it is not clear how these results were actually determined. More qualitative descriptions of variability suggest that the epidermis of the eyelid, knee and elbow possess an architecture described as "slightly verrucous." The epidermis of the eyelid and ear gives rise to vellus hair follicles. Axillary epidermis gives rise to apocrine glands. Large sebaceous glands are found on the nose. Skin over the knee and elbow shows a prominent stratum corneum. Palms and soles show a thick and compact cornified layer with loss of basket weave pattern (Elder *et al* 2004, Gray *et al* 1995, Sternberg 1997). The stratum lucidum is a layer of epidermis just deep to the stratum corneum found only on glabrous skin (Kanitakis *et al* 2002). With all these differences noted one could ask what exactly is meant by “normal skin?”

Montagna (1969) wrote, **“*Although a great deal has been written about the microscopic anatomy of the skin of man, relatively little is known about that of the chin, lips, nose, eyelids, eyebrows and auricula for the obvious reason that its removal would cause disfigurement and mutilation.*”** The lack of detailed study of the skin in these regions is noted, and it seems surprising that in the intervening 38 years little new information has been added to this knowledge. The cosmetic importance of these areas alluded to in this quotation is given as a reason for lack of their study.

In this study, in contrast to using operative samples from “live” tissue, sampling material from cadavers donated to medical science has allowed skin to be sampled from areas not accessible during routine surgery and that may not be permitted during a hospital post-mortem.

The six sites that have been sampled from cadavers (eyelid, earlobe, post-auricular, abdomen, sternum and deltoid) can be considered to belong to a body region in two ways. Firstly skin was sampled from different topographic regions, namely the head (eyelid, earlobe and post-auricular) and the trunk (abdomen, sternum and deltoid). Secondly they can be grouped according to a body region's potential to form scars of different quality, as based on previous studies of keloid forming potential in different areas (Jacobsson 1947, Cosman *et al* 1961, Crockett 1964, Ramakrishnan *et al* 1974, Bayat *et al* 2004). Regions with greater potential to form good quality scars were the eyelid and abdomen. Regions with greater potential to form poor quality scars were the earlobe, post-auricular, sternum and deltoid.

I have studied a number of parameters: epidermal thickness, collagen bundle orientation and density of epidermal appendages. These are all reliably identified with Herovici's stain.

4.5.1 Epidermal thickness

Looking at graph 3.2 we can see that the epidermal thickness varies slightly between regions. On closer inspection, the trend is for the epidermis to be thicker in skin sampled from the head compared with that sampled from the trunk. This is confirmed when all the regions sampled from the head and trunk are grouped together, as seen on graph 3.3.

This was surprising given that skin on the eyelids is generally thought to be significantly thinner than that of the trunk (Kanitakis 2002) supporting observations from clinical practice, operating on these regions. However it should be noted that only the epidermis was measured and I make no reference to the absolute thickness of the dermis as its deeper boundary was not possible to determine exactly in some cases. The dermis was not measured because; on observation of the specimens it is difficult to determine exactly where the dermis ends. In some sections this is shown by a clear demarcation between the collagen bundles of the reticular dermis and a thin, delicate network of connective tissue, which would surround the subcutaneous adipose tissue. In other sections this is not so clear. During tissue sampling every measure was taken to ensure that the dermis was completely excised, however sampling errors may have occurred to account for this discrepancy between sections. On balance I felt it was better not to assess dermal thickness rather than present inaccurate or incomplete data. Other methods to study skin thickness in vivo using ultrasound have reported difficulty in determining exact interface between dermis and hypodermis. (De Rigal *et al* 1989)

Comparing the epidermal thickness between body regions grouped by their scarring potential did not reveal any statistically significant differences. This may be because scarring is more a phenomenon of the dermis rather than epidermis.

4.5.2 Epidermal appendage density

Looking at graph 3.5 we can clearly see variations in the density of sebaceous glands, sweat glands and hair follicles between regions. When all the regions sampled from the head and trunk are grouped together, we see statistically significant differences in the density of each type of epidermal appendage. There are more sweat glands in the trunk than the head, but more hair follicles and sebaceous glands in the head. When we look at graph 3.6 we see that the total epidermal appendage density is greater in skin samples obtained from the head.

Comparing the appendage density between body regions grouped by their scarring potential did not reveal any statistically significant differences at all. This again may be because scarring is more a phenomenon of the dermis rather than epidermis. This however presented an interesting finding in relation to hair follicles. It has been suggested that hair follicle dermal sheath fibroblasts play an important role in wound healing (Jahoda *et al* 2001). Based on this I would have expected a significantly higher number of hair follicles in areas with better scarring potential. However on further consideration the hair follicles present in the areas studied will be vellus hairs and perhaps it is the dermal sheath fibroblasts of terminal hairs that contribute to wound healing.

4.5.3 Collagen fibre orientation

Looking at graph 3.8 we can clearly see variations in the proportions of collagen fibres orientated parallel, oblique or perpendicular to the coronal plane. These observations were only possible by meticulous orientation of tissues during sampling.

The direction of relaxed skin tension lines varies considerably with body region, though there is some disagreement over their exact arrangement (Borges 1973, 1984). Over 30 different lines have been proposed to describe the axis of tension in the skin (Borges 1984). Cox (1941) suggested that collagen fibres run parallel to lines of "cleavage," though his paper contains a photograph illustrating this point clearly, it appears to be an isolated observation without further quantification or supporting statistical analysis. In considering which of the many tension lines to compare my own samples to, I felt that Langer's lines themselves were the most appropriate. This is because his work was performed on cadaveric tissue. If we consider each of the regions studied and then look at the direction of the greatest proportion of fibres, we see there is very little correlation between Langer's lines and dominant direction of fibres. This is shown in table 4.4.

Table 4.4 Direction of fibres compared to Langer's lines adapted from Gibson (1978) and Langer (1978)

Body Region	**Direction of Langer's Lines**	**Predominant direction of Collagen Fibres**
Eyelid	Transverse	Transverse
Earlobe	Transverse	Oblique
Post-auricular	N/A	Oblique
Deltoid	Transverse	Transverse=Oblique
Abdomen	Transverse	Transverse
Sternum	Oblique to Perpendicular	Transverse

We see that only the eyelid and abdominal skin correlate to Langer's lines. Unfortunately the original paper made no reference to post-auricular skin and so this could not be assessed. This may appear at odds with Gibson's (1965) observations that collagen fibres align when tension is applied to them. However Pierard and Lapiere (1987) suggested that the thin fibres of the papillary dermis were aligned with tension. Whilst the methodology to preserve skin tension in the samples excised appears prior to excision appears meticulous, the observations are only based on two samples. In my own observations I felt that light microscopy was not sensitive enough to fully define the direction of the thinnest collagen fibres, perhaps electron microscopy (EM) is a more appropriate tool. However, the complexity of EM would make such a study extremely difficult because orientation of tissue samples in the mm cubes the technique uses would be impossible. Clearly more work is needed to fully address this question.

When the skin samples are grouped according to their topographical region, we see that there is a statistically significantly higher proportion of parallel fibres in trunk skin, oblique fibres in head skin and no difference in the proportion of perpendicular fibres. This may suggest a more orderly, parallel appearance of trunk skin compared to that of the head, reflecting different demands placed on their movements.

When skin samples are grouped according to their scarring potential we see that there is a statistically significantly higher proportion of parallel fibres in regions with better scarring potential. We also see a statistically significantly higher proportion of oblique fibres in regions with poorer scarring potential. The proportion of perpendicular fibres is similar in both groups. It is interesting to note that the proportion of perpendicular fibres is fairly constant throughout the body. As these fibres are not variable, it seems reasonable to discount them and focus on the parallel and oblique fibres.

Looking at the ratio of parallel to oblique fibres we see that that it is statistically significantly higher in samples of skin from the head, as one would expect, given the higher proportion of parallel fibres in the trunk. We also see a higher ratio of parallel to oblique fibres in regions with poorer scarring potential.

It would seem that a more parallel, orderly collagen fibre arrangement correlated with better scarring. Wound tension has often been implicated in unfavourable scarring (Borges 1973). Meyer *et al* (1991) demonstrated the direction of tension in puncture wounds in pre-sternal skin at various levels. They found that tension existed in a multidirectional plane, evidenced by the wound expanding in all directions. Interestingly although sternal skin is subject to expansion and relaxation of the thorax an average 12 times per minute during respiration and is an area that classically has a tendency towards keloid formation, parallel fibres predominate. Skin tension is clearly not the only factor governing the orientation of collagen fibres. If we consider the earlobe, looking at figure 3.17 we see what appears at first glance to be an almost random arrangement of collagen fibres. This is a region that also has a strong tendency to form keloids, but is not subject to any obvious tension. It has long been known that scars along lines of tension heal better than those across them (Borges 1973). It is tempting to speculate that the relationship of skin tension to scar formation is that scars may heal better in the presence of a dominant axis of tension and that they will not heal as well where there is no overall axis of tension. It is disappointing that literature on this subject is somewhat limited.

When I further subdivided the regions according to their scarring potential and body region, the ratio of parallel to oblique fibres was statistically significantly higher in regions from the head with poorer scarring potential, but there was no significant difference in scarring potential in samples from the trunk. I think that the numbers involved in examining the data in this manner are too small to draw any definitive conclusions.

4.5.4 Topographical Variability

Eyelid skin is worthy of separate mention. Its structure is qualitatively very different to any of the regions studied fig (3.16) with more thin collagen fibres, mostly type III. Clinically operations such as blepharoplasty heal with good scars. Indeed searching the literature for evidence of keloids in eyelids has only produced 2 case reports in French (Offret *et al* 1993, D'Hermies *et al* 2003). Many studies have incorporated fibroblasts into dermal substitutes. Often the original location of the fibroblast may not be of direct concern to the researcher. Konstantinova *et al* (1997) compared fibroblasts taken from normal eyelids with other normal body regions and pathological lesions and embedded them into a constructed skin equivalent. It was found that the eyelid fibroblasts were superior at producing well-differentiated skin equivalents, compared to other regions. Indeed another study (Sorell *et al* 2004) compared characteristics of site matched fibroblasts in the papillary and reticular dermis and found they exhibited certain differences. These studies add further value to exploring the structure and behaviour of skin at different sites of the body.

We can see that qualitative and quantifiable regional variations exist in human skin. These differences in structure perhaps reflect adaptation to the differing stresses and functions of the skin at different sites of the body. For example, the soles of the feet have to withstand a person's entire bodyweight for hours at a time; the skin covering the shoulder joint has to move in many different directions; eyelid skin has to facilitate the rapid movements of blinking. The idea of specialized areas of skin is not new, but perhaps all areas of skin are specialized to a greater or lesser degree and I would repeat the question, "what is normal skin?"

In conclusion, this may have clinical implications when we look to replacing areas of skin loss with skin grafts and dermal substitutes. Fitzgerald *et al* (1996) reported when studying human skin with Herovici's stain that a layer of type III collagen was visible in the sub-epidermal region. He suggested that this could provide a guide to the future design of superior dermal substitutes. Over 10 years later a dermal substitute has yet to be produced that replicates the normal structure of skin. In order to produce a more anatomically correct dermal substitute we need to take this idea further and map the structure of skin at all areas of the body to determine characteristics such as dermal thickness, quantities of type I and type III collagen, orientation of collagen fibres in both the superficial and papillary dermis, and fibroblast characteristics. I have looked at several characteristics of skin from several areas of the body in this thesis, and it is surprising that nobody has attempted a similar study in the past. Extending these ideas to generate a "skin map" of the human body would provide an accurate template for future dermal substitutes. How can we hope to replace like tissue with like tissue if we do not know exactly what we are replacing? This concept may be of benefit in the shorter term, the cosmetic results of skin grafts are often disappointing for patients and doctors alike. The thigh is often used as a convenient donor site, but are the characteristics of thigh skin always a good match to the recipient sites? There are many occasions when we have little or no choice of donor sites, but knowledge of which areas of the body share similar characteristics may improve the cosmetic outcome of skin grafts in certain cases. Clearly more remains to be done before simple answers can be provided for ongoing clinical problems.

Further work

The next, natural step would be to expand this study to examine all areas of the human body and generate a “skin map.” The aim is to fully understand how skin structure varies with location. This would involve taking multiple of samples from adjacent areas. It would also entail exploring further characteristics including: dermal thickness, proportions of type I and III collagen, using an image analysis software package and Herovici’s stain, and fibroblast characteristics.

More detailed study should also be made of the unique characteristics of eyelid skin and fibroblasts to elucidate the lack of keloid formation in this region.

References

Bayat A, Arscott G, Ollier WE, McGrouther DA, Ferguson MW.

Keloid disease: clinical relevance of single versus multiple site scars.

Br J Plast Surg. 2005 Jan;58(1):28-37.

Bayat A, Arscott G, Ollier WE, Ferguson MW, Mc Grouther DA.

Description of site-specific morphology of keloid phenotypes in an Afrocaribbean population.

Br J Plast Surg. 2004 Mar;57(2):122-33

Bayat A, McGrouther DA, Ferguson MW.

Skin scarring.

BMJ. 2003 Jan 11;326(7380):88-92. Review.

Becker U, Nowack H, Gay S, Timpl R.

Production and specificity of antibodies against the aminoterminal region in type III collagen.

Immunology. 1976 Jul;31(1):57-65

Borges AF

Scar prognosis of wounds.

Br J Plast Surg. 1960 Apr;13:47-54.

Borges AF

Relaxed Skin Tension Lines (RSTL) Versus Other Skin Lines

Plas Recon Surg 1984:73:144-50

Borges AF

Elective incisions and scar revisions 1973: Chapter 1: pp1-14

Bosset S, Barré P, Chalon A, Kurfurst R, Bonté F, André P, Perrier P, Disant F, Le Varlet B, Nicolas JF

Skin ageing: clinical and histopathologic study of permanent and reducible wrinkles.

Eur J Dermatol. 2002 May-Jun;12(3):247-52.

Boutros S, Kattash M, Wienfeld A, Yuksel E, Baer S, Shenaq S.

The intradermal anatomy of the inframammary fold.

Plast Reconstr Surg. 1998 Sep;102(4):1030-3.

Breslow A

Thickness, cross-sectional areas and depth of invasion in the prognosis of cutaneous melanoma.

Ann Surg. 1970 Nov;172(5):902-8.

Brody GS.

Keloids and hypertrophic scars.

Plast Reconstr Surg. 1990 Oct;86(4):804.

Brzeziński PM, Godlewski A

The assessment of post mortem structural changes in the human epidermis

Folia Histochem Cytobiol. 2002;40(2):211-2

Büttner P, Garbe C, Bertz J, Burg G, d'Hoedt B, Drepper H, Guggenmoos-Holzmann I, Lechner W, Lippold A, Orfanos CE, et al.

Primary cutaneous melanoma. Optimized cutoff points of tumor thickness and importance of Clark's level for prognostic classification.

Cancer. 1995 May 15;75(10):2499-2506

Calnan JS, Copenhagen HJ.

Autotransplantation of keloid in man.

Br J Surg. 1967 May;54(5):330-5.

Canham PB, Finlay HM, Dixon JG, Ferguson SE.

Layered collagen fabric of cerebral aneurysms quantitatively assessed by the universal stage and polarized light microscopy.

Anat Rec. 1991 Dec;231(4):579-92

Canham PB, Talman EA, Finlay HM, Dixon JG.
Medial collagen organization in human arteries of the heart and brain by polarized light microscopy.
Connect Tissue Res. 1991;26(1-2):121-34

Drury RAB, Wallington EA
Carleton's Histological techniques 5th Edition
Oxford University Press 1980 pp186-190

Clark WH Jr, From L, Bernardino EA, Mihm MC.
The histogenesis and biologic behavior of primary human malignant melanomas of the skin.
Cancer Res. 1969 Mar;29(3):705-27.

Constantine VS, Mowry RW.
Selective staining of human dermal collagen. II. The use of picrosirius red F3BA with polarization microscopy.
J Invest Dermatol. 1968 May;50(5):419-23

Cosman B, Crikelair GF, Ju DMC, Gaulin JC, Lattes R
The surgical treatment of keloids
Plast Recons Surg 1961:27(4):335-357

Cox HT

The Cleavage Lines of the Skin

Br J Surg 1941:29:234-40

Crockett DJ.

Regional keloid susceptibility.

Br J Plast Surg. 1964 Jul;17:245-53

D'Hermies F, Dollé C, Verola O, Meyer A, Morel X, Dighiero P, Than Trong T, Behar Cohen F, Halhal M, Vu TA, Elmaleh C, Renard G.

[Hypertrophic eyelid conjunctival scar. A tarsal keloid]

J Fr Ophtalmol. 2003 Mar;26(3):315-8. French

Dayan D, Hiss Y, Hirshberg A, Bubis JJ, Wolman M.

Are the polarization colors of picrosirius red-stained collagen determined only by the diameter of the fibers?

Histochemistry. 1989;93(1):27-9.

de Rigal J, Escoffier C, Querleux B, Faivre B, Agache P, Lévêque JL

Assessment of aging of the human skin by in vivo ultrasonic imaging.

J Invest Dermatol. 1989 Nov;93(5):621-5.

Elder DE, Elenitsas R, Johnson BL, Murphy GF

Lever's Histopathology of the Skin 9th edition 2004

Epstein EH Jr, Munderloh NH.
Human skin collagen. Presence of type I and type III at all levels of the dermis.
J Biol Chem. 1978 Mar 10;253(5):1336-7

Escoffier C, de Rigal J, Rochefort A, Vasselet R, Lévêque JL, Agache PG.
Age-related mechanical properties of human skin: an in vivo study.
J Invest Dermatol. 1989 Sep;93(3):353-7

Ferguson MW, Whitby DJ, Shah M, Armstrong J, Siebert JW, Longaker MT.
Scar formation: the spectral nature of fetal and adult wound repair.
Plast Reconstr Surg. 1996 Apr;97(4):854-60. Review.

Fitzgerald AMP
Histology and immunochemistry of dermal collagen
M Phil Thesis, University of Bradford 1997

Fitzgerald AM, Kirkpatrick JJ, Foo IT, Naylor IL.
Human skin histology as demonstrated by Herovici's stain: a guide for the improvement of dermal substitutes for use with cultured keratinocytes?
Burns. 1996 May;22(3):200-2.

Fitzgerald AM, Kirkpatrick JJ, Foo IT, Naylor IL.
A picropolychrome staining technique applied to Dupuytren's tissue.
J Hand Surg [Br]. 1995 Aug;20(4):519-24.

Furuzawa-Carballeda J, Rodríquez-Calderón R, Díaz de León L, Alcocer-Varela J.
Mediators of inflammation are down-regulated while apoptosis is up-regulated in rheumatoid arthritis synovial tissue by polymerized collagen.
Clin Exp Immunol. 2002 Oct;130(1):140-9. Erratum in: Clin Exp Immunol 2002 Dec;130(3):565-6

Gabe M
Histological Techniques 1976

Gazoti Debessa CR, Mesiano Maifrino LB, Rodrigues de Souza R
Age related changes of the collagen network of the human heart
Mech Ageing Dev. 2001 Jul 31;122(10):1049-58.

Gibson T, Kenedi RM, Craik JE.
The mobile micro-architecture of dermal collagen: a bio-engineering study.
Br J Surg. 1965 Oct;52(10):764-70.

Gibson T

Karl langer (1819-1887) and his lines

Br J Plast Surg. 1978 Jan;31(1):1-2

Glegg RE, Eidinger D, Leblond CP

Some carbohydrate components of reticular fibers

Science 1953:118: 614-616

Gray H, Bannister LH, Berry MM, Williams PL

Gray's Anatomy: The Anatomical Basis of Medicine & Surgery

38th Edition: 1995

Griffioen FM, Smit-Vis JH, Brugman P, de Groot IJ, Sinnige WG.

Regeneration in surgically produced cleft palate in rabbits. A microscopical study.

Acta Morphol Neerl Scand. 1987;25(4):215-25.

Hale DM, Cromartie WJ, Dobson RL.

Luxol fast blue as a selective stain for dermal collagen.

J Invest Dermatol. 1960 Nov;35:293-5.

Murray RK, Granner DK, Mayes PA, Rodwell VW

Harper's illustrated biochemistry 26th Edition 2003: chapter 5: pp37-39, chapter 48 pp535-539

Har-Shai Y, Amar M, Sabo E.

Intralesional cryotherapy for enhancing the involution of hypertrophic scars and keloids.

Plast Reconstr Surg. 2003 May;111(6):1841-52

Herovici C

Picropolchorme. Histoligical technic for the study of supporting tissue.

Pathol Biol (Paris). 1961 Feb;9:387-8. French.

Herovici C

A polychrome stain for differentiating precollagen from collagen

Stain Tech 1963 204-205

Hess MW, Klima G, Pfaller K, Künzel KH, Gaber O.

Histological investigations on the Tyrolean Ice Man

Am J Phys Anthropol. 1998 Aug;106(4):521-32.

Hino H, Ammitzbøll T, Møller R, Asboe-Hansen G.

Ultrastructure of skin and hair of an Egyptian mummy. Transmission and scanning electron microscopic observations.

J Cutan Pathol. 1982 Feb;9(1):25-3

Hirschberg A, Buchner A, Dayan D.

The central odontogenic fibroma and the hyperplastic dental follicle: study with Picrosirius red and polarizing microscopy.

J Oral Pathol Med. 1996 Mar;25(3):125-7

Hirshberg A, Sherman S, Buchner A, Dayan D.

Collagen fibres in the wall of odontogenic keratocysts: a study with picrosirius red and polarizing microscopy.

J Oral Pathol Med. 1999 Oct;28(9):410-2.

Hiss J, Hirshberg A, Dayan DF, Bubis JJ, Wolman M.

Aging of wound healing in an experimental model in mice.

Am J Forensic Med Pathol. 1988 Dec;9(4):310-2

Hwang K, Kim DJ, Kim SK

Does the upper eyelid skin become thinner with age?

J Craniofac Surg. 2006 May;17(3):474-6

Jahoda CA, Reynolds AJ.

Hair follicle dermal sheath cells: unsung participants in wound healing.

Lancet. 2001 Oct 27;358(9291):1445-8.

Jacobsson F
The treatment of keloids at Radiumhemmet 1921-1941
Acta Radiologica 1947 XXIX 251-267

Junqueira LC, Cossermelli W, Brentani R.
Differential staining of collagens type I, II and III by Sirius Red and polarization microscopy.
Arch Histol Jpn. 1978 Jun;41(3):267-74

Junqueira LC, Bignolas G, Brentani RR.
A simple and sensitive method for the quantitative estimation of collagen
Analytical Biochemistry 1979:94;96-99

Junqueira LC, Bignolas G, Brentani RR.
Picrosirius staining plus polarization microscopy, a specific method for collagen detection in tissue sections.
Histochem J. 1979 Jul;11(4):447-55.

Junqueira LC, Bignolas G, Mourão PA, Bonetti SS.
Quantitation of collagen - proteoglycan interaction in tissue sections.
Connect Tissue Res. 1980;7(2):91-6.

Junqueira LC, Montes GS, Sanchez EM.

The influence of tissue section thickness on the study of collagen by the Picrosirius-polarization method.

Histochemistry. 1982;74(1):153-6.

Junqueira LC, Montes GS, Martins JE, Joazeiro PP.

Dermal collagen distribution. A histochemical and ultrastructural study.

Histochemistry. 1983;79(3):397-403.

Junqueira LCU, Carneiro J

Basic histology: Text and atlas 10th Edition 2002: Chapter 5: pp 106-126

Kanitakis J.

Anatomy, histology and immunohistochemistry of normal human skin.

Eur J Dermatol. 2002 Jul-Aug;12(4):390-9; quiz 400-1. Review.

Kiernan JA

Histological and histochemical methods. Theory and practice 2nd Edition :1990:pp115-130

Konstantinova NV, Lemak NA, Duong DM, Chuang AZ, Urso R, Duvic M.

Artificial skin equivalent differentiation depends on fibroblast donor site: use of eyelid fibroblasts.

Plast Reconstr Surg. 1998 Feb;101(2):385-91.

Koren R, Yaniv E, Kristt D, Shvero J, Veltman V, Grushko I, Feinmesser R, Sulkes J, Gal R.
Capsular collagen staining of follicular thyroid neoplasms by picrosirius red: role in differential diagnosis.
Acta Histochem. 2001 Apr;103(2):151-7.

Lamme EN, van Leeuwen RT, Jonker A, van Marle J, Middelkoop E.
Living skin substitutes: survival and function of fibroblasts seeded in a dermal substitute in experimental wounds.
J Invest Dermatol. 1998 Dec;111(6):989-95.

Langer K
On the anatomy and physiology of the skin. I. The cleavability of the cutis. (Translated from Langer, K. (1861). Zur Anatomie und Physiologie der Haut. I. Uber die Spaltbarkeit der Cutis. Sitzungsbericht der Mathematisch-naturwissenschaftlichen Classe der Kaiserlichen Academie der Wissenschaften, 44, 19.).
Br J Plast Surg. 1978 Jan;31(1):3-8

Levame M, Meyer F.
[Herovici's picropolychromium. Application to the identification of type I and III collagens]
Pathol Biol (Paris). 1987 Oct;35(8):1183-8. French.

Lillie RD

The allochrome procedure; a differential method segregating the connective tissues collagen, reticulum and basement membranes into two groups.

Am J Clin Pathol. 1951 May;21(5):484-8.

Lillie RD, Reynolds C, Pizzolato P.

Phosphomolybdic and phosphotungstic acid--Victoria Blue R stains two histochemically distinct collagens: dense dark blue and loose areolar pale green.

J Histochem Cytochem. 1979 Jul;27(7):1092-4.

López-De León A, Rojkind M.

A simple micromethod for collagen and total protein determination in formalin-fixed paraffin-embedded sections.

J Histochem Cytochem. 1985 Aug;33(8):737-43.

Lovell CR, Smolenski KA, Duance VC, Light ND, Young S, Dyson M

Types I and III collagen content and fibre distribution in normal skin during ageing

Br J Derm 1987:117:419-428

Macbride RG

Potential use of embalmed cadavers to study mast cell presence

Anat Rec. 1998 Jan;250(1):117-20

Mackay EV, Khoo SK.
Reactions in the rabbit Fallopian tube after plastic reconstruction. II. Histopathology. Fertil Steril. 1972 Mar;23(3):207-16.

Madruga de Melo EC, Lemos M, Aragao Ximenes Filho J, Sennes LU Nascimento Saldiva PH, Tsuji DH
Distribution of collagen in the lamina propria of the human vocal fold
Laryngoscope. 2003 Dec;113(12):2187-91

Marghoob AA, Koenig K, Bittencourt FV, Kopf AW, Bart RS.
Breslow thickness and clark level in melanoma: support for including level in pathology reports and in American Joint Committee on Cancer Staging.
Cancer. 2000 Feb 1;88(3):589-95.

Meyer M, McGrouther DA.
A study relating wound tension to scar morphology in the pre-sternal scar using Langers technique.
Br J Plast Surg. 1991 May-Jun;44(4):291-4.

McKee PH
Essential Skin Pathology
Mosby 1999

Meigel WN, Gay S, Weber L.

Dermal architecture and collagen type distribution.

Arch Dermatol Res. 1977 Jul 21;259(1):1-10

Melis P, Noorlander ML, van der Horst CM, van Noorden CJ.

Rapid alignment of collagen fibers in the dermis of undermined and not undermined skin stretched with a skin-stretching device.

Plast Reconstr Surg. 2002 Feb;109(2):674-80; discussion 681-2

Montagna W

The Structure and Function of Skin

Academic Publishers 1962

Montagna W, Ford DM.

Histology and cytochemistry of human skin. 3. The eyelid.

Arch Dermatol. 1969 Sep;100(3):328-35.

Montagna W, Giacometti L.

Histology and cytochemistry of human skin. XXXII. The external ear.

Arch Dermatol. 1969 Jun;99(6):757-67.

Montagna W

Histology and cytochemistry of human skin. XXXIV. The eyebrows.

Arch Dermatol. 1970 Mar;101(3):257-63

Montagna W

Structural changes in ageing skin.

Br J Dermatol. 1990 Apr;122 Suppl 35:61-70

Montes GS, Krisztán RM, Shigihara KM, Tokoro R, Mourão PA, Junqueira LC.

Histochemical and morphological characterization of reticular fibers.

Histochemistry. 1980 Feb;65(2):131-41

Montes GS, Krisztán RM, Junqueira LC.

Preservation of elastic system fibers and of collagen molecular arrangement and stainability in an Egyptian mummy.

Histochemistry. 1985;83(2):117-9

Montes GS, Junqueira LC.

The use of the Picrosirius-polarization method for the study of the biopathology of collagen.

Mem Inst Oswaldo Cruz. 1991;86 Suppl 3:1-11.

Morton DL, Davtyan DG, Wanek LA, Foshag LJ, Cochran AJ.

Multivariate analysis of the relationship between survival and the microstage of primary melanoma by Clark level and Breslow thickness.

Cancer. 1993 Jun 1;71(11):3737-43.

Muir IF.
On the nature of keloid and hypertrophic scars.
Br J Plast Surg. 1990 Jan;43(1):61-9.

Noorlander ML, Melis P, Jonker A, Van Noorden CJ.
A quantitative method to determine the orientation of collagen fibers in the dermis.
J Histochem Cytochem. 2002 Nov;50(11):1469-74

Offret H, Quillard J.
[Cheloid nodule of the free edge of the eyelid]
J Fr Ophtalmol. 1993;16(10):552-3. French.

Pérez-Tamayo R, Montfort I.
The susceptibility of hepatic collagen to homologous collagenase in human and experimental cirrhosis of the liver.
Am J Pathol. 1980 Aug;100(2):427-42

Perrin C, Noly V, Mourer R, Schmitt D
Preservation of cutaneous structures of egyptian mummies. An ultrastructural study
Ann Dermatol Venereol. 1994;121(6-7):470-5

Piérard GE, Lapiere CM

Microanatomy of the dermis in relation to relaxed skin tension lines and langer’s lines

Am J Dermatopath 1987:9:219-224

Piérard GE

Sirius red polarization method is useful to visualize the organization of connective tissues but not the molecular composition of their fibrous polymers.

Matrix. 1989 Jan;9(1):68-71

Prockop DJ, Kivirikko KI.

Collagens: molecular biology, diseases, and potentials for therapy.

Annu Rev Biochem. 1995;64:403-34. Review

Rabau MY, Hirshberg A, Hiss Y, Dayan D.

Intestinal anastomosis healing in rat: collagen concentration and histochemical characterization by Picrosirius red staining and polarizing microscopy.

Exp Mol Pathol. 1995 Jun;62(3):160-5.

Rabau MY, Dayan D.

Polarization microscopy of picrosirius red stained sections: a useful method for qualitative evaluation of intestinal wall collagen.

Histol Histopathol. 1994 Jul;9(3):525-8

Ramakrishnan KM, Thomas KP, Sundararajan CR.

Study of 1,000 patients with keloids in South India.

Plast Reconstr Surg. 1974 Mar;53(3):276-80

Ranne J, Kalimo H, Pyykkö K, Scheinin M, Aaltonen V, Niinikoski J, Laato M

Wound healing in denervated rat groin skin flap.

Eur Surg Res. 2000;32(3):197-20

Rawlins JM, Lam WL, Karoo RO, Naylor IL, Sharpe DT.

Quantifying collagen type in mature burn scars: a novel approach using histology

and digital image analysis.

J Burn Care Res. 2006 Jan-Feb;27(1):60-5

Rockwell WB, Cohen IK, Ehrlich HP.

Keloids and hypertrophic scars: a comprehensive review.

Plast Reconstr Surg. 1989 Nov;84(5):827-37. Review

Ebling FJG, Eady RAJ, Leigh IM

Rook’sTextbook of dermatology 5th Edition 1992 Vol 1 Chapter 3 pp49-89

Royal College of Pathologists

Standards and minimum datasets for reporting cancers: Minimum dataset for the histopathological reporting of common skin cancers: 2002

Sadler TW

Langman’s medical embryology 6th Edition 1990: Chapter 19: pp347-351.

Shoobridge MP.

A new principle in polychrome staining: a system of automated staining, complementary to hematoxylin and eosin, and usable as a research tool.

Stain Technol. 1983 Sep;58(5):245-58

Sorrell JM, Baber MA, Caplan AI.

Site-matched papillary and reticular human dermal fibroblasts differ in their release of specific growth factors/cytokines and in their interaction with keratinocytes.

J Cell Physiol. 2004 Jul;200(1):134-45

Sternberg SS

Histology for pathologists 2nd Edition 1997 Chapter 2: pp 25-44

Stücker M, Bechara FG, Bacharach-Buhles M, Pieper P, Altmeyer P.

What remains of the skin after 2000 years in a bog?

Hautarzt. 2001 Apr;52(4):316-21

Sweat F, Puchtler H, Rosenthal SI.

Sirius Red F3BA as a stain for connective tissue.

Arch Pathol. 1964 Jul;78:69-72

Tajima S, Nagai Y.

Distribution of macromolecular components in calf dermal connective tissue.

Connect Tissue Res. 1980;7(2):65-71.

Tan CY, Statham B, Marks R, Payne PA

Skin thickness measurement by pulsed ultrasound: its reproducibility, validation and variability

Br J Derm 1982: 106: 657-667

Trau H, Dayan D, Hirschberg A, Hiss Y, Bubis JJ, Wolman M.

Connective tissue nevi collagens. Study with picrosirius red and polarizing microscopy.

Am J Dermatopathol. 1991 Aug;13(4):374-7

Uitto J, Paul JL, Brockley K, Pearce RH, Clark JG.
Elastic fibers in human skin: quantitation of elastic fibers by computerized digital image analyses and determination of elastin by radioimmunoassay of desmosine.
Lab Invest. 1983 Oct;49(4):499-505.

van Zuijlen PP, Ruurda JJ, van Veen HA, van Marle J, van Trier AJ, Groenevelt F, Kreis RW, Middelkoop E.
Collagen morphology in human skin and scar tissue: no adaptations in response to mechanical loading at joints.
Burns. 2003 Aug;29(5):423-31.

Weedon D
The Skin (Systemic Pathology)
Churchill Livingstone 3rd Edition 1993